Elucidating the Regulation of the Metaphase-to-Anaphase Transition During Mitosis in *Candida albicans*

Samantha Sparapani

AThesis

In the Department

of

Biology

Presented in Partial Fulfillment of the Requirements

For the Degree of

Doctor of Philosophy (Biology) at

Concordia University

Montréal, Quebec, Canada

September 2019

Abstract

**Elucidating the Regulation of the Metaphase-to-Anaphase Transition
During Mitosis in *Candida albicans***

Samantha Sparapani, Ph.D.

Concordia University, 2019

Candida albicans is an important fungal pathogen of humans. Understanding the regulation of its cell cycle and mechanisms governing the metaphase-to-anaphase transition may reveal new targets for therapeutic development. This process is dependent on several factors including; separase, a conserved cohesin protease, the separase regulator securin, the Anaphase Promoting Complex/Cyclosome (APC/C) and its cofactors Cdc20p and Cdh1p, as well as the cohesin complex. Although Cdc20p and Cdh1p have been previously characterized in *C. albicans*, a detailed framework of metaphase-to-anaphase progression remains elusive. We provide the first characterization of separase in *C. albicans*, and demonstrate its putative interactors, collectively implying conserved and novel functions. We hypothesized one putative interactor; a divergent securin called Eip1p (Esp1-Interacting Protein 1). Subsequent characterization demonstrated that Eip1p is *Candida*-specific, important for chromosome segregation, and exhibited conserved securin-like features including stabilization in the presence of DNA damage/stress agents. Moreover, Eip1p depletion partially suppressed a metaphase block induced by these agents. Eip1p was reduced upon Cdc5p depletion, suggesting regulation via degradation, a diagnostic feature of securins. A proportion of Eip1p-depleted cells also exhibited novel phenotypes including misoriented spindles and maintenance of elongated spindles. However, Eip1p was not consistently or strongly enriched in the absence of Cdc20p unlike other securins, and its mechanisms of action remained unclear.

Since Eip1p is functioning like a securin, we hypothesized that its regulation includes degradation mediated by the APC/C Cdc20p, and inconsistent modulation in Cdc20p-depleted cells may be due to an incomplete Cdc20p-arrest phenotype. To test this, we investigated the APC/C subunit Cdc16p and provide the first characterization of an APC/C subunit in *C. albicans*. Bioinformatic analyses revealed sequence conservation of Cdc16p. Its depletion caused an early

mitotic arrest, and showed enrichment of the mitotic cyclin Clb2p. Eip1p was strongly enriched upon Cdc16p depletion, suggesting conserved function of Cdc16p in *C. albicans*. Mechanisms of action of Eip1p were addressed through affinity purification of Eip1p and mass spectrometry, revealing some unique putative protein interactors. Overall, we present evidence of a new securin, a potential drug target, and novel insights on mitotic regulation in *C. albicans*.

Acknowledgements

I would like to extend my deepest gratitude to my supervisor, Dr. Catherine Bachewich, for your continuous guidance and support. Catherine, you have provided me with the knowledge and techniques to think independently and have helped with my growth as a scientist and for this I am forever grateful. I would also like to thank Dr. Malcolm Whiteway for allowing me to integrate with your lab and participate in general discussions. I am grateful for your additional expertise and vision for my project and other endeavors. To my committee member, Dr. Alisa Piekny; Thank you for your support and guidance and for kindly being a member of my committee for my thesis.

In addition, I would also like to thank my former collegue Amandeep Glory, for your patience and guidance throughout each and every day in the lab.

Also, I would like to extend a special thank you to Dr. Chris Law of The Center for Miscroscopy and Cellular Imaging (CMCI) for providing me with tools and techniques that improved my microscopy techniques. I also thank Dr. Eric Bonneil from the Proteomic Centre of University of Montreal who helped with mass spectrometry.

Contribution of Authors

All figures presented in this thesis were contributed by Samantha Sparapani

Table of Contents

List of Figures

List of Tables

List of Acronyms

ACN   Acetonitrile
APC/C   Anaphase promoting complex/Cyclosome
ARM   Armadillo repeats
bp   base pair(s)
BSA   Bovine Serum Albumin
cAMP   Cyclic adenosine monophosphate
CD   Catalytic domain
CDC   Cell division cycle
CDK   Cyclin-dependent kinase
Co-IP   Co-immunoprecipitation
CID   Collision induced dissociation
DAPI   4', 6'diamidino-2-phenylindole dihydrochloride
DIC   Differential interference contrast
DNA   Deoxyribonucleic acid
dNTP   Deoxyribonucleotide triphosphate
DOX   Doxycycline
EDTA   Ethylenediaminetetraacetic acid
FA   Formic acid
FEAR   Fourteen early anaphase release
GAP   GTPase activating protein
gDNA   Genomic DNA
HDAC   Histone deacetylase
GEF   Guanine exchange factor
GFP   Green fluorescent protein
HA   Hemaglutinin
HU   Hydroxyurea
hr   Hour(s)
kb   kilo base pair(s)
L   Litre(s)
LiAc   Lithium acetate
MAP   Mitogen-activated protein
MAPK   MAP Kinase
MEN   Mitotic exit network
MMS   Methyl Methanesulfate
-MC   MM medium lacking methionine and cysteine.
             MM medium supplemented with 2.5mM methionine and 0.5mM
+MC   cysteine
MIC   Minimum inhibitory concentration
min   Minute(s)
ml   Milliliter(s)
MPF   Mitosis promoting factor

μl	Microlitre (s)
nt	nucleotides
O.D.	Optical Density
PCR	Polymerase chain reaction
PEG	Polyethylene glycol
PHYRE	Protein homology/analogy recognition engine
PI	Propidium iodide
PVDF	Polyvinylidene difluoride
Rcf	Relative Centrifugal Force
RNA	Ribonucleic acid
rpm	Rotations per minute
SCF	Skp-cullin F-box
SD	0.67% yeast nitrogen base without amino acids, 2% glucose
SD	Substrate binding domain
SDS	Sodium Dodecyl Sulfate
sec	Second(s)
SMC	Structural maintenance of chromosomes
ssDNA	Salmon Sperm DNA
TAP	Tandem affinity purification
TCEP	Tris (2-carboxyethyl) phosphine hydrochloride
TEV	Tobacco etch virus
TPR	Tetratricopeptide repeat
TRIS	Tris(hydroxymethyl)aminomethane
YPD	1% yeast extract, 2% peptone, 2% dextrose

1.0 Introduction

1.1 Cell Proliferation and the Cell Cycle

1.1.1 Overview

The cell cycle is the process that governs duplication of DNA, chromosome segregation, and subsequent division of the cell. Cell proliferation is defined by a network of interconnected metabolic wiring that balances cell division and cell death (Zhu and Thompson, 2019). Cell proliferation falls under control of the cell cycle. The cell cycle consists of various stages including G1, S, G2 and M phase followed by cytokinesis (Behl and Ziegler, 2007). During G1 phase, many cell types will grow. S phase is characterized by duplication of genetic material and expression of histones required for DNA assembly. During G2 phase, growth can again occur in some cell types (Behl and Ziegler, 2007). Mitosis involves the alignment of duplicated chromosomes on a spindle, and their separation to opposite poles. Mitosis is then followed by cytokinesis, which results in the formation of daughter cells (Behl and Ziegler, 2007).

1.1.2 Mitosis

Mitosis is the cell cycle stage where duplicated chromosomes condense, align on a spindle, and separate to opposite poles of the cell (Behl and Ziegler, 2007). Specifically, mitosis begins with prophase, where in mammalian cells, chromatin condense into chromosomes and centrosomes nucleate microtubules. The nuclear envelope and nucleolus break down, and the chromosomes are captured by the spindle microtubules. During metaphase, the chromosomes align at the cell equator. During anaphase, the chromosomes separate through degradation of the cohesin "glue" that held them together and move to opposite poles of the cell. Finally, telophase consists of sister chromosomes reaching opposite poles of the spindle and the reformation of the nuclear envelope. Telophase is followed by cytokinesis where the daughter cells separate. In the model yeast *Saccharomyces cerevisiae*, differences are seen with respect to the nuclear envelope which does not break down, but does form pores (De Souza et al., 2007), and spindle assembly which occurs earlier in S phase (Kitamura et al., 2007).

1.1.3 Major regulators of mitosis

1.1.3a Mitotic Cyclins and CDK

A major regulator of cell cycle transitions involves a Cyclin Dependent Kinase (CDK) interacting with a phase-specific cyclin. For entry into mitosis, a CDK interacts with a mitotic Cyclin B to form Mitosis Promoting Factor (MPF). In *S. cerevisiae*, MPF consists of the CDK Cdc28p and the cyclin B Clb2p (Dabrieva et al., 2003). The Cdc28p/Clb2p complex is held inactive at the G2/M transition by inhibitory phosphorylation from Swe1p kinase. The phosphatase Mih1p can activate Cdc28p/Clb2p by removing the inhibitory phosphate. Targets of MPF include factors required for spindle assembly, chromosome condensation and activation of other processes required for mitotic progression. Cdc28p/Clb2p activity must be down regulated for cells to exit mitosis, which occurs in part through targeted degradation of the B-type cyclin (Weiss, 2012; Marston et al., 2014).

1.1.3b Separase

Separase is a critical regulator of the metaphase-to-anaphase transition and mitotic exit, and is highly conserved amongst various organisms (Moschou and Bozhkov, 2002), including Esp1p from *S. cerevisiae* (Yamamoto et al., 1996a), Cut1p from *Shizosaccharomyces pombe* (Yanagida et al., 2000), Esp1p from *Homo sapiens* and other mammals (Waizenegger et al. 2002), and Sep-1p from *Caenorhabditis elegans* (Siomos et al., 2001), for example. They are composed of three main domains; the catalytic domain (CD), the substrate-binding domain (SD) and the α-helical domain (Luo and Tong, 2018), otherwise known as the head, tail and trunk domains, respectively. The head domain in the C-terminus is the most conserved and contains catalytic caspase-like domains, whereas the tail in the N-terminus consists of Armadillo (ARM) repeats that form a super helix of alpha helices divided between four domains that mediate protein-protein interactions (Uhlmann et al., 1999; Moschou and Bozhkov, 2002). Separases are cysteine-rich proteases that help cleave the cohesin structure holding sister chromosomes together. In *S. cerevisiae*, the cohesin complex is composed of two core SMC proteins Smc1p and Smc3p, as well as two non-SMC kleisin proteins, Mcd1p/Scc1p and Scc3p, which are highly conserved (Peters et al., 2008). The alpha-kleisin subunit of the cohesin complex (Mcd1p/Scc1p)

is one of the main substrates of separase. Scc1p phosphorylation by the polo-like kinase Cdc5p enhances its cleavage by Esp1p during the metaphase-to-anaphase transition. In *S. cerevisiae*, *ESP1* is essential since its absence results in large-budded cells with unsegregated chromatin, spindle defects and extra spindle pole bodies (McGrew et al., 1992). Spindles were abnormal in most cells, resembling discontinuous microtubule arrays that were often curved around the perimeter of the cell, or were very weak in staining, while a smaller proportion of cells contained a short G2 spindle (McGrew et al., 1992). Defects in sister chromatid segregation are also observed in Esp1p-depleted cells in humans (Chestukhin et al., 2003). Separases have additional functions (Kumar et al., 2017). For example, Esp1p is a component of the Fourteen Early Anaphase Release Pathway (FEAR), where it aids in the release of the mitotic phosphatase Cdc14p from inhibition in the nucleolus by downregulating the PP2A-Cdc55p complex (Weiss, 2012). This was thought to be important for spindle elongation and priming of the Mitotic Exit Network (see below) and downregulation of Cdc28p/Clb2p, resulting in mitotic exit. However, more recent evidence suggests that the FEAR pathway functions in rDNA segregation and may alternatively restrain mitotic exit (Yellman and Roeder, 2015). Esp1p is also important for stabilization of the anaphase spindle (Luo and Tong, 2018).

1.1.3c Securin

Another major regulator of mitotic progression, including the metaphase-to-anaphase transition and mitotic exit, is securin (Jensen et al., 2001; Moschou and Bozhkov, 2002). Securins exist in various organisms including Pds1p in *S. cerevisiae* (Yamamoto et al., 1996a), Cut2p in *S. pombe* (Funabiki et al., 1996), PTTG1 in humans (Zou et al., 1999), Pimp in *Drosophila melanogaster* (Jäger et al., 2001), IFY-1 in *C. elegans* (Kitigawa et al., 2002) and Pans1p/Pans2p in *Arabidopsis* (Cromer et al., 2019), but are highly divergent in sequence, making their identification difficult. To date, they have not been characterized in several organisms including in several fungi, for example (Moschou and Bozhkov, 2002). Securins function through binding separase at specific sites which differ slightly between different organisms. For example, in *S.*

pombe, the N-terminus of separase binds the C-terminus of securin, whereas in budding yeast the C-terminus of Pds1p binds the first 155 amino acids of the N-terminus of separase as well as other sites (Moschou and Bozhkov, 2002; Luo and Tong, 2018). This binding pattern is also observed in *C. elegans*. However, structural analysis of the securin-separase complex show the location of securin on the surface of the third domain in the helical domain of separase differs significantly, underscoring the weak sequence homology between different securins (Luo and Tong, 2018). Securin acts as both a negative and positive regulator of separase. First, securin binds and inhibits separase prior to metaphase, and must be targeted for degradation at the metaphase-to- anaphase transition to release separase, allowing it to cleave the cohesin subunit Mcd1p/Scc1p and permit synchronous chromosome segregation. In *S. cerevisiae*, some securin remains in order to inhibit separase and prevent mitotic exit during anaphase, but is subsequently degraded later in mitosis, promoting mitotic exit (Hatano et al., 2016). Securin also acts as a chaperone of separase where it assists in folding. In *S. cerevisiae,* it also contributes to efficient localization of Esp1p to the nucleus from the cytoplasm (Agarwal and Cohen-Fix, 2002; Hellmuth et al., 2015).

Securins are essential for growth in *S. pombe*, *D. melanogaster* and *C. elegans* (Funabiki et al., 1996; Stratmann and Lehner, 1996; Jäger et al., 2001; Kitigawa et al., 2002) but not in vertebrates due to additional inhibitory regulation of phosphorylation by the CDK/Cyclin B complex (Hellmuth et al., 2015). In *S. cerevisiae*, *pds1* mutants were identified by screening for precocious dissociation of chromosomes in the presence of microtubule inhibitors (Guacci et al. 1993; Yamamoto et al. 1996a). In the absence of the drugs, *pds1Δ* cells are viable but show growth defects such as micro-colony formation and chromosome loss (Yamamoto et al., 1996a). Moreover, temperature sensitive mutants of *PDS1* show that *PDS1* is essential at higher temperatures due to a temperature-sensitive defect at G1/S that prevents normal spindle elongation, and Esp1p from entering the nucleus, thus cells arrest with a single mass of DNA (Yamamoto et al., 1996a; Jensen et al., 2001). Other phenotypes include loss of synchrony in chromosome separation and multi-nucleate cells, which imply precocious mitotic exit (Holt et al., 2008; Hatano et al., 2016).

1.1.3d The Anaphase Promoting Complex/Cyclosome (APC/C)

The APC/C is essential for progression through mitosis. The APC/C is a ubiquitin ligase system that targets proteins for degradation through assembling a chain of ubiquitin tags on substrates (McLean et al., 2011). Such tags are recognized by the 26S proteosome and destroyed at the appropriate time. The APC/C is a large complex composed of 11 to 13 subunits (Barford, 2011). In *S. cerevisiae*, a catalytic domain consists of the cullin subunit Apc2 and the RING H2 domain subunit Apc11, which are responsible for binding the E2-ubiquitin conjugate as well as APC core components, which include Apc6p/Cdc16p, Apc3p/Cdc27p and Apc8p/Cdc23p, for example (Peters, 2006; Barford, 2011; McClean et al., 2011). The non-catalytic core subunits such as Apc4p, Apc5p, Apc7p (humans), Apc9p and Apc10p, Apc11p, Apc12p, Apc13p, Apc15p and Apc16p act as scaffold and stabilizing factors, many of which contain the tetratricopeptide repeat (TPR) motif, a 34-amino acid region that acts to anchor proteins during complex formation and interactions (Figure 1.1) (Barford, 2011). Several subunits, including Cdc16p, Cdc23p and Cdc27p of *S. cerevisiae* are essential; temperature-sensitive mutants arrest as large-budded cells that contain a large mass of DNA lying either at or through the bud neck, and demonstrate chromosome loss (Lamb et al. 1994; Heichman and Robert, 1996).

APC/C activity is regulated by two cofactors; Cdc20p and Cdh1p (Morgan, 2007). During the early stages of mitosis, Cdc20p binds Cdc23p and Cdc26p through its N-terminus, anchoring it to the APC/C and directing APC/C activity towards mitotic proteins such as securin and a proportion of the cyclin Clb2p, for example (Acquaviva and Pines, 2006; Barford, 2011; Qiao et al., 2016). Degradation of securin permits activation of separase, and the metaphase-to-anaphase transition. In *S. cerevisiae*, *CDC20* mutants arrest in metaphase with elevated Clb2p and Pds1p levels (Cohen-fix et al., 1996), similar to the situation with absence of Cdc16p (Irniger and Nasmyth, 1997). Simultaneous absence of the securin *PDS1* in the *CDC20* mutant background results in a telophase arrest, suggesting that Cdc20p is also important for mitotic exit (Lim et al., 1998). Later in mitosis, the APC/C falls under control of Cdh1p. Cdh1p also binds Cdc23p and Cdc26p and assists the APC/C in targeting additional mitotic regulators such as the polo-like kinase Cdc5p, the remainder of Clb2p, securin, as well as Cdc20p for degradation, permitting mitotic exit (Lianga et al., 2018). In *S. cerevisiae*, APC/C subunits and cofactors are regulated in

part by phosphorylation by the CDK-cyclin complex Cdc28p/Clb2p. Phosphorylation of Cdc16p and Cdc23p during anaphase helps with the stabilization and binding of Cdc20p (Acquaviva and Pines, 2006). Phosphorylation of Cdh1p keeps the cofactor inactive until late mitosis (Harkness, 2018).
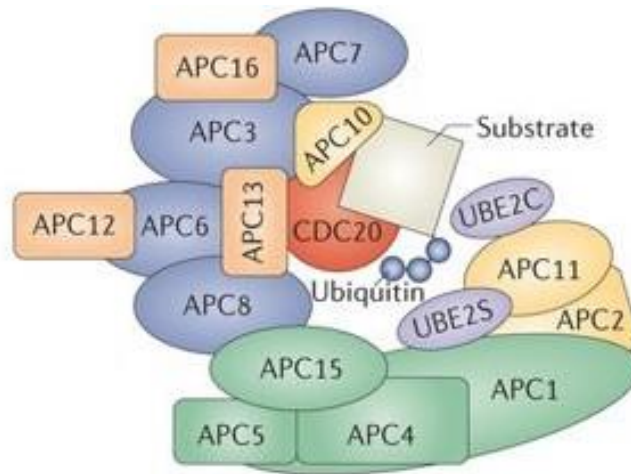
Figure 1.1. Components of the Anaphase Promoting Complex/Cyclosome in humans (Sivakumar and Gorbsky, 2015).

1.1.3e Cdc14 Early Anaphase Release (FEAR) and Mitotic Exit Network (MEN) Pathways

In *S. cerevisiae*, additional pathways exist to ensure timely progression through mitosis. Two pathways that are involved in this process include the Cdc14 Early Anaphase release (FEAR) and Mitotic Exit network (MEN) which both function to ensure the proper release of the phosphatase Cdc14p from its inhibitor, Net1p (Figure 1.2) (Yellman and Roeder, 2015). During anaphase, the separase Esp1p, Slk19p, and Spo12p, act to inactivate the protein phosphatase PP2Ap-Cdc55p complex, resulting in the phosphorylation of Net1p by the Cdk-cyclin complex Cdc28p/Clb2p, releasing Cdc14p from inhibition (Yellman and Roeder, 2015). Accumulation of Cdc14p contributes to the activation of the MEN pathway during late mitosis. Simultaneously, MEN pathway activation maintains Cdc14p release, allowing eventual mitotic exit. During this process, the polo-like kinase Cdc5p negatively regulates the GTPase activating protein (GAP) complex Bub2p-Bfa1p. This in turn negatively regulates the Ras-like GTPase Tem1p. Tem1p is localized to the daughter spindle pole bodies where it is activated by Lte1p, a guanine exchange

6

factor (GEF) for Tem1p (Queralt and Uhlmann, 2008). The active form of Tem1p leads to a protein kinase signaling cascade including Cdc15p, Dbf2p and Mob1p, which function in the release of remaining Cdc14p to the cytoplasm (Yellman and Roeder, 2015).
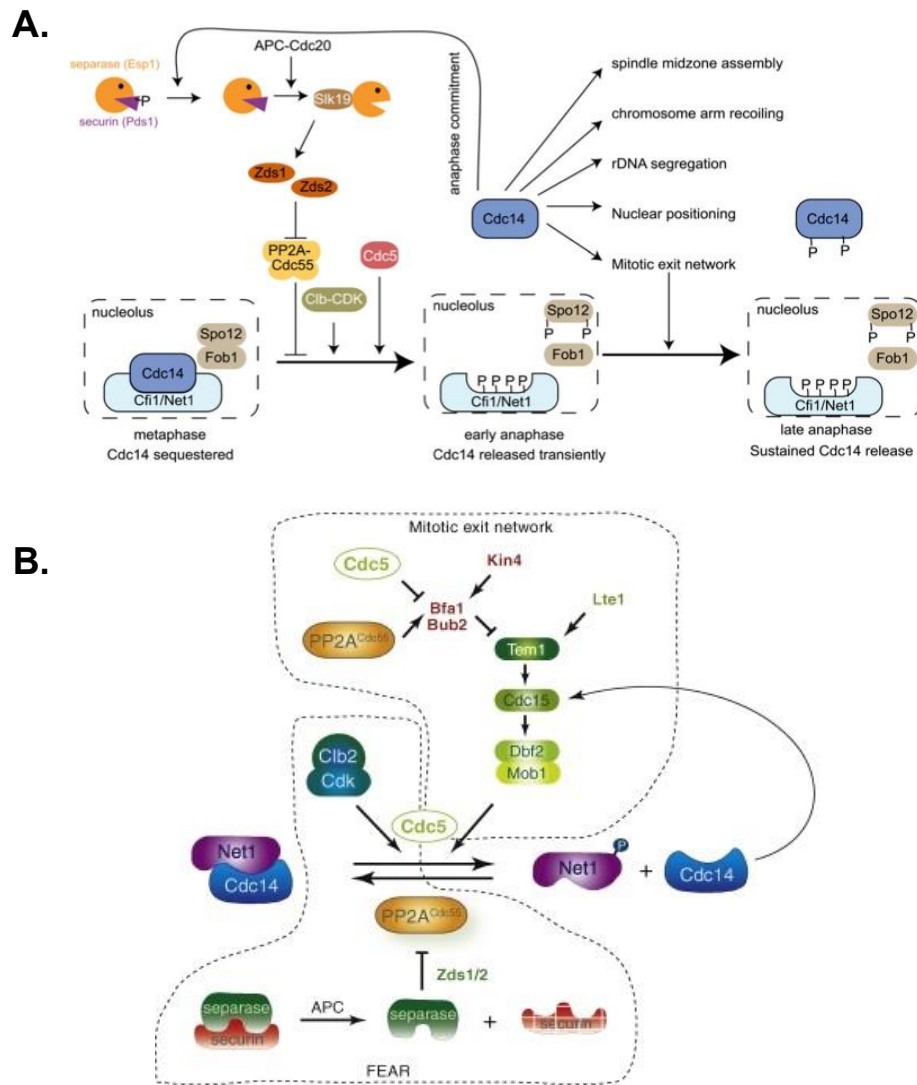
Figure 1.2. Regulatory pathways in mitosis Mitotic regulatory pathways.
(A) Cdc14p early anaphase release pathway (FEAR) (Marston et al., 2014). (B) Mitotic exist network (MEN) (Queralt and Ulhmann, 2008).

1.1.3f Mitotic Checkpoint Pathways

Several checkpoint pathways impinge on the regulation of the metaphase-to-anaphase transition to ensure mitosis does not progress under abnormal conditions or until damage is corrected. For example, in *S. cerevisiae,* Cdc20p is a target of the spindle checkpoint pathway. Upon spindle damage, checkpoint factors such as Mad2p form an inhibitory complex with Cdc20p, sequestering Cdc20p from binding to the APC/C and thus preventing the APC/C from activating anaphase by targeting Pds1p for degradation (Sudakin et al., 2001; May and Hardwick, 2006). Moreover, in the presence of DNA damage induced by exposure to DNA damaging agents such as methyl methane sulfate (MMS) or the replicative stress agent hydroxyurea (HU), Pds1p becomes phosphorylated by the kinase Chk1p through a signaling cascade directly activating Chk1p kinase activity by Rad53p (Sanchez et al., 1999; Palou et al., 2017). This phosphorylation renders Pds1p resistant to degradation by the APC/C$_{Cdc20p}$ complex and results in a cell cycle block during early mitosis (Sanchez et al., 1999; Palou et al., 2017). Mad2p also prevents the premature association of the APC/C with Cdh1p and mitotic exit by sequestering Cdh1p, allowing it to remain inactive following its phosphorylation by Cdc28p (Listovsky and Sale, 2013).

1.2 *Candida albicans*: Opportunistic Pathogen
1.2.1 General Overview

C. albicans is a diploid ascomycete asexual fungus that exists normally as a commensal in the human gastrointestinal, urogenitary, and mucotaneous tracts (Lim et al., 2012). However, it can cause infection under conditions of immune suppression, including mucosal infections such as thrush or vaginitis, or more serious systemic infections that involve entry into the bloodstream and invasion of organ tissues. Systemic infections are associated with up to 50% mortality rates (Delaloye et al., 2014; da Silva Dantas et al., 2016). The human gut comprises a multitude of microorganisms that co-exist to maintain a symbiotic relationship, and the immune system employs a variety of mechanisms in order to discriminate between commensal and pathogenic organisms (Williams et al., 2012). Immunocompromised individuals become susceptible to *C. albicans* infection because of disruption of epithelial cell junctions, or when homeostasis is no longer maintained (Williams et al., 2012). Infections caused by *C. albicans* are commonly treated

by targeting fungal-specific factors. For example, azoles such as fluconazole affect cell membrane development by inhibiting cytochrome P450 from synthesizing ergesterol, a key component of fungal cell membranes, and are fungistatic (Cannon et al., 2007). However, current treatments are exhibiting toxic side effects on the host such as nephrotoxicity caused by Amphotericin B, for example (Li et al., 2015). Moreover, *C. albicans* is showing greater resistance to current drug therapies such as employing upregulation of drug efflux mechanisms for example (Robbins et al., 2017). Additionally, in the presence of echinocandins, *C. albicans* cells activate salvaging pathways by introducing mutations in specific amino acid sequences coding for 1,3-β-D-glucan synthase; the enzyme responsible for synthesis of the cell wall component β-1,3-glucan biosynthesis (Parente-Rocha et al., 2017). Recent studies have suggested combinatorial drug therapies as a means of reducing drug resistance and toxic side effects (Cui et al., 2015) since targeting multiple non-essential factors simultaneously with anti-fungal therapies may lower the chance of developing resistance (Cui et al., 2015). Susceptibility to fungal infections is measured as the minimum inhibitory concentration (MIC) following 24 h in the presence of a drug (Rosenberg et al., 2018). It has recently been shown that highly tolerant cells, defined as the residual growth of *Candida* cells in the presence of antifungal drugs, have been associated with persistent candidemia (Rosenberg et al., 2018). This suggests that a greater understanding of the tolerance levels rather than the levels of resistance of *Candida* infections is vital for therapeutic development (Rosenberg et al., 2018). Given this, there is a need to identify additional drug targets and develop new anti-fungal therapies. This in turn requires a more comprehensive understanding of the basic biology of *C. albicans*' growth and virulence traits.

1.2.2 Virulence Trait: Morphogenesis

Virulence in *C. albicans* is dependent on a number of factors and processes including morphogenesis (Kabir et al., 2012; Lim et al., 2012). *C. albicans* can undergo morphological changes between different types of yeast, pseudohyphae, hyphae, and chlamydospores. This plasticity is important for cells to survive in different environments (Si et al., 2013). *C. albicans* hypae cells are important for macrophage lysis, where *C. albicans* cells undergo remodeling of the proteins at the cell surface upon ingestion by the host (O'Meara et al., 2015), penetrating

endothelial cells and invading epithelial cells. *C. albicans* in its yeast form is important for dissemination throughout the blood stream to various tissue (Kadosh, 2017). The switching between cell types is important for virulence, as cells locked in one morphological form are significantly less pathogenic (Lo et al., 1997). Regulation of morphogenesis involves several environmental cues. For example, yeast, pseudohyphae and hyphae grow at 30, 36 or 37°C, respectively. Hyphae additionally require factors such as serum, a pH between 6 and 7, or alternative carbon sources to form (Sudbery, 2011). The yeast-to-hyphal transition has been extensively investigated, where environmental cues are mediated by a diversity of signaling pathways, including the mitogen-activated protein kinase (MAPK) and cyclic AMP (cAMP), among others (Carlisle et al., 2013). Moreover, cell cycle arrest due to depletion of essential cell cycle proteins in *C. albicans* contributes to the formation of elongated filaments with some hyphal traits, yet involve distinct forms of regulation. This response to cell cycle arrest has been proposed to represent a virulence trait, as it may assist a yeast cell to escape a harmful environment that imposes stress on the cell cycle (Bachewich et al., 2003; Bachewich et al., 2005; Wang et al., 2019). The various cell types and plasticity in differentiation also contribute to biofilms. Biofilms are defined as communities of cells that adhere to surfaces, producing an intracellular matrix, and have distinct morphological properties that differ from single cells (Gulati et al., 2016). *C. albicans* biofilms are composed of several cell types mostly of which include hyphae with a combination of yeast cells and pseudohyphal cells (Gulati et al., 2016). A network of genes including *EFG1*, *TEC1*, *BCR1* and *ROB1* compose the circuitry governing biofilm formation through activation of downstream and upstream factors (Gulati et al., 2016) however recent studies suggest the possibility of diversity in the overall network with respect to clinical isolates (Huang et al., 2019). Thus, understanding how the various morphological forms of *C. albicans* are regulated is an essential component of understanding its virulence.

1.2.3 Virulence Trait: Cell Proliferation

1.2.3a Regulation of the cell cycle in *C. albicans*: general overview

Another process that is critical for virulence in *C. albicans* is cell proliferation. This process is fundamental for survival in the host. Further, aneuploidy and a significant degree of

chromosomal loss are prevalent and tolerated in *C. albicans*, which in addition to its parasexual cycle, have been proposed to help generate diversity (Bouchonville et al., 2009). Cell cycle regulation has not been well characterized in *C. albicans*. At a transcriptional level, there exist many similarities in cell cycle phase-specific modulated genes compared to other yeast systems including *S.cerevisiae* and *S. pombe* (Côte et al., 2009). However, there were also many differences, including modulation of *Candida*-specific and/or uncharacterized genes. Several putative cell cycle-associated and regulatory proteins remain to be characterized in *C. albicans*. Intriguingly, of those that have been analyzed, many show variation in function compared to homologues in other systems, including yeast and mammals (Bachewich et al., 2003; Bachewich et al., 2005; Chou et al., 2011). This suggests the existence of novel factors and/or functions in the cell cycle circuitry in *C. albicans*, which may be exploited for the purpose of new drug target discovery.

1.2.3b Regulation of the metaphase to anaphase transition and mitotic exit in *C. albicans*

In *C. albicans*, little is known about the regulation of mitosis, and the circuitry controlling the metaphase-to-anaphase transition and mitotic exit have not been well defined. Of the factors that have been characterized, several show differences in function in *C. albicans* compared to orthologues in *S. cerevisiae*, suggesting re-wiring in the mitotic networks. For example, with respect to MEN and FEAR pathways, the latter being non-established in *C. albicans*, Tem1p, the Ras-like GTPase, is important for mitotic exit and cytokinesis in *C. albicans*, consistent with *S. cerevisiae*. However, its depletion generates polarized growth, in contrast to Tem1p mutants in *S. cerevisiae* (Milne et al., 2014). In *C. albicans*, Dbf2p is essential, and important for cytokinesis, mitotic exit, septum formation and mitotic spindle organization (González-Novo et al., 2009). However, in *S. cerevisiae,* Dbf2p is not essential, and is required for cytokinesis and mitotic exit (González-Novo et al., 2009). *C. albicans* contains a homologue of *CDC14*. Unlike *S. cerevisiae,* Cdc14p in *C. albicans* is not essential, is regulated in part by degradation at the end of mitosis, and is required for telophase (Kaneva et al., 2019). In most systems including *S. cerevisiae* and humans, Cdc14p is regulated in part by being sequestered in the nucleolus, however in *C. albicans* Cdc14p is targeted for degradation towards the end of mitosis rather than being

sequestered (Clemente-Blanco et al., 2005). Moreover, C. *albicans* also contains a homologue of the polo-like kinase, Cdc5p, but it may be required earlier in the cell cycle compared to *S. cerevisiae* (Bachewich et al., 2003). *C. albicans* also contains homologues of several key regulators of the metaphase-to-anaphase transition, including separase, the cohesin subunits, as well as most of the APC/C subunits and their cofactors Cdc20p and Cdh1p. However, of these, only orthologues of the APC/C cofactors Cdc20p and Cdh1p were previously characterized, and demonstrated to have some conservation in mitotic function (Chou et al., 2011). In *C. albicans*, Cdc20p is important for both metaphase and telophase, and results in enrichment of Clb2p upon its depletion, consistent with *S. cerevisiae*. However, Cdc20p-depleted cells form elongated filaments, in contrast to Cdc20p in *S. cerevisiae* (Chou et al., 2011). Moreover, *CDH1* is not essential in *C. albicans* and Cdh1p depletion results in Clb2p enrichment, consistent with *S. cerevisiae*. However, Cdh1p-depleted cells demonstrate a pleiotropic phenotype consisting of larger yeast cells, in contrast to Cdh1p- depletion in *S. cerevisiae* (Chou et al., 2011). In addition, *C. albicans* does not contain a sequence homologue of the separase regulator; securin, despite being an ascomycete like *S. cerevisiae* and *S. pombe.* Thus, collectively, little is known about the regulatory factors governing the metaphase-to-anaphase transition and mitotic exit in *C. albicans*. During my MSc studies, I attempted to address this problem by partially characterizing the *C. albicans* homologue of separase Esp1p. We hypothesized that a divergent securin in *C. albicans* may be revealed by identifying Esp1p-interacting factors, and isolated a novel protein, Orf19.955p (S. Sparapani, MSc thesis, https://spectrum.library.concordia.ca/980588). However, these studies were preliminary, and the function of Orf19.955p remained unclear.

1.3 Objectives

It is important to understand cell cycle regulation in *C. albicans* because it is critical for survival in the host and virulence. Moreover, several *Candida*-specific genes show cell cycle-specific modulation in expression, and several conserved cell cycle regulators that have been characterized demonstrate variation in function (Bachewich et al., 2003; Bachewich et al., 2005; Chou et al., 2011). This suggests the existence of novel features that could be further exploited for controlling growth. We hypothesize that regulation of the metaphase-to-anaphase transition in

C. albicans involves conserved as well as distinct proteins, and these may be revealed through characterizing the separase homologue Esp1p as well as its interacting factors. My specific objectives include; 1) Further explore the functions of *C. albicans* separase Esp1p by confirming whether it plays a conserved role in influencing chromosome segregation, and obtaining data that may support additional roles; 2) comprehensively characterize Orf19.955p, an Esp1p-interacting factor, and determine whether it functions as a securin; 3) explore the regulation of Eip1p in part by characterizing Cdc16p, a putative APC/C subunit; and 4) investigate Eip1p mechanisms of action. Collectively, this will provide a better understanding of the mechanisms governing mitotic progression in *C. albicans*, new insights on mitotic regulatory factors in eukaryotic cells in general, as well as uncover potential fungal-specific targets for therapeutic development.

Chapter 2. Characterization of a Novel Separase-Interacting Protein and Candidate new Securin, Eip1p, in the Fungal Pathogen *Candida albicans*

2.1 Abstract

Proper chromosome segregation is crucial for maintaining genomic stability, and dependent on separase, a conserved and essential cohesin protease. Securins are key regulators of separases, but remain elusive in many organisms due to sequence divergence. Here, we demonstrate that the separase homologue Esp1p in the ascomycete *Candida albicans*, an important pathogen of humans, is essential for chromosome segregation. However, *C. albicans* lacks a sequence homologue of securins found in model ascomycetes. We sought a functional homologue through identifying Esp1p interacting factors. Affinity purification of Esp1p and mass spectrometry revealed Eip1p/Orf19.955p, an uncharacterized protein specific to *Candida* species. Functional analyses demonstrated that Eip1p is important for chromosome segregation but not essential, and modulated in an APC$_{Cdc20}$-dependent manner, similar to securins. Eip1p is strongly enriched in response to MMS or HU treatment, and its depletion partially suppresses an MMS or HU-induced metaphase block. Further, Eip1p depletion reduces Mcd1p/Scc1p, a cohesin subunit and separase target. Thus, Eip1p may function as a securin. However, other defects in Eip1p-depleted cells suggest additional roles. Overall, the results introduce a candidate new securin, provide an approach for identifying these divergent proteins, reveal a putative anti-fungal therapeutic target, and highlight variations in mitotic regulation in eukaryotes.

2.2 Introduction

Segregation of duplicated chromosomes to two daughter cells during mitosis is essential for maintaining genomic stability. Errors in this process have profound consequences, and can lead to numerous disorders including cancer (Kumar et al., 2017). During metaphase, sister chromatids align at the equatorial region of the cell, and are under tension due to mutual attachment and kinetochore binding to spindle microtubules (Piskadlo and Oliveira, 2017). Chromatids are joined by cohesin, a conserved protein complex (Mehta et al., 2013). In the yeast *Saccharomyces cerevisiae*, this consists of Structural Maintenance of Chromosomes (SMC) proteins Smc1p and Smc3p, the kleisin subunit Mcd1p/Scc1p, and Scc3p. Together these form a ring structure on chromatids after DNA replication (Mehta et al., 2013). In order to progress to anaphase, cohesin must be cleaved.

Separase is a highly conserved and essential cysteine protease responsible for cleaving Mcd1p/Scc1p and triggering anaphase (Kumar, 2017). In *S. cerevisiae*, absence of the separase homologue *ESP1* results in large-budded cells with unsegregated chromatin, spindle defects and extra spindle pole bodies (McGrew et al., 1992). In humans, depletion of separase also results in defects in sister chromatid separation (Chestukhin et al., 2003). Cleavage of cohesin by separase is enhanced by phosphorylation of the Scc1p subunit by Polo-like kinases, including PLK-1 in humans or Cdc5p in *S. cerevisiae*, respectively (Alexandru et al., 2001; Hornig et al., 2002; Hauf et al., 2005). Separases have several additional functions (Kumar, 2017). In *S. cerevisiae,* for example, Esp1p is part of the Fourteen Early Anaphase Release or FEAR network, where it contributes to initial release of the phosphatase Cdc14p from the nucleolus, which in turn is required for rDNA segregation (Yellman and Roeder, 2015). Cdc14p is released by phosphorylation of the inhibitor Net1p by mitotic cyclin-dependent kinase (CDK), as well as downregulation of the PP2A$_{CDC55}$ phosphatase by Esp1p and other FEAR components in a non-proteolytic manner (Stegmeier et al., 2002; Sullivan et al., 2003). The bulk of Cdc14p is released into the cytoplasm later in mitosis by the Mitotic Exit Network (MEN). This permits Cdc14p-dependent dephosphorylation of several substrates, resulting in down-regulation of mitotic Cyclin-Dependent Kinase (CDK) activity and mitotic exit (Weiss 2012). Esp1p also cleaves Slk19p, a kinetochore-associated protein, and both are important for several spindle functions

(Havens et al., 2010). Esp1p contributes to mitotic exit through promoting spindle elongation and spindle pole body entry into the bud, a requirement for activation of the MEN pathway (Lu and Cross, 2009; Yellman and Roeder, 2015)

Securin is a critical regulator of separase, and homologues have been characterized in *S. cerevisiae* (Pds1p) (Yamamoto et al., 1996a), *Shizosaccharomyces pombe* (Cut2p) (Funabiki et al., 1996), *Homo sapiens* and other mammals (PTTG1) (Zou et al., 1999), *Drosophila melanogaster* (Pimp) (Jäger et al., 2001), and *Caenorhabditis elegans* (IFY-1) (Kitigawa et al., 2002). Securin is positively required for separase folding, localization and stability, but also inhibits enzyme activity (Hornig et al., 2002; Argawal and Cohen-Fix, 2002; Hellmuth et al., 2015; Luo and Tong, 2018). Securins are initially targeted for degradation at the metaphase-to-anaphase transition to permit rapid activation of separase and abrupt, synchronous chromosome segregation. In *S. cerevisiae*, some securin remains in order to inhibit separase and prevent mitotic exit during anaphase, but is subsequently degraded later in mitosis (Hatano et al., 2016). Degradation is mediated by the Anaphase Promoting Complex/Cyclosome (APC/C) and its cofactors Cdc20p and Cdh1p (Kramer et al., 2000; Hilioti et al., 2001; Hatano et al., 2016). In *S. cerevisiae*, *pds1* mutants were initially identified by screening for precocious separation of chromosomes in the presence of microtubule inhibitors (Guacci et al., 1993; Yamamoto et al., 1996a). In the absence of inhibitory drugs, *pds1Δ* cells are viable but show growth defects in the form of heterogeneous and micro-colony formation and chromosome loss (Yamamoto et al., 1996a). However, *PDS1* is essential at higher temperature due to a temperature-sensitive defect at G1/S that prevents normal spindle elongation and Esp1p from entering the nucleus, resulting in most cells containing a single DNA mass (Yamamoto et al., 1996a; Jensen et al., 2001). Additional phenotypes include loss of synchrony in separation of sister chromatid pairs, and some multi-nucleate cells, implying precocious mitotic exit (Holt et al., 2008; Hatano et al., 2016). Securins are essential for growth in *S. pombe, D. melanogaster* and *C. elegans* (Funabiki et al., 1996; Stratmann and Lehner, 1996; Jäger et al., 2001; Kitigawa et al., 2002) but not in vertebrates, due to additional inhibitory regulation of separase by CDK/cyclin B phosphorylation (Hellmuth et al., 2015). Securin becomes essential in *S. cerevisiae* when spindle assembly or kinetochore function is defective, or in response to γ irradiation-induced activation of DNA

damage in G2 phase. Under these conditions, it is stabilized through sequestration of Cdc20p by the spindle checkpoint protein Mad2p, or Chk1p-dependent phosphorylation, respectively (Yamamoto et al., 1996a,b; Cohen-Fix and Koshland, 1997; Wang et al., 2001; Palou et al., 2017). Pds1p is also regulated by CDK/Cyclin B phosphorylation, which enhances binding to Esp1p and localization to the nucleus (Agarwal and Cohen-Fix, 2002). Despite the fact that separase, cohesin, and the APC/C are conserved, securins are divergent in sequence and have not been identified in several organisms, including plants and many fungi, for example (Moschou and Bozhkov, 2012).

Candida albicans is a diploid multi-morphic ascomycete that exists in many morphological forms including yeast, pseudohyphal, hyphal or chlamydospore cells, and is one of the most common opportunistic fungal pathogens of humans. A commensal in the gastrointestinal tract, *C. albicans* can also be invasive and cause systemic infections are associated with mortality rates reaching 50% (da Silva Dantas et al., 2016). Limited treatments and growing drug resistance (O'Meara et al., 2015) compel identification of new therapeutic targets and anti-fungal therapies, which is dependent on a thorough understanding of the basic biology of the organism (Sellam and Whiteway, 2016).

Cell proliferation is important for survival of *C. albicans* in the host and virulence. However, the cell cycle networks, including those governing chromosome segregation and mitotic progression, are not well defined*,* and some conserved players show variations in function. For example, several *C. albicans* homologues of MEN factors are required for mitotic exit in a manner similar to the situation in *S. cerevisiae* (Milne et al., 2014; Bates, 2018; Orellana-Muñoz et al., 2018), but others have alternative functions (Clemente-Blanco et al., 2005; González-Novo et al., 2009). With respect to the metaphase-to-anaphase transition, *C. albicans* homologues of the APC/C cofactors Cdc20p and Cdh1p are conserved in regulating anaphase onset, telophase, and mitotic exit through targeting the mitotic cyclin Clb2p and the polo kinase Cdc5p for degradation, (Chou et al., 2011). However, variations in function were suggested by the pleiotropic phenotype of *cdh1Δ/Δ/* cells, which included enlarged yeast-form cells. In contrast, *S. cerevisiae cdh1Δ* cells were significantly reduced in size due to a role for Cdh1p in repressing START (Jorgensen and Tyers, 2004). Further, Cdc20p depletion resulted in

filament formation, contrary to the large doublet arrest of *S. cerevisiae cdc20* mutants (Lim et al., 1998). *C. albicans* has a separase homologue, Esp1p, and its depletion also resulted in filamentous growth (O'Meara et al., 2015). However, its functions remain unclear. Cohesin homologues are also present, including Mcd1p/Scc1p, but not characterized. Similar to many other fungi, *C. albicans* lacks a sequence homologue of securin. Together with other examples of functional variation in cell cycle regulatory factors (Bachewich et al., 2003; Atir-Lande et al., 2005; Shi et al., 2007; Ofir and Kornitzer, 2010; Ofir et al., 2012) and cell cycle phase expression of *C. albicans*-specific genes (Côte et al., 2009), the data imply unique facets of the cell cycle circuitry in *C. albicans,* which could be exploited for the purpose of controlling growth. *C. albicans* is tolerant of aneuploidy and exploits this feature as a mechanism for adapting to different environments (Selmecki et al., 2010), further underscoring the need to understand the mechanisms governing chromosome segregation in this organism.

In order to gain new insights on the regulation of the metaphase-to-anaphase transition and mitotic progression in *C. albicans*, we characterized the separase homologue Esp1p, and demonstrate that it is essential for sister chromatid segregation. Further, we identified a novel Esp1p-binding protein, called Eip1p. Eip1p is *Candida*-specific, important for chromosome segregation, and has other features consistent with it being a candidate securin with additional functions.

2.3 Materials and Methods

2.3.1 *Strains, Oligonucleotides, plasmids, culture conditions*

Strains, oligonucleotides and plasmids used in this study are listed in Tables S2.1-2.3 respectively. Strains were cultured in rich media (YPD) containing 1.0% yeast extract, 2.0% peptone, 2.0% glucose and 50 μg/ml of uridine (Bensen et al., 2002). Alternatively, strains containing genes under control of the *MET3* promoter were incubated in synthetic defined (SD) yeast culture medium containing 0.67% of yeast nitrogen base, 2.0% dextrose, amino acid supplements (2.0 g adenine, 2.5 g uridine, 2.0 g tryptophan, 1.0 g histidine, 1.0 g arginine, 1.5 g tyrosine, 1.5 g isoleucine, 7.45 g valine, 1.5 g lysine, 2.5 g phenylalanine, 5.0 g glutamic acid, 10.0 g threonine and 3.0 g leucine per 50 L) that either lacked methionine and cysteine for promoter induction (-MC), or contained 2.5 mM methionine and cysteine for promoter repression (Care et al., 1999). For *TET*-regulated strains, cells were incubated in YPD medium with or without 100 μg/ml doxycycline hyclate (Sigma-Aldrich). Uridine, histidine and/or arginine were omitted under conditions of prototroph selection. For growth assays or protein extraction, overnight cultures of cells were diluted into fresh medium to an $O.D._{600nm}$ of 0.1 or 0.2, and collected after incubation at either an $O.D._{600nm}$ of 0.8-1.0 or at indicated time points. Alternatively, cells from plates were mixed in small volumes of liquid media, from which large dilutions were made. Cultures that were in low exponential phase the next day were then collected and diluted into fresh medium to an $O.D._{600nm}$ of 0.1 or 0.2 for subsequent incubation as described. For colony growth assays on solid media, overnight cultures of cells were washed in water, diluted to an $O.D._{600nm}$ of 0.1, serial diluted (100x) and spotted (4.0 μl) on plates. For affinity purification of Esp1p-TAP in a *CDC20* conditional background, strains were incubated overnight in inducing medium, diluted to an $O.D._{600nm}$ of 0.4 in repressing medium and collected after 4 h incubation. In order to measure the levels of Eip1p-MYC in response to methylmethane sulfate (MMS) or hydroxyurea (HU), overnight cultures were diluted to an $O.D._{600nm}$ of 0.1 in YPD medium containing either 0.02% MMS (Sigma-Aldrich), 200 mM HU (Sigma-Aldrich) or no drug and incubated for 5 h. Cells were then collected and processed for Western blotting. In order to determine the effects of MMS on cells with or without Eip1p, low exponential cultures of strains were diluted into fresh inducing or repressing medium at a starting $O.D._{600nm}$ of 0.25,

incubated for 2.5 h, collected, diluted into fresh inducing or repressing medium containing 0.02% MMS, and incubated for a further 5 h before fixation. Unless otherwise noted, all experiments were performed at 30°C, and repeated at least two times.

2.3.2 Strain Construction

In order to tag the C-terminus of *ESP1* with the TAP epitope (Protein A and Calmodulin-binding protein separated by a tobacco etch virus (TEV) protease cleavage site) (Lavoie et al., 2008), the 3.0 kb *TAP-URA3* cassette was amplified from plasmid pFA-TAP-*URA3* (Lavoie et al. 2008) with primer pair AG103F and AG103R. The 3.0 kb construct was transformed into strain BWP17, resulting in strain AG636. Correct integration was confirmed using primer pair AG104F and AG3R. The second copy of *ESP1* was replaced using a two-step PCR reaction. Primer pairs SS1F, SS1R and SS2F, SS2R were used to amplify sequences lying upstream from the START or downstream from the STOP codon for *ESP1*, respectively. The *HIS1* cassette fragment from plasmid pBS-Ca*HIS1* (Chou et al., 2011) was amplified with primers SS3F and SS3R. The products were combined in a fusion PCR reaction with primer pair SS1F and SS2R. The fusion construct was transformed into strain AG636 resulting in strain SS1. Correct integration was confirmed using PCR with primer pair SS10F and CaHIS1R. Transformant gDNA was extracted according to Rose et al., 1990. In order to tag *ESP1* with TAP in a *CDC20* conditional strain, the approach described above was used, and the product was transformed into strain HCCA109 (Chou et al., 2011) resulting in strain SS3. In order to create a strain containing a single copy of *ESP1* under control of the *MET3* promoter, one copy of *ESP1* was deleted from strain BWP17 using the strategy described previously, with the exception of amplifying the *URA3* cassette from pBS-Ca*URA3* with primer pair SS3F and SS3R, resulting in strain SS20. Correct integration was confirmed with primer pairs SS10F and CaURA3R. Primer pairs SS19F, SS19R and SS20F, SS20R were used to amplify sequences upstream and downstream of the *ESP1* START codon, respectively, while primers SS21F and SS21R amplified a *HIS1-MET3* fragment from the pFA-*MET*-Ca*HIS1* plasmid (Gola et al., 2003). The three fragments were combined in a fusion PCR with primers SS19F and SS20R. The final construct was transformed into strain SS20 resulting in strain SS35. Correct integration was confirmed using primers SS26F and CaHIS1R. In order to

tag the C-terminus of *ESP1* with three copies of the hemaglutinin epitope (HA), a *HA-URA3* cassette was amplified from plasmid pFA-HA-*URA3* (Lavoie et al., 2008) with primers AG4F and AG4R. The product was used as a template in a fusion PCR with primers AG103F and AG103R. The fusion construct was transformed into strain BWP17 resulting in strain SS16. Correct integration was confirmed using primer pair CaURA3F and AG104R.

For creating a strain containing a single copy of *EIP1* under the control of the *MET3* promoter, primer pairs SS22F, SS22R and SS23F, SS23R were used to amplify sequences lying upstream from the *EIP1* START codon or downstream from the STOP codon, respectively. Primer pair SS24F and SS24R amplified the *URA3* cassette from the pBS-*URA3* plasmid. The three fragments were combined in a fusion PCR with primers SS22F and SS23R. The final product was transformed into strain BWP17, resulting in strain SS10. Correct integration of product was confirmed by PCR with primers caURA3F and SS25R. To place the second copy of *EIP1* under the control of the *MET3* promoter, primer pairs SS27F, SS27R and SS28F, SS28R were used to amplify sequences lying upstream and downstream of the *EIP1* START codon, respectively, while primers SS29F and SS29R amplified a *HIS1-MET3* fragment from the pFA-*MET*-Ca*HIS1* plasmid. The three fragments were combined in a fusion PCR with primers SS27F and SS28R. The final construct was transformed into strain SS10 resulting in strain SS25. Correct integration of the construct was confirmed by PCR with primers SS25F and caHIS1R.

In order to create a strain lacking both copies of *EIP1*, the remaining allele of *EIP1* in strain SS10 was replaced as described for SS10, with the exception of amplifying a *HIS1* cassette from pBS-*HIS1* with primers SS24F and SS24R. The final fusion PCR product was transformed into strain SS10 resulting in strains SS63-65. Strains were confirmed with primer pairs CaURA3F/CaHIS1F and SS25R to confirm allele replacements with *HIS1* and *URA3*, as well as SS25F and SS25R to screen for presence of the *EIP1* ORF.

In order to construct a strain that contained a single copy of *EIP1* tagged at the C terminus with the TAP epitope, the *TAP-ARG4* cassette was amplified from plasmid pFA-TAP-*ARG4* with primers SS33F and SS33R, and transformed into strain SS10. The resulting strain SS40 was confirmed by PCR with primer pair CaARG4F and SS25R. A similar approach was used to tag *EIP1* with TAP in strain HCCA109, resulting in strain SS41. Alternatively, *EIP1* was tagged

with TAP in strain AG500 by amplifying a *TAP-URA3* construct from pFA-TAP-*URA3* as described, resulting in strain SS43. To tag the C-terminus of *EIP1* with thirteen copies of the MYC epitope (Bensen et al., 2005), a *MYC-HIS1* cassette was amplified from plasmid pMG2093 with oligonucleotides SS18F and SS18R. The product was transformed into strain SS10 resulting in strain SS22, or strain SS16 resulting in strain SS29. Correct integration of the PCR product was confirmed with primer pair CaHIS1F and SS25R.

In order to tag the C-terminus of *TUB2* with the green fluorescent protein (GFP), the *GFP-ARG4* cassette (Gola et al., 2003) was amplified from plasmid pFA-GFP-*ARG4* with primer pair CB135F and CB135R. The final fragment was transformed into strains SS25 and SS35 resulting in strains SS37 and SS38, respectively. In order to tag the C-terminus of *HTB1* with the green fluorescent protein (GFP) epitope, the *GFP-ARG4* cassette was amplified from plasmid pFA-GFP-*ARG4* with primers SS37F and SS37R. The construct was transformed into strain SS25, resulting in strain SS44. Strains were screened for protein expression using epifluorescence microscopy.

In order to tag the C-terminus of *MCD1* with the with the TAP epitope, the 3.0 kb *TAP-ARG4* cassette was amplified from plasmid pFA-TAP-*ARG4* with primer pair SS47F and SS47R. The 3.0 kb construct was transformed into strain SS25, resulting in strain SS86. Correct integration was confirmed using primer pair SS48F and SS48R.

2.3.3 Protein extraction and Western blotting

In order to measure the levels of Eip1p in response to manipulation of Cdc20p or Cdc5p, cells were collected as indicated above. Protein extracts were prepared using HK buffer according to Liu et al., 2010. Extracted protein was quantified using the Bradford assay (Bio-Rad, Mississauga). Briefly, 30μg of protein was loaded onto SDS-PAGE gels and proteins were transferred to a polyvinylidene difluoride (PVDF) membrane (BioRad). Membranes were blocked with Tris-buffered saline Tween (TBST; Tris [pH 7.5], 137 mM NaCl, 0.1% Tween 20) containing 5% skim milk for 1.5 h. Blots were washed three times for 15 min in TBST and incubated for 2 h in 0.2 g/ml anti-TAP antibody (Thermo Scientific), diluted in TBST. Blots were rinsed three times for 15 min in TBST and incubated for 1 h in a 1/10,000 dilution of horseradish

peroxidase-conjugated anti-rabbit secondary antibody (Santa Cruz). After washing, blots were developed using Amersham ECL Western blotting analysis system (GE Healthcare). Blots were stripped and incubated with 1.0 μg/ml anti-GAPDH (Protein Tech) or 1/1000 dilution of anti-α tubulin (Sigma-Aldrich) antibodies as a loading control. For detecting Esp1p-HA or Eip1p-MYC, membranes were incubated for 2 h in either 0.4 g/ml anti-HA antibody (12CA5; Roche) or 1.0 μg/ml of anti-MYC antibody (Santa Cruz) diluted in TBST. Secondary antibodies including horseradish peroxidase-conjugated anti-mouse (KPL) or anti-rabbit (Santa Cruz) were diluted 1/10:000. Anti-PSTAIRE (Santa Cruz Biotechnology) was used as a loading control at 0.2 μg/ml. Western blots were quantified using ImageJ as described previously (Chou et al., 2011).

2.3.4 Co-immunoprecipitation and Affinity purification

For Co-immunoprecipitation assays, overnight cultures of cells were diluted into 2.0 L of YPD medium and incubated at 30°C until the O.D.$_{600nm}$ reached 0.8-1.0. The culture was centrifuged for 5 min at 3000 rpm, and the remaining pellet was immersed in dry ice and stored at - 80°C. Protein was extracted as described above. Co-immunoprecipitation was performed according to Lavoie et al., 2008. Briefly, 40 μl of Mono HA 11 Affinity beads (Covance) was centrifuged at 1500g for 2 min at 4°C, washed three times with 500 μl of HK buffer (Liu et al., 2010), and centrifuged again. Beads were then added to 40 mg of protein extract, and samples were incubated overnight at 4°C with rocking. After centrifugation, the supernatant was transferred to fresh Eppendorf tubes. Beads were washed five times with 1.0 mL of HK buffer, centrifuged, and re-suspended in 500 μl of buffer. The contents were transferred to fresh Eppendorf tubes and centrifuged to pellet the beads. The supernatant was removed and protein was eluted by boiling in 50 μl of 1X SDS sample buffer (50 mM Tris pH 6.8, 2% SDS, 0.01% Bromophenol blue, 10% Glycerol, 100mM DTT) for 10 min. After centrifugation, the supernatant was removed and beads were boiled in 40 μl of 1X SDS sample buffer for 10 min. Eluted samples were loaded on 7.5 or 10% SDS PAGE gels for Western blotting. Affinity purification assays were carried out according to Rigaut et al. 1999 and Liu et al. 2010. Briefly, cultures from strains AG153 and SS3 were prepared as described above, and 4 L resulted in 330 mg of input protein. Protein was pre-cleared by adding 500 μl of prewashed Sepharose 6B beads

(Sigma) (1:1 slurry in HK buffer) and rocking at 4°C for 30 min. After removing beads, protein extracts were incubated with prewashed IgG Sepharose 6 Fast Flow (GE Healthcare) (1:1 slurry in HK buffer; 250 µl bead volume) overnight at 4°C. The extract and beads were poured into a Poly-Prep Chromatography Column (BIO-RAD). The eluate was discarded and beads were washed twice with 10 ml ice cold IPP300 buffer (25 mM Tris-HCl pH 8.0, 300 mM NaCl, 0.1% NP-40), twice with 10 ml IPP150 buffer (25 mM Tris-HCl pH 8.0, 150 mM NaCl, 0.1% NP-40) and once with 10 ml TEV-CB (25 mM Tris-HCl pH 8.0, 150 mM NaCl, 0.1% NP40, 0.5 mM EDTA and 1 mM DTT). After adding 1.0 ml of TEV CB buffer containing 10 U of Ac-TEV protease (Invitrogen), the column was rocked overnight at 4°C. The eluate was collected and beads were washed with another 1.0 ml TEV CB buffer. To the final 2.0 ml eluate, 3.0 ml of CBB (25 mM Tris-HCl pH 8.0, 150 mM NaCl, 1 mM Mg acetate, 1 mM Imidazole, 2 mM CaCl2), 24.0 µl of 1.0 M $CaCl_2$ and 300 µl of Calmodulin Sepharose 4B (GE Healthcare) was added. The mixture was rocked for 1 h at 4°C. After centrifugation, beads were washed twice with 1.0 ml CBB (0.1% NP-40), and once with 1.0 ml CBB (0.02% NP-40). Protein was eluted by two subsequent additions of 1.0 ml CEB (25 mM Tris-HCl pH 8.0, 150 mM NaCl, 0.02% NP-40, 1 mM Mg acetate, 1 mM Imidazole, 20 mM EGTA, 10 mM β- mercaptoethanol). The elutions were combined and protein was precipitated by adding 25% volume of 50% Trichloroacetic acid (TCA). The samples were kept on ice for 30 min, then centrifuged for 10 min at 4°C. The supernatant was removed, and 1.0 ml of 80% acetone was added to wash the precipitate. The contents were then centrifuged for 10 min at 4°C to remove the acetone, and the sample dried on ice for 60 min. The pellet was re-suspended in 30 µl 1 X SDS sample buffer, and boiled for 10 min. Samples were loaded on an SDS-PAGE gel and run on gels until just entering the resolving gel (Liu et al., 2010). The gel was stained with Coomassie blue (BioRad), and gel pieces from tagged and untagged strains were cut and sent for analysis via Orbitrap LC/MS (IRIC, University of Montreal). Bands were destained in 50% MeOH (Sigma-Aldrich). Each band was shrunk in 50% acetonitrile (ACN), reconstituted in 50 mM ammonium bicarbonate with 10 mM TCEP [Tris(2-carboxyethyl) phosphine hydrochloride; Thermo Fisher Scientific], and vortexed for 1 h at 37°C. Chloroacetamide (Sigma-Aldrich) was added for alkylation to a final concentration of 55 mM. Samples were vortexed for another hour at 37°C. One microgram

of trypsin was added, and digestion was performed for 8 h at 37°C. Peptide extraction was conducted with 90% ACN. The extracted peptide samples were dried down and solubilized in 5% ACN-0.2% formic acid (FA). The samples were loaded on a home-made C_{18}precolumn (0.3-mm inside diameter [i.d.] by 5 mm) connected directly to the switching valve. They were separated on a home-made reversed-phase column (150-µm i.d. by 150 mm) with a 56-min gradient from 10 to 30% ACN-0.2% FA and a 600-nl/min flow rate on a Nano-LC-Ultra-2D (Eksigent, Dublin, CA) connected to an Q-Exactive Plus (Thermo Fisher Scientific). Each full MS spectrum acquired at a resolution of 70,000 was followed by 12 tandem-MS (MS-MS) spectra on the most abundant multiply charged precursor ions. Tandem-MS experiments were performed using collision-induced dissociation (CID) at a collision energy of 25%. The data were processed using PEAKS 8.5 (Bioinformatics Solutions, Waterloo, ON) and a concatenated *Candida albicans* database. Mass tolerances on precursor and fragment ions were 10 ppm and 0.01 Da, respectively. Variable selected posttranslational modifications were carbamidomethyl (C), oxidation (M), deamidation (NQ), and phosphorylation (STY). The data were visualized with Scaffold 4.3.0 (protein threshold, 99%, with at least 2 peptides identified and a false-discovery rate [FDR] of 0.1% for peptides).

2.3.5 Cell imaging

In order to visualize DNA, cells were fixed in fresh 70% ethanol for 20 min, washed with sterile water, incubated in 1.0 µg/ml of 4′, 6′-diamidino-2-phenylindole dihydrochloride (DAPI; Sigma-Aldrich) for 20 min, washed twice with sterile water, and mounted on slides. For visualization of *TUB2-GFP* or *HTB1-GFP* in living cells, cultures were diluted into repressing or inducing medium, incubated for 8 h, centrifuged at 3000 rpm for 3 min, washed twice in water and mounted on regular slides. In order to determine cell viability, cells were stained with 10 µg/ml propidium iodide (Sigma-Aldrich) as previously described (Bachewich et al., 2003). Cells were imaged on a LeicaDM6000B microscope (Leica Microsystems Canada Inc., Richmond Hill, ON, Canada) equipped with a Hamamatsu-ORCA ER camera (Hamamatsu Photonics, Hamamatsu City, Japan) and the HCX PL APO 63x NA 1.40-0 oil or HCX PLFLUO TAR 100x NA 1.30-0.6 oil objectives. Differential Interference Contrast (DIC) optics, or epifluorescence

with DAPI (460nm), FITC (500nm) or Texas Red (615 nm) filters were utilized. Images were captured with Volocity software (Improvision Inc., Perkin-Elmer, Waltham, MA). Alternatively, time lapse imaging of Htb1p-GFP or Tub2p-GFP was performed by diluting overnight cultures of cells into inducing or repressing medium to O.D$_{600nm}$ 0.1 and incubating for 8 h. Cells were diluted 100-fold and transferred to an 8-well µSlide (Ibidi), containing similar media. Cells were imaged on a Nikon TI microscope equipped with a Photometrics Evolve 512 camera using a 63x objective (NA1.4) with the optical path defined for Differential Interference Contrast (DIC) and GFP (488nm ex/550nm longpass emission filters). Images were captured every 5 minutes for 3 hours using NIS Elements software.

2.3.6 Bioinformatic Analysis

Comparative analysis of the amino acid sequence of *ESP1* began with the alignment of its sequence alongside the sequences of Esp1 (*S. cerevisiae*), Cut1 (*S. pombe*), Sep-1 (*C. elegans*), and Espl-1 (*H. sapiens*) using ClustalW (Larkin et al., 2007). Aligned sequences obtained from ClustalW were further analyzed using ESPript software (Robert et al., 2014). Parameters used included sequence similarity (% similarity), alignment output layout (flashy, portrait), and a global score of 0.7, as set by the program. Analysis of the amino acid sequence of *EIP1* was completed as described for *ESP1*, using Pds1p (*S. cerevisiae*), Cut2p (*S. pombe*), IFY-1 (*C. elegans*), and PTTG1 (*H. sapien*), respectively. Three dimensional protein simulation was generated using the Protein Homology/Analogy Recognition Engine V 2.0 (PHYRE 2.0). Eip1 and Esp1 amino acid sequences were downloaded from the Candida Genome Database (http://www.candidagenome.org) and entered into PHYRE2.

2.4 Results

2.4.1 Depletion of Esp1p results in growth inhibition, bud enlargement and filamentation

We previously characterized the *C. albicans* APC/C cofactor Cdc20p and demonstrated that it is important for the metaphase-to-anaphase transition (Chou et al., 2011). However, its precise mechanisms of action remained unclear. Securins are targets of Cdc20p, but highly divergent in sequence (Bachmann et al., 2016). *C. albicans* lacks a sequence homologue of the few known securins in other ascomycetes. We hypothesized that a functional homologue may be revealed by identifying factors that co-purify with a protein that is known to bind securin. Since the interaction between Cdc20p and securin is transient (Hilioti et al., 2001), we focused on another conserved securin partner, separase. *C. albicans* contains a separase homologue, *ESP1/ORF19.3356* (http://www.candidagenome.org). Esp1p is similar to other separases with respect to the catalytic domain, armadillo (ARM) repeats and regions of disorder (Figure 2.1A), and is 23.2% identical and 40.5% similar to Esp1p from *S. cerevisiae.* A screen of *C. albicans* strains under control of the *TET* promoter demonstrated that *ESP1* was essential, and its repression resulted in filamentous growth (O'Meara et al., 2015). However, the functions of Esp1p, including a role in mitosis, remain unclear. We first addressed this question by creating a strain carrying a single copy of *ESP1* under control of the *MET3* promoter. When plated on solid repressing medium at 30°C for 24 h, the strain grew poorly and was filamentous. In contrast, normal growth was observed for wild-type cells on repressing medium, or both strains on inducing medium (Figure 2.1B). In liquid repressing medium, cells lacking Esp1p were predominantly large-budded by 5 h, and filamentous by 24 h. In contrast, normal yeast-form cells were observed under inducing conditions, and in the control strain in both media (Figure 2.1C, Table 2.1). Similar results were obtained when we repressed *ESP1* with the *TET* promoter using doxycycline (Figure S2.1), in agreement with previous results (O'Meara et al. 2015). In comparison, *S. cerevisiae* cells lacking Esp1p arrest as large doublets (Baum et al., 1998). Thus, absence of Esp1p in *C. albicans* impairs yeast cell division, resulting in bud enlargement and filamentation.
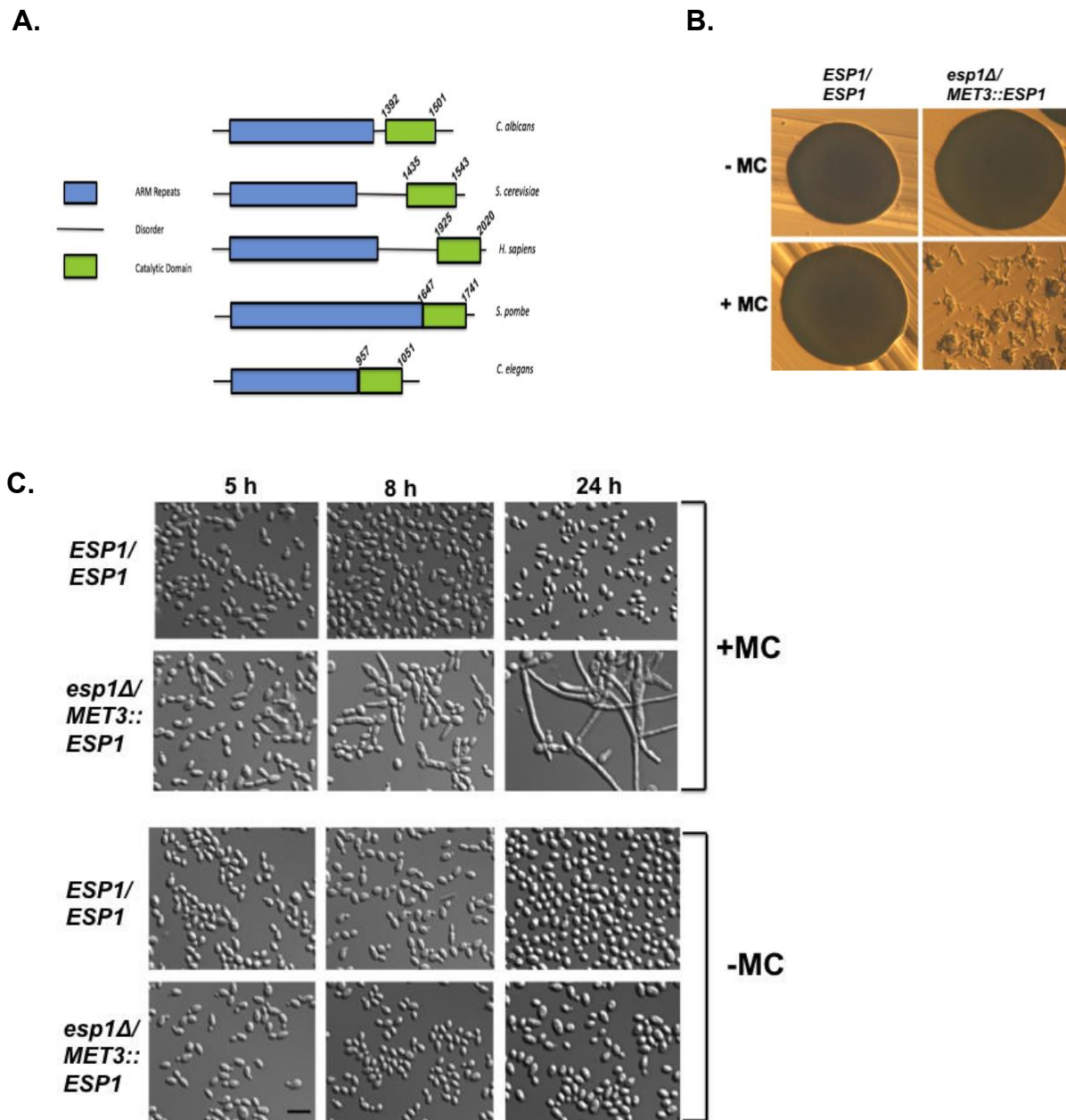
Figure 2.1. *C. albicans* **Esp1p is conserved in sequence and its depletion results in large bud formation, filamentation and growth inhibition.**

(A) Comparative analysis of amino acid sequences of separase homologues from *C. albicans* (Esp1p), *S. cerevisiae* (Esp1p), *H. sapiens* (Espl1p), S. *pombe* (Cut1p) and *C. elegans* (Sep-1p). ARM repeat domains are highlighted in blue, regions of disorder are represented by solid black lines, and catalytic domains are illustrated in green. Amino acid sequences were obtained from

the *Saccharomyces* Genome Database (https://www.yeastgenome.org), *Candida* Genome Database (http://www.candidagenome.org), WormBase (https://www.wormbase.org/#012-34-5), Pombase (https://www.pombase.org) and UniProt (https://www.uniprot.org), respectively. Sequences were analyzed with InterPro (https://www.ebi.ac.uk/interpro/) and information in Bachmann *et al.,* 2016. (B) Strains BH440 (*ESP1/ESP1*, *URA+HIS+)* and SS35 (*esp1::URA3/MET3::ESP1-HIS1*) were streaked onto solid repressing (+MC) or inducing (-MC) medium and incubated at 30°C for 24 h. (C) Overnight cultures of strains BH440 or SS35 were diluted into liquid -MC or +MC medium and incubated at 30°C for the indicated time periods. Bar: 10 μm.

Table 2.1. Number and distribution of nuclei in Esp1p-depleted cells[1]

+MC							
esp1Δ/MET3::ESP1 (n=155)	19.3	22.4	22.4	6.2	4.3	15.5	9.9
ESP1/ESP1 (n=161)	63.0	15.5	0	5.2	0	1.0	15.4
-MC							
esp1Δ/MET3::ESP1 (n=269)	70.9	12.0	0	2.6	0	0	14.5
ESP1/ESP1 (n=253)	57.0	24.0	0	3.1	0	0	19.4

[1]Percentage of cells showing the indicated patterns. Strains SS35 (*esp1::URA3/MET3::ESP1-HIS1*) and BWP17 (*ESP1/ESP1)* were incubated in -MC or +MC medium for 8 h, fixed and stained with DAPI.

2.4.2 Depletion of Esp1p prevents chromosome segregation and impairs spindle elongation

In *S. cerevisiae*, absence of functional Esp1p prevents chromosome segregation and proper spindle formation (McGrew et al., 1992). In order to determine whether *C. albicans* Esp1p has similar functions, the conditional *ESP1* and control strains were incubated in inducing or repressing medium for 8 h, fixed and stained with DAPI. In repressing medium, approximately 55% of cells depleted of Esp1p contained enlarged buds with a single mass of DNA near or within the bud neck. In contrast, this was observed in approximately 20% of cells under inducing conditions, or in wild-type cells in both media (Figure 2.2; Table 2.1). Similar results were obtained when *ESP1* was repressed with doxycycline in a strain carrying a single copy of *ESP1* under control of the *TET* promoter (Figure S2.1B). This localization reflects metaphase/early anaphase (Hazan et al., 2002) or movement of a pre-anaphase nucleus into the bud, which is associated with many conditions that arrest early mitosis in *C. albicans* (Bai et al., 2002; Bachewich et al., 2003, Bachewich et al., 2005; Bensen et al., 2005). Thus, Esp1p is important for chromosome segregation in *C. albicans*, consistent with it functioning as a separase.

Esp1p in *S. cerevisiae* is also important for spindle formation and elongation (Jensen et al., 2001). In order to determine whether *C. albicans* Esp1p influences spindle organization, *β*-tubulin was tagged with GFP (Hazan et al., 2002; Finley and Berman, 2005) in the *MET3::ESP1* conditional strain. After incubating in inducing medium for 7 h, 7.0 % (n=186) of cells contained short rod-like spindles characteristic of metaphase or early anaphase, while 8.1% contained elongated late anaphase spindles that spanned the mother and daughter cells (Figure 2.2). The remaining cells contained a spot of Tub2p-GFP signal, representing a spindle pole body in G1 phase, or an enlarged spot corresponding to a duplicated spindle pole body in S/G2 phase (Hazan et al., 2002). In repressing medium, 45.3% (n=148) of cells contained short rod spindles (Figure 2.2), and elongated late anaphase spindles were not observed. The remaining cells demonstrated a spindle pole body, at times more than one, cytoplasmic microtubules or abnormal microtubule organization. Notably, the Tub2p-GFP-tagged strain showed transient filamentation when transferred from overnight to fresh medium, irrespective of composition. However, by 7 h, the majority of cells in inducing medium were in a yeast form, while those in repressing medium

resembled the phenotype of the untagged conditional strain. The results suggest that Esp1p is important for spindle elongation.
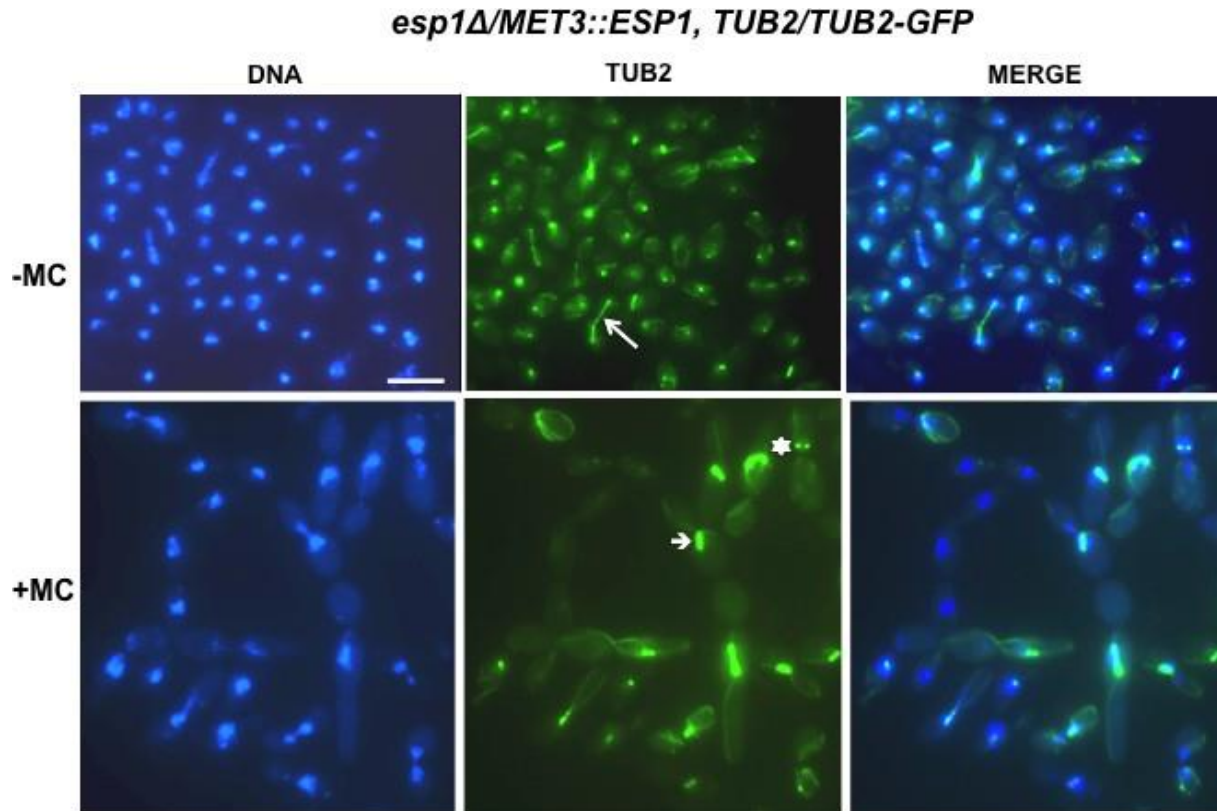
Figure 2.2. Depletion of Esp1p impairs chromatin separation.
Strain SS37 (*TUB2-GFP-ARG4/TUB2, esp1::URA3/MET3::ESP1-HIS1*) was incubated in inducing (-MC) or repressing (+MC) medium for 7 h, mounted and imaged live. An arrowhead denotes a G2-M/early anaphase spindle. The star denotes two spindle pole bodies within one cell. Bar: 10μm.

2.4.3 Identification of Esp1p-interacting factors reveals strong enrichment of an uncharacterized protein, Eip1p/Orf19.955p

If Esp1p is a separase, we reasoned that one of its interacting proteins may be a functional homologue of a securin. In order to test this hypothesis, strains carrying a single copy of *ESP1* tagged at the C-terminus with the Tandem Affinity Purification (TAP) tag composed of Protein A and calmodulin-binding peptide, separated by a Tobacco Etch Virus (TEV) protease cleavage site (Lavoie et al., 2008) were created. Since cells expressed the protein and grew at normal rates (data not shown), Esp1p-TAP was deemed functional. Affinity purification of Esp1p-TAP was performed in exponential-phase cells, but co-purifying proteins were not greatly enriched (data not shown). We thus tagged *ESP1* with TAP in a *CDC20* conditional strain to allow for a synchronized block in mitosis and potential enhancement of interacting proteins. Cells from the TAP-tagged and an untagged control strain were incubated in inducing medium overnight, diluted into repressing medium, incubated for 4 h prior to collection, and processed for LTQ-Orbitrap Elite with nano-ES analysis. After removal of peptides that were also present in the untagged strain, the data revealed strong enrichment of Esp1p, the phosphatase Cdc14p, and Orf19.955p, a previously uncharacterized protein with no close sequence homologues (Figure 2.3A, Table S2.4). Additional co-purifying peptides corresponded to proteins of varying function, including the heat shock protein *HSP70*, the filamentation regulator *DEF1,* and the endocytosis-associated protein *CTA3,* for example. Notably, homologues of proteins that interact with Esp1p in *S. cerevisiae*, including the protein kinase Cdc5p (Rahal and Amon, 2008a), the protein phosphatase regulatory subunit Cdc55p (Queralt and Uhlmann, 2008), the cohesin complex protein Mcd1p/Scc1p (Uhlmann et al., 2000), and the kinetochore-associated protein Slk19p (Rahal and Amon, 2008a) did not co-precipitate with *C. albicans* Esp1p. A previous report of phenotypes of *TET*-regulated strains of *C. albicans* indicated *ORF19.955* was essential and influenced filamentous growth (O'Meara et al., 2015), but its precise functions remain unclear. Since Orf19.955p was one of the most enriched Esp1p-interacting proteins and of novel sequence, we hypothesized that it may be a candidate functional securin. The remainder of the study focussed on this protein, which we call Esp1p-Interacting Protein1 (Eip1p).

To confirm that Eip1p and Esp1p physically interact, we performed co-immunoprecipitation. For this purpose, strains containing *EIP1* tagged at the C-terminus with the MYC epitope alone or in combination with *ESP1* tagged with the HA epitope were constructed. Immunoprecipitation of Esp1p-HA with anti-HA beads co-purified Eip1p-MYC (Figure 2.3B; full blot in Figure S2.2). Eip1p-MYC did not co-purify from cells with untagged Esp1p.Thus, Esp1p and Eip1p physically interact.

2.4.4 Eip1p is a novel, *Candida*-specific protein that contains putative KEN and Destruction Boxes

EIP1 encodes a potential protein of 325 amino acids and a predicted molecular weight of 36.4 kDa (http://www.candidagenome.org). A BLAST search of the *EIP1* sequence against all known organisms (http://blast.ncbi.nlm.nih.gov/Blast.cgi) or against fungi alone (http://www.yeastgenome.org) revealed that the only homologues were in several *Candida* species (Figure S2.3). Securins are not well conserved at the sequence level (Bachmann et al., 2016) and consistently, an alignment of Eip1p with securins Pttg1p, Pds1p or Cut2p showed little similarity (Figure S2.4). However, Eip1p has some features consistent with securins. It contains putative Destruction Boxes (Cohen-Fix et al., 1996) and a KEN box (Yamamoto et al., 1996a) (Figure 2.3C). Eip1p also contains one consensus phosphorylation site for CDK, similar to Pttg1p (Ramos-Morales et al., 2000), and numerous sites for polo-like kinase phosphorylation (Figure 2.3C). In contrast, Pds1p contains five phosphorylation sites for CDK (Agarwal and Cohen Fix, 2002). In order to explore the *EIP1* sequence further, a 3D structure analysis comparison using the program Phyre2 Protein Folder was performed. Intriguingly, the results demonstrated 50% confidence in alignment at a specific region with Pds1p, and some similarity in the predicted 3D structure based on this alignment (Figure 2.3D). Thus, Eip1p is a *Candida*-specific protein but has some features consistent with other securins.

A.

Orbitrap LC/MS analysis of putative Esp1p-interacting proteins

PROTEIN ID	Peptides	ORF	Identified Proteins
CAL0004160	63	ESP1	Putative caspase-like cysteine protease;
CAL0005886	24	CDC14	Protein involved in exit from mitosis and morphogenesis
CAL0003715	11	ORF19.955	UNCHARACTERIZED, protein of unknown function
CAL0000006	8	HSP70	Putative hsp70 chaperone;
CAL0005977	6	CDC19	Pyruvate kinase at yeast cell surface; Gcn4/Hog1/GlcNAc regulated;
CAL0000121	4	DEF1	RNA polymerase II regulator; role in filamentation, epithelial cell escape

B.
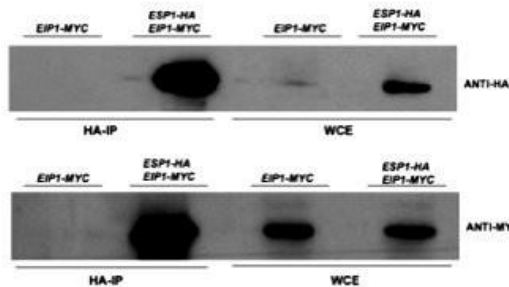
C.
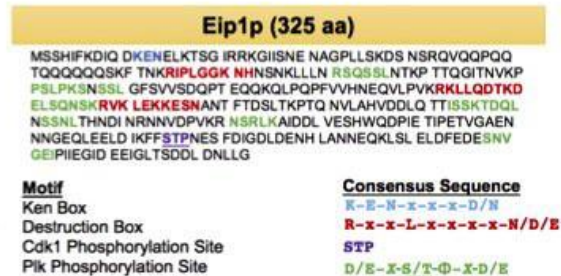
D.
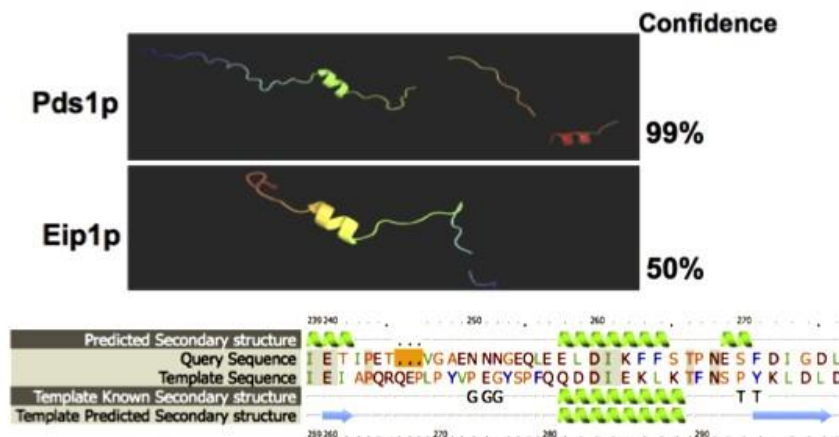
Figure. 2.3. Identification of Esp1p-interacting proteins reveals Eip1p/Orf19.955p.

(A) Select interacting factors of Esp1p-TAP identified by Orbitrap LC/MS analysis. (B) Co-immunoprecipitation demonstrates confirms a physical interaction between Esp1p and Eip1p. Western blots of whole cell extracts (WCE) and immune-precipitates (HA-IP) of strains SS22 (*eip1::URA3/EIP1-MYC-HIS1*) and SS29 (*EIP1/EIP1-MYC-HIS1, ESP1/ESP1-HA-URA3*), using anti-HA agarose (HA-IP). Blots were incubated with anti-MYC or anti-HA antibody. (C) Eip1p

34

amino acid sequence (Candida Genome Data base; http://www.candidagenome.org), with motifs indicated. (D) 3D protein simulation using PHYRE 2.0, demonstrating some similarity at a specific region with Pds1p from *S. cerevisiae*. Bottom portion represents the region of amino acid sequence homology between the template strain (Pds1p) and query strain (Eip1p). Green coils and blue arrows represent regions of α-helices and β-pleaded sheet arrangements, respectively. Polar properties of the protein sequences are shown in colored amino acids. Secondary structures are represented by the number of "G" and "T" segments present, where G indicates a 3-turn α-helix and T represents a hydrogen-bonded turn.

2.4.5 Depletion of Eip1p impairs cell growth and morphology

In order to address the function of Eip1p, we created a conditional strain containing a single copy of the gene under control of the *MET3* promoter. When plated on solid repressing medium at 30°C for 24 h, growth was severely restricted. Only a few small colonies formed, in contrast to the situation with wild-type cells or when both strains were plated on inducing medium (Figure 2.4A). In order to explore the growth defect further, serial dilutions of strains were spotted onto plates, and incubated for 24, 48 or 72 h. The *ESP1* conditional strain was included for comparison. By 72 h, growth of the *EIP1* conditional strain remained impaired relative to wild-type cells on repressing medium (Figure 2.4B). However, a low level of colony growth was observed. Intriguingly, this was variably more than that of Esp1p-depleted cells. With the *TET*-regulated strains, Eip1p vs. Esp1p-depleted cells consistently demonstrated some residual growth (8/8 trials) (Figure S2.5A, B). This result prompted an attempt to create a strain lacking both alleles of *EIP1* (*eip1::URA3/eip1::HIS1*). From three separate transformations yielding twenty-three total transformants, three were positive for replacement of *EIP1* alleles with *HIS1* and *URA3* markers, and absence of *EIP1* (Figure S2.6A). The strains grew very slowly (Figure S2.6B) and resembled Eip1p-depleted cells (Figure S2.6C). We cannot rule out the possibility of secondary mutations or chromosomal alterations that permit growth in *eip1Δ/Δ* strains, but it is noteworthy that the strains were recovered from independent transformations. Weak growth could reflect variable accumulations of abnormal events that eventually prevent proliferation. In comparison, securins from *S. pombe* and *D. melanogaster*, for example, are essential (Funabiki et al.,1996, Jager et al., 2001), as well as *PDS1* of *S. cerevisiae* at 37°C, where cells arrest in a large-budded form due to a temperature-sensitive defect at the G1/S transition that affects spindle elongation and Esp1p localization into the nucleus (Yamamoto et al., 1996a; Jensen et al., 2001; Agarwal & Cohen-Fix, 2002). At lower temperature, however, *pds1Δ* cells are viable but chromosome loss is frequent and many cells cannot form colonies (Yamamoto et al., 1996a; Liang et al., 2013). Eip1p-depleted cells did not show any temperature sensitivity (data not shown) and the defects were more severe than those of *pds1Δ* cells at permissive temperature. In order to determine the dynamics of Eip1p depletion on cell viability, the proportions of cells that stained with propidium iodide during a time course were determined.

After 5, 8 or 24 h in repressing medium, 11.3 (n=194), 9.5 (n=158) or 30.0% (n=166) of Eip1p-depleted cells stained with propidium iodide, compared to 2.9 (n=171), 1.3 (n=157) or 1.5% (n=198) of cells in inducing medium. Many more Eip1p-depleted cells were clearly inviable at 24 h but lacked cytoplasm, which precluded staining (Figure S2.7). Thus, Eip1p is critical for growth, but its absence does not immediately lead to death for all cells.

In order to investigate the phenotype of cells lacking Eip1p, the *EIP1*-conditional and control strains were incubated in liquid medium at 30°C for set times. After 5 h in repressing medium, Eip1p-depleted cells were in various stages of yeast cell budding (Figure 2.4C). By 8 h, a pleiotropic phenotype was observed, including enlarged single yeast cells, chains of yeast, or pseudohyphae (Figure 2.4C, Table 2.2). When Eip1p was depleted using the *TET* promoter, similar results were obtained (Figure S2.5C). The results suggest that Eip1p is also important for proper yeast cell morphology.

A.

B.

C.
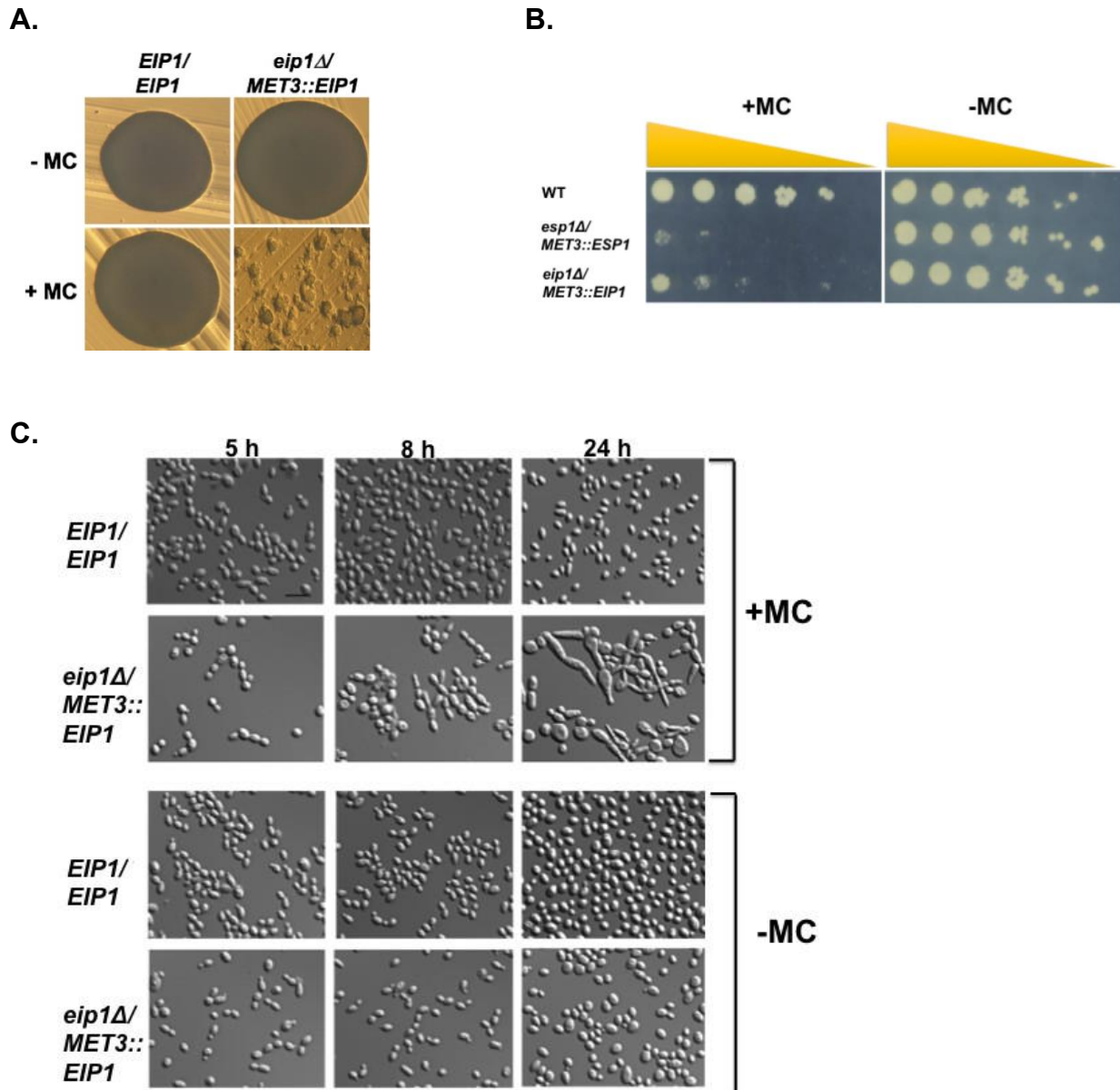
Figure 2.4. Depletion of Eip1p in yeast impairs growth and results in a pleiotropic phenotype including cell enlargement, formation of chains of cells and pseudohyphae.
(A)Strains BH440 (*EIP1/EIP1, URA3+HIS1+)* and SS25 (*eip1::URA3/MET3::EIP1-HIS1*) were streaked onto repressing (+MC) or inducing (-MC) solid medium and incubated at 30°C for 24 h. (B) Strains SS25, BH440 and SS35 (*esp1::URA3/MET3::ESP1-HIS1*) serial diluted onto solid inducing or repressing medium and incubated for 72 h at 30°C. (C) Overnight cultures strains

BH440 and SS25 were incubated at 30°C, diluted into inducing (-MC) or repressing (+MC) medium and incubated for the indicated time periods. Bar: 10 μm.

Table 2.2. Number and distribution of nuclei in Eip1p-depleted cells[1]

							[2]	[3]	[4]
+MC									
eip1Δ/MET3::EIP1 (n=242)	51.2	14.5	11.6	3.7	19.0		20.7	5.0	18.2
EIP1/EIP1 (n=279)	77.4	11.1	1.8	9.7	0		12.5	0	5.7
-MC									
eip1Δ/MET3::EIP1 (n=269)	75.1	17.5	1.9	5.2	0		5.2	0	7.4
EIP1/EIP1 (n=253)	85.4	5.5	4.7	4.3	0		12.6	0	2.4

[1]Percentage of cells showing the indicated patterns. Strains BH440 (*EIP1/EIP1, URA3+HIS1+*) and SS25 (*eip1::URA3/MET3::EIP1-HIS1*) were incubated in +MC or -MC medium for 8 h, fixed, and stained with DAPI.
[2] Proportion of cells lacking visible DAPI staining
[3]Proportion of cells containing more than one DAPI-staining body
[4] Proportion of cells with abnormal DAPI-stained organization

2.4.6 Absence of *EIP1* influences chromosome organization

Absence of essential securins, such as Cut2p, prevents chromosome segregation and phenocopies separase mutants, due to the positive and negative effects of securin on separase (Funabiki et al., 1996; Hellmuth et al., 2015). In contrast, chromosomes segregate successfully and initiate anaphase in a timely fashion in the absence of *S. cerevisiae* Pds1p at lower temperature, since it is not essential under these conditions. However, an increase in chromosome loss was noted (Yamamoto et al., 1996; Alexandru et al., 1999; Liang et al., 2013). At restrictive temperature when *PDS1* is essential, the majority of *pds1Δ* cells are large-budded with an unseparated mass of DNA. Spindles cannot elongate properly, the synchrony of chromatid pair separation is reduced, and some cells are multinucleate, suggesting precocious mitotic exit (Yamamoto et al., 1996a; Ciosk et al., 1998; Holt et al., 2008; Hatano et al., 2016). In order to determine whether Eip1p influences chromosome segregation, the *EIP1* conditional and wild-type strains were incubated in inducing or repressing medium for 8 h, fixed, and stained with DAPI. Under inducing conditions, the *EIP1*-conditional strain demonstrated normal DNA patterns including single compacted masses per cell compartment, a stretched organization within the bud neck indicative of anaphase, or two separate DNA masses at opposite poles of mother and daughter cells, reflecting late anaphase and/or mitotic exit. Similar patterns were observed in wild-type cells under inducing and repressing conditions (Figure 2.5A). In contrast, Eip1p-depleted cells demonstrated numerous defects, including irregular shaped, enlarged DNA masses, more than one DNA mass per cell compartment, and either small fragments or no DNA in some other cells (Figure 2.5A, Table 2.2). Further, more cells showed an anaphase-like organization of chromosomes, where DNA was localized within the bud neck, suggesting a delay in mitosis (Table 2.2). Notably, most cells contained DNA, indicating that chromosome segregation was not homogeneously inhibited. Similar defects were detected when Eip1p was depleted using the *TET* promoter (Figure S2.5C), when both alleles were deleted (Fig. S2.6C) or in Eip1p-depleted cells at 37°C (data not shown).

In order to investigate the effects of depleting Eip1p on chromosome segregation in living cells, Histone *HTB1* was tagged with green fluorescent protein (GFP) (Sherwood and Bennett, 2008) in the *EIP1*-conditional strain. Cells were incubated in inducing or repressing medium for

8 h, and analysed live with microscopy. Under inducing conditions, cells showed normal DNA patterns as described for DAPI-stained cells. However, in repressing medium, pleiotropic effects were observed, including large irregular-shaped masses of DNA, cells containing two DNA masses, or cells with fragments or no detectable DNA (Figure 2.5B,C), similar to fixed cells stained with DAPI. We next performed time-lapse microscopy to analyse the dynamics of chromosome segregation. Cells incubated in inducing medium were transferred to either fresh inducing or repressing medium for 5 h, mounted on an 8-well µSlide and recorded for 3 h, with images captured every 5 min. In inducing medium, a representative unbudded cell with a single mass of Htb1p-GFP signal demonstrated bud formation followed by anaphase, represented by DNA stretching through the bud neck, by 75 min. This was followed by complete separation of signal between mother and daughter cell by 90 min (Figure 5Da). In repressing medium, a representative large budded cell with a large mass of DNA within one compartment did not demonstrate any segregation during the length of the time course (Figure 2.5Db), while another cell demonstrated uneven separation of Htb1p-GFP signal within the mother cell (Figure 2.5Dc). In another example, an unbudded cell within a cell group demonstrated a stretching of Htb1p-GFP signal and separation into two masses within 60 min, and remained separated for the duration of the time course (Figure 2.5Dd, arrow). Within a separate cell group, a small-budded cell demonstrated stretching of the Htb1p-GFP signal by 45 min within the mother cell (Figure 2.5De, bottom arrow). This was oriented perpendicular to the mother/bud axis, but subsequently rearranged parallel to the axis and separated into two masses, one of which entered the small bud 120 min following the initial stretching of Htb1p-GFP signal. Within this same group, a budded cell demonstrated anaphase by 30 min and chromosome segregation between mother and bud (Figure 2.5De, top arrow). However, 60 min after anaphase, the single Htb1p-GFP mass within the mother cell migrated into the bud, then translocated back to the mother cell 15 min later. A different cell within this group appeared to lack Htb1p-GFP signal (Figure 2.5De, bottom cell), and imploded 90 min into the time course. Thus, Eip1p-depleted cells can segregate chromosomes, but variably show multiple defects as well as abnormal nuclear movements, supporting a role for Eip1p in these processes.

A.

eip1Δ/MET3::EIP1   EIP1/EIP1

+MC

-MC

C.

eip1Δ/MET3:: EIP1, HTB1/HTB1-GFP

■ +MC
■ -MC

B.

eip1Δ/MET3::EIP1, HTB1/HTB1-GFP

HTB1   DIC   MERGE

-MC

+MC

D.

-MC

+MC
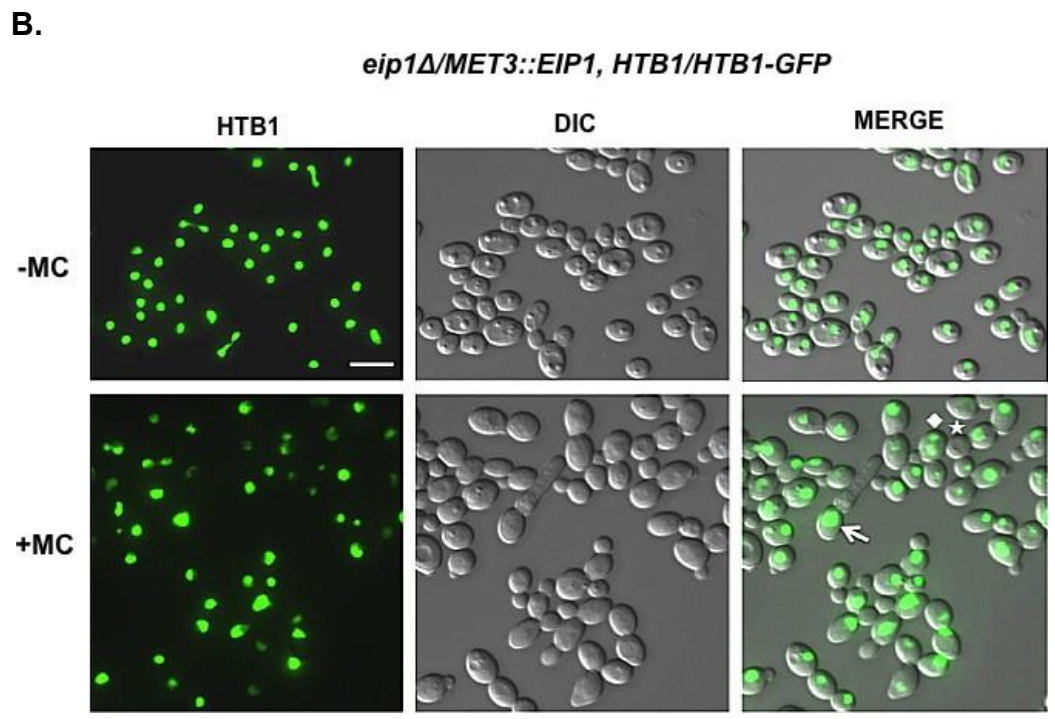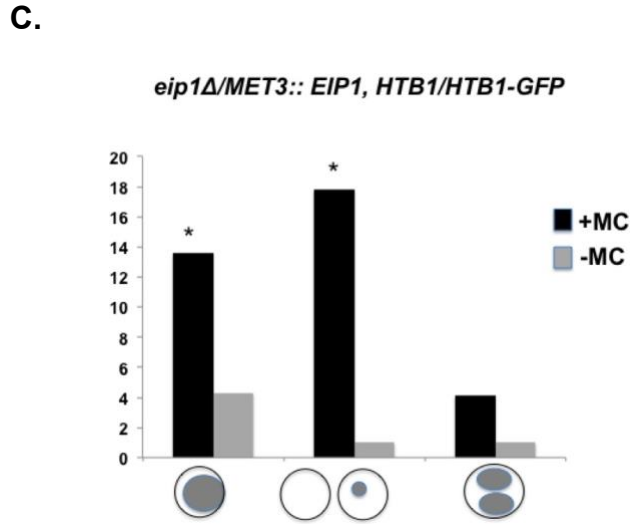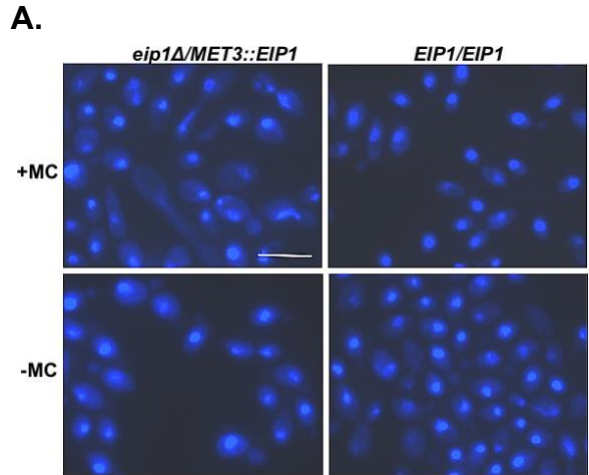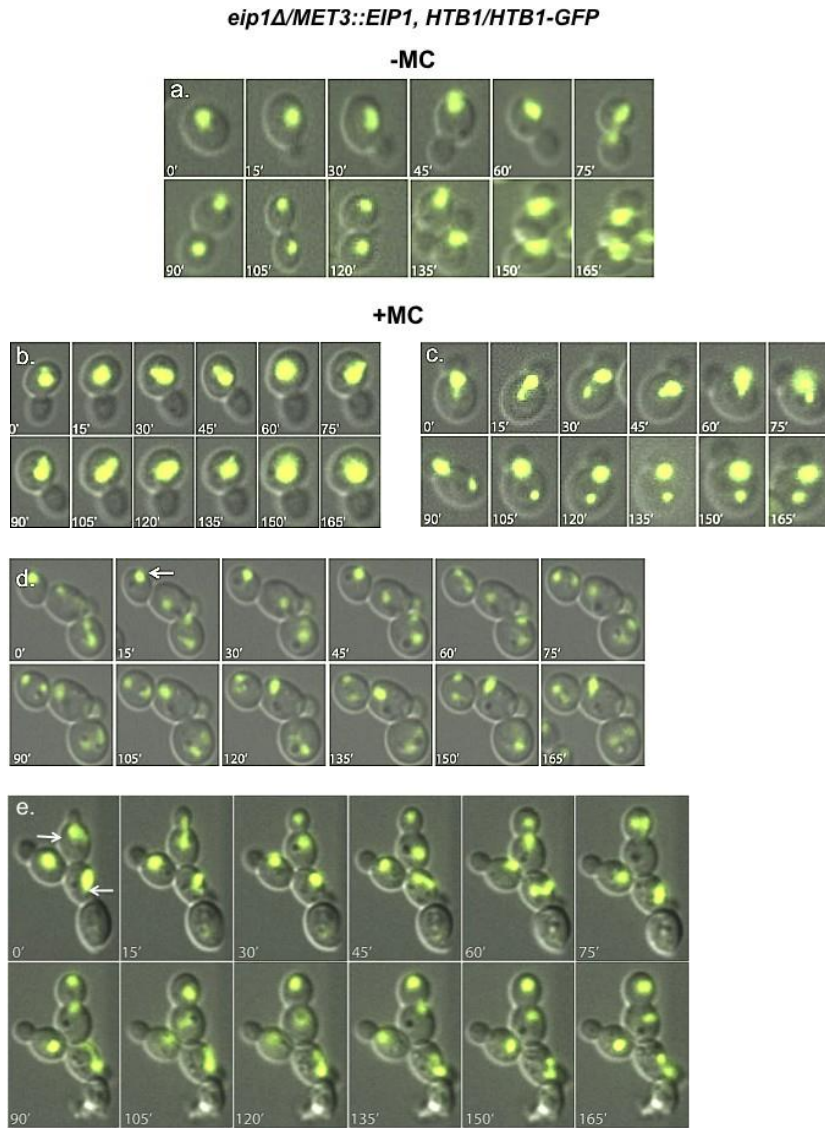
Figure 2.5. Cells depleted of Eip1p can segregate chromosomes but show multiple defects.
(A) Strains SS25 (*eip1::URA3/MET3::EIP1-HIS1*) and BWP17 (*EIP1/EIP1*) were incubated in inducing (-MC) or repressing medium (+MC) for 8 h, fixed and stained with DAPI. (B) Strain SS44 (*HTB1/HTB1-GFP-ARG4, eip1::URA3/MET3::EIP1-HIS1)* was incubated in −MC or +MC medium for 7 h, mounted and imaged live. Abnormal features including two DNA masses within one cell (diamond), empty cell compartments (star) and large DNA masses (arrow) are indicated. (C) Proportions of cells in (B) containing enlarged DNA masses, fragments or no DNA, or two DNA masses within a single cell compartment. Sample sizes include 286 (+MC) and 277 (-MC)

cells. Significance was measured with a Fisher Exact Test, 2-tailed, where * indicates p<0.05. (D). Time-lapse imaging of strain SS45 in -MC or +MC medium. Images were captured every 5 min for 180 min. Bars: 10 μm.

2.4.7 Absence of *EIP1* affects spindle orientation and disassembly

Since defects in chromosome segregation can reflect deregulated spindle function, we next analysed microtubules by tagging β-tubulin with GFP in the Eip1p-conditional strain. Cells were incubated in either inducing or repressing medium and imaged live (Figure 2.6A) or fixed and stained with DAPI (Figure 2.6B,C). In inducing medium, 15.9 % and 3.4% (n-387) of cells showed short bar-like spindles, characteristic of metaphase/early anaphase, or elongated late anaphase spindles that spanned the mother daughter cells, respectively. The remaining cells contained spindle pole bodies (Figure 2.6A). In repressing medium, however, approximately 45% (n= 309) of Eip1p-depleted cells contained mitotic spindles, where 29.4% were short bars and 14.6% were elongated (Figure 2.6A-C). Some spindles appeared normal while others were abnormal in shape or misoriented with respect to the mother/bud axis. Abnormal microtubule structures were also observed (Figure 2.6A, B). Some Eip1p-depleted cells also contained single DNA masses with more than one spindle pole body or short spindle, or demonstrated uneven chromosome segregation (Figure 2.6B, C). In order to investigate spindle dynamics, time-lapse imaging of Tub2p-GFP was performed, as described for Htb1p-GFP. Under inducing conditions, the length of time that cells maintained a short bar spindle, indicative of metaphase or early anaphase, was 9.1 ± 0.8 min (n=17; s.e.m.), while elongated late anaphase spindles were maintained for 7.9 ± 0.8 min (n=17; s.e.m.) (Figure 2.6Da). The timing is approximate due to the 5 min intervals for image capture. In contrast, a sample of cells under repressing conditions maintained early anaphase spindles for 98.3 ± 16 min (n=15; s.e.m.), or elongated late anaphase spindles for 59.2 ± 16.6 min (n=12; s.e.m.). Variation within these groups was great, however, with some cells maintaining spindles for the duration of the time course (Figure 2.6Db) and others demonstrating normal timing. We also noted random and severe oscillations of some spindles or spindle pole bodies, at times back and forth between the mother cell and buds, as described for Htb1p-GFP (Figure 2.6Db,c). In comparison, *pds1Δ* cells of *S. cerevisiae* at

permissive temperature form spindles and have normal cell cycle progression and DNA content (Yamamoto et al., 1996a). At restrictive temperature, spindles frequently fail to elongate or retract back to shorter structures (Yamamoto et al., 1996a; Holt et al., 2008), due to the temperature-sensitive step at G1/S that requires Pds1p for localizing Esp1p to the nucleus and spindle elongation (Jensen et al., 2001; Agarwal and Cohen Fix, 2002). Excess spindle pole bodies are also present since cells do not arrest the cell cycle. However, if *pds1Δ* cells are shifted to 37°C after S phase, spindles can elongate (Yamamoto et al., 1996a). Thus, Eip1p is not essential for spindle formation, but its absence can influence spindle behavior and microtubule organization.

A.

eip1Δ/MET3::EIP1, TUB2/TUB2-GFP

B.

eip1Δ/MET3::EIP1, TUB2/TUB2-GFP

C.

eip1Δ/MET3::EIP1, TUB2/TUB2-GFP
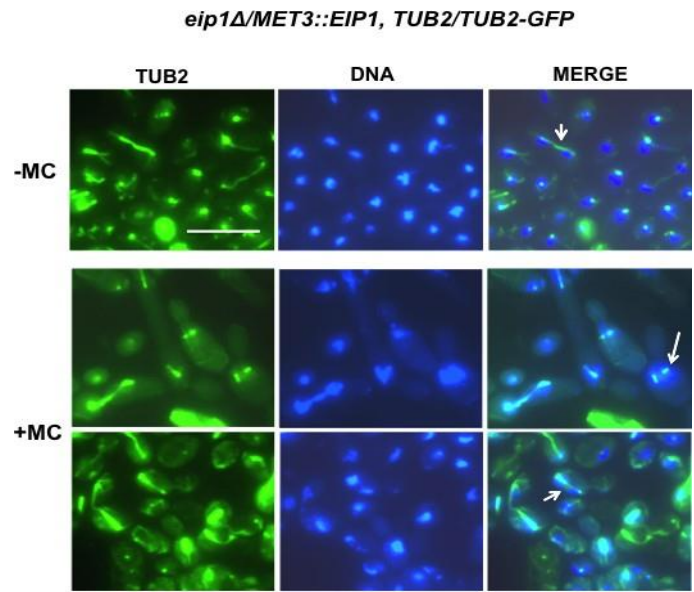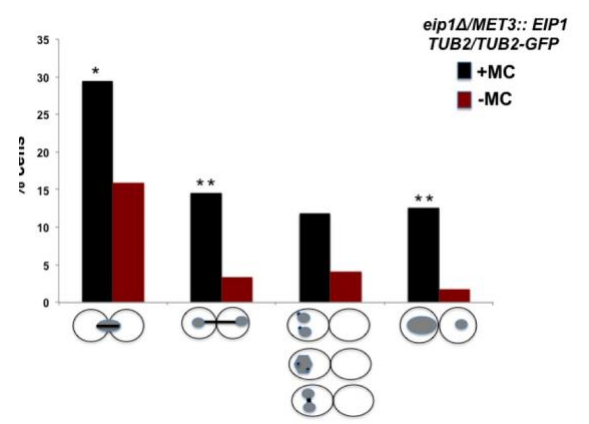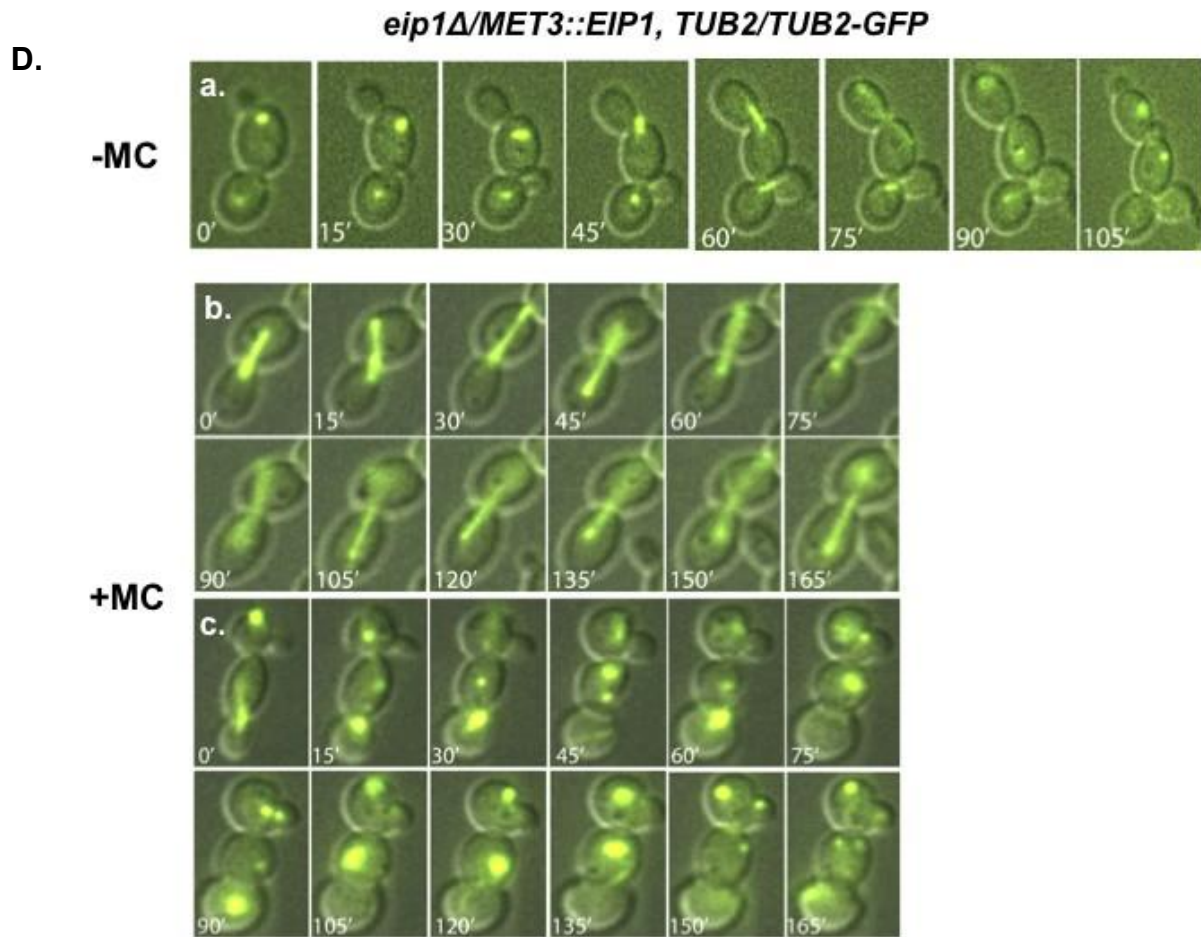
Figure 2.6. Eip1p depletion results in a higher proportion of cells with mitotic spindles.
(A) Strain SS38 (*TUB2-GFP-ARG4/TUB2, eip1::URA3/MET3::EIP1-HIS1*) was incubated in inducing (-MC) or repressing medium (+MC) for 7 h, and imaged live. (B). Strain SS38 was prepared as in (A), then fixed and stained with DAPI. Late anaphase spindles are designated by short arrows. The short arrow in the +MC condition also highlights a misoriented spindle and uneven chromosome segregation. The long arrow indicates two short spindles in a single DNA mass. (C) Proportions of cells in (B) with short spindles at the bud neck; elongated late anaphase spindles that spanned the mother daughter cells; one DNA mass with two spindle pole bodies, two DNA masses in the mother cell connected by a spindle or with separate spindle pole bodies; or uneven segregation of DNA between mother and daughter cell. Sample sizes include 387 (+MC) and 309 (-MC) cells. Significance was determined with a Fisher Exact Test, 2-tailed, with $p < 0.05$ (*), $p < 0.01$ (**). (D) Time-lapse imaging of strain SS38 showing normal spindle
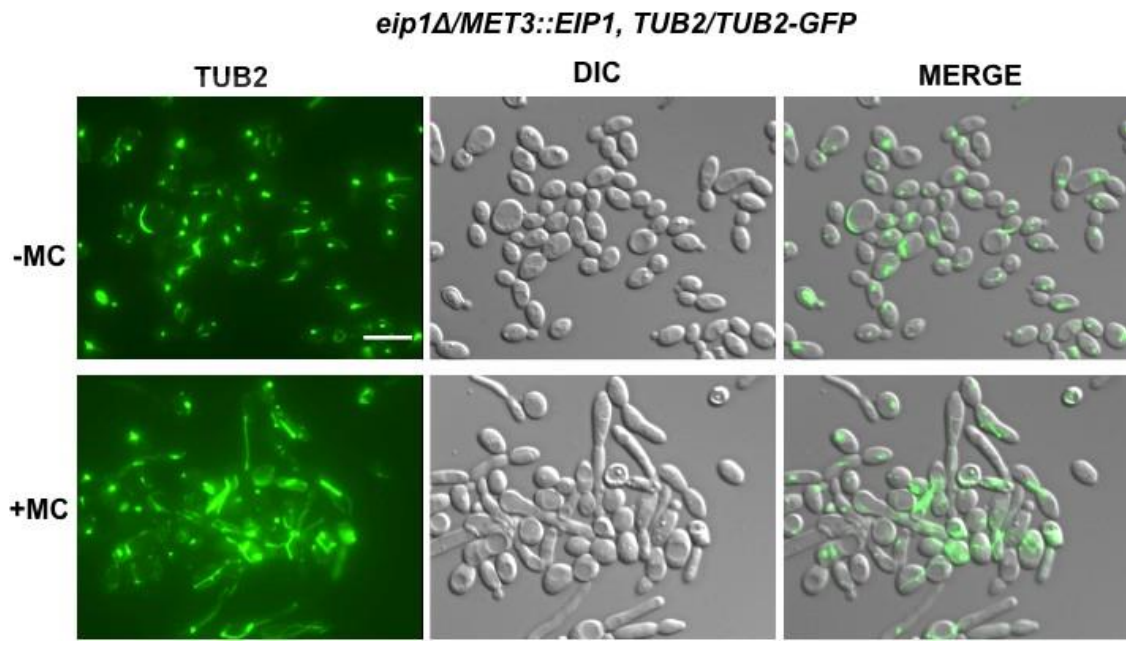
formation and disassembly in -MC medium, or defects in +MC medium. Images were captured every 5 min for 180 min. Bars: 10 μm.

2.4.8 Eip1p is significantly reduced when cells are blocked in mitosis through depletion of Cdc5p, but not Cdc20p

Securins are regulated in part through APC/C-dependent degradation. In *S. cerevisiae,* for example, the securin Pds1p is targeted for degradation at the metaphase-to-anaphase transition by the APC/C in association with its cofactor Cdc20p (Cohen-Fix et al., 1996; Funabiki et al., 1996). Residual Pds1p is subsequently targeted by Cdh1p-dependent APC/C activity to permit mitotic exit (Hatano et al., 2016). Pds1p is thus unstable and significantly reduced in late stages of mitosis or G1 phase. Although the APC/C has not been extensively investigated in *C. albicans*, cofactors Cdc20p and Cdh1p were demonstrated to be important for mitotic progression. Depletion of Cdc20p initially resulted in an early mitotic arrest, but most cells subsequently progressed to late mitosis with two separate DNA masses and elongated spindles (Figure 2.7B) (Chou et al., 2011). If Eip1p acts as a securin, it may demonstrate APC/C-dependent modulation in mitosis. In order to test this hypothesis, Eip1p was tagged with the TAP epitope in a *CDC20-*conditional strain (Chou et al, 2011). This and a wild-type strain carrying a TAP-tagged copy of Eip1p were incubated in inducing or repressing medium for set times and processed for Western Blotting. In repressing medium, Eip1p was induced in half of the trials (n=4) at 3 h and two-thirds of the trials (n=3) at 6 h, with levels ranging from 1.3 to 1.7 times that of Eip1p-TAP in the control strain (Figure 2.7A). In inducing medium where cells overexpressed *CDC20,* Eip1p-TAP was mildly reduced in three-quarters of the trials at 3 h and half the trials at 6 h, with values ranging from 0.1 to 0.8 times that of the control strain in the same medium (Figure 2.7A). Pds1p is also reduced or enriched upon overexpression or depletion, respectively, of Cdc20p, in *S. cerevisiae* (Visintin et al., 1997; Raspelli et al., 2015), although the effects are more pronounced. Variability in Eip1p responses may reflect heterogeneity in the *C. albicans* Cdc20p-depleted cell phenotype (Chou et al., 2011), and/or other factors that contribute to Eip1p regulation.

A.

B.B

cdc20Δ/MET3::CDC20, EIP1-TAP/EIP1

+MC 6 h

C.C

D.D.

cdc5Δ/MET3::CDC5, EIP1-TAP/EIP1

+MC 6 h
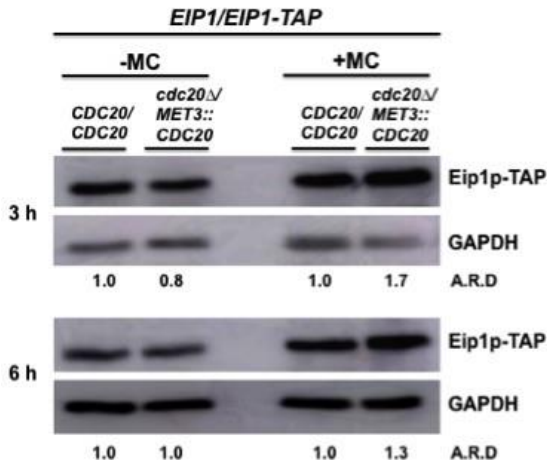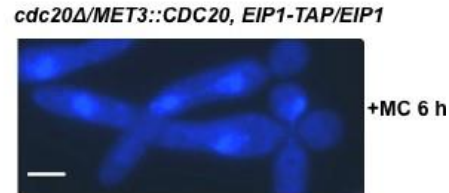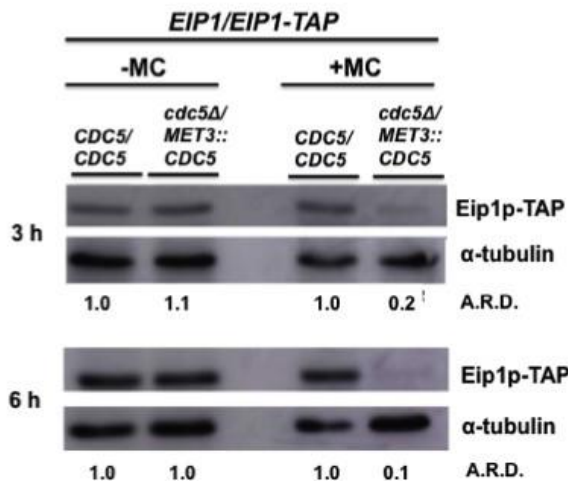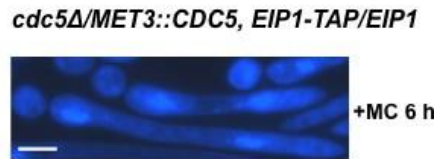
Figure 2.7. Eip1p is reduced in cells depleted of Cdc5p, but not Cdc20p.

(A) Strains SS40 (*eip1::URA3/EIP1-TAP-ARG4*) and SS41 (*eip1::URA3/EIP1-TAP-ARG4, cdc20::URA3/MET3::CDC20-HIS1*) were incubated in inducing (-MC) or repressing (+MC) medium. Samples were collected at 3 or 6 h and processed for Western blot analysis using anti-TAP antibody and anti-GAPDH antibodies. Adjusted relative densities (A.R.D) of Eip1p-TAP bands were determined using strain SS40 in either -MC or +MC medium as a reference. (B) Strain SS41 incubated in +MC medium for 6 h, fixed, and stained with DAPI. (C) Strains SS40 and SS43 (*EIP1/EIP1-TAP-URA3, cdc5::hisG/ MET3::CDC5-ARG4*) were incubated and analyzed with Western blotting as described in (A), with the exception of using anti-α tubulin

antibody as a loading control. (D) Strain SS43 was incubated in +MC medium for 6 h, fixed, and stained with DAPI. Bars: 5 μm.

In order to further investigate the hypothesis that Eip1p is regulated in part by degradation during mitosis, Eip1p was tagged with the TAP epitope in a strain carrying a single conditional copy of another mitotic regulator, the polo-like kinase *CDC5*. In *S. cerevisiae*, Pds1p is not affected by *CDC5* overexpression, but is reduced in the absence of Cdc5p due to the fact that cells arrest past the point when most Pds1p is degraded (Charles et al., 1998). In *C. albicans*, Cdc5p depletion results in a phenotype similar to that described for Cdc20p depleted cells (Figure 2.7D) (Bachewich et al., 2003; 2005; Chou et al., 2011). However, the precise initial arrest point in either condition remains unclear. When cells were incubated in inducing medium to overexpress *CDC5*, the level of Eip1p was similar to that of the control strain (Figure 2.7C). However, upon depletion of Cdc5p in repressing medium, Eip1p-TAP was significantly and consistently reduced (Figure 2.7C). Thus, Eip1p is turned over during a block in mitosis induced by Cdc5p depletion, but this does not occur in the absence of Cdc20p. This suggests that Cdc20p may be required in part for Eip1p degradation in mitosis, similar to other securins.

2.4.9 Eip1p levels increase in response to MMS or HU treatment

The securin Pds1p in *S. cerevisiae* is essential for preventing anaphase initiation and mitotic exit in response to *γ*-irradiation-induced DNA damage in G2 or spindle defects. It is stabilized by phosphorylation in a Mec1p and Chk1p-dependent manner, and Mad2p-dependent sequestration of Cdc20p, respectively (Yamamoto et al., 1996b; Cohen-Fix and Koshland, 1997; Sanchez et al., 1999; Tinker -Kulberg and Morgan, 1999; Palou et al., 2017). Pds1p is also stabilized in response to hydroxyurea (HU) or methyl methanesulfate (MMS), but this is not sufficient to block cell cycle progression; *pds1Δ* cells remain arrested due to Swe1p and Rad53p-mediated down-regulation of mitotic CDK activity (Palou et al., 2015, 2017). In order to determine whether Eip1p is important for a mitotic arrest during the response to DNA damage, cells containing Eip1p tagged with the MYC epitope were incubated in the presence or absence of MMS for 5 h, and processed for Western blotting. The mobility of Eip1p-MYC was not grossly affected by MMS, unlike the situation for Pds1p. We cannot rule out the possibility of undetectable phosphorylation under the current conditions, but it is noteworthy that Eip1p has only one CDK consensus phosphorylation site, vs. five in Pds1p (Agarwal and Cohen Fix, 2002). However, Eip1p levels were significantly enriched in response to MMS (Figure 2.8A). This may be due to a high proportion of cells blocked in early mitosis in response to MMS (Wang et al., 2012; Figure 2.8C), or stabilization or induction of Eip1p. When the experiment was repeated with the exception of using 200 mM hydroxyurea (HU), Eip1p levels were also enhanced (Figure 2.8B). Thus, Eip1p is strongly enriched in response to DNA damage and replication stress.

If enrichment of Eip1p is important for mediating the MMS or HU-induced arrest in mitosis, then absence of Eip1p may allow cells to progress through the block. To test this hypothesis, the *EIP1* conditional strain carrying a copy of *TUB2* tagged with GFP was incubated in inducing or repressing medium for 2.5 h, transferred to fresh media containing 0.02% MMS or 200 mM HU, incubated for 5 h, then fixed and stained with DAPI. In the presence of Eip1p, the majority of MMS-treated cells demonstrated a very short spindle and localization of DNA near the bud neck (Figure 2.8C,D). In the absence of Eip1p, however, the proportion of cells with this pattern was greatly reduced, and more cells were in later stages of mitosis (Figure 2.8C,D). This contrasts to the situation in *S. cerevisiae Δpds1* cells, which remain arrested when treated with

MMS or HU due to Swe1p and Rad53p-mediated down-regulation of mitotic CDK (Palou et al., 2015, 2017). Similar results were obtained when *C. albicans* cells were alternatively treated with HU (Figure 2.8E,F). The results suggest that Eip1p may be critical for blocking anaphase under conditions of MMS or HU-induced DNA stress, providing additional support for Eip1p acting as a securin, and underscoring unique features of the mitotic regulatory networks in *C. albicans*.

A.

EIP1/EIP1-MYC

30 µg		10 µg		5 µg		
−	+	−	+	−	+	MMS

Eip1p-MYC

PSTAIRE

| 1 | 1.8 | 1 | 2.1 | 1 | 1.4 | A.R.D |

B.

EIP1/EIP1-MYC

30 µg		10 µg		5 µg		
−	+	−	+	−	+	HU

Eip1p-MYC

PSTAIRE

| 1 | 2.2 | 1 | 5.1 | 1 | 3.3 | A.R.D |

C.

eip1Δ/MET3::EIP1
TUB2/TUB2-GFP
+ MMS

■ −MC
■ +MC

D. *eip1Δ/MET3::EIP1, TUB2/TUB2-GFP +MMS*

TUB2	DNA	MERGE

−MC

+MC

53

E.

F.
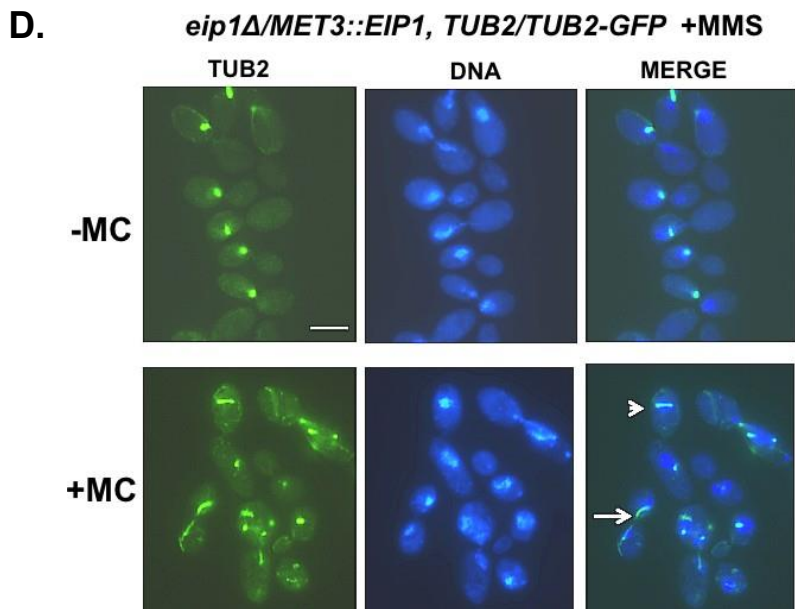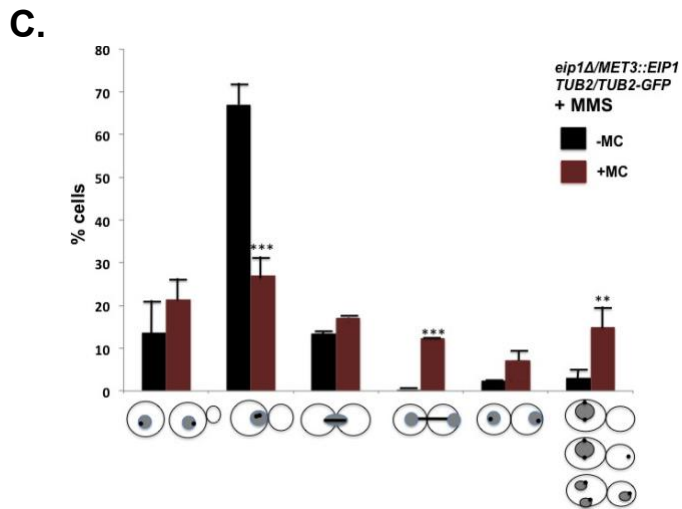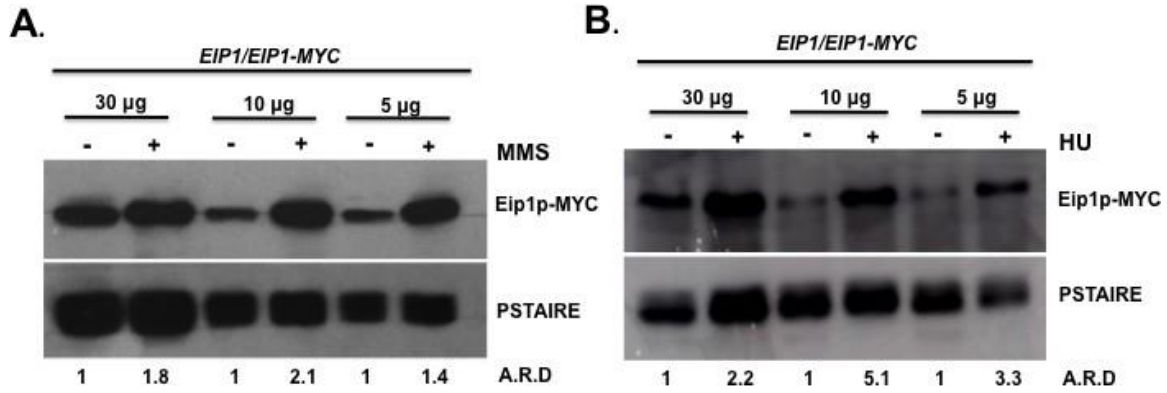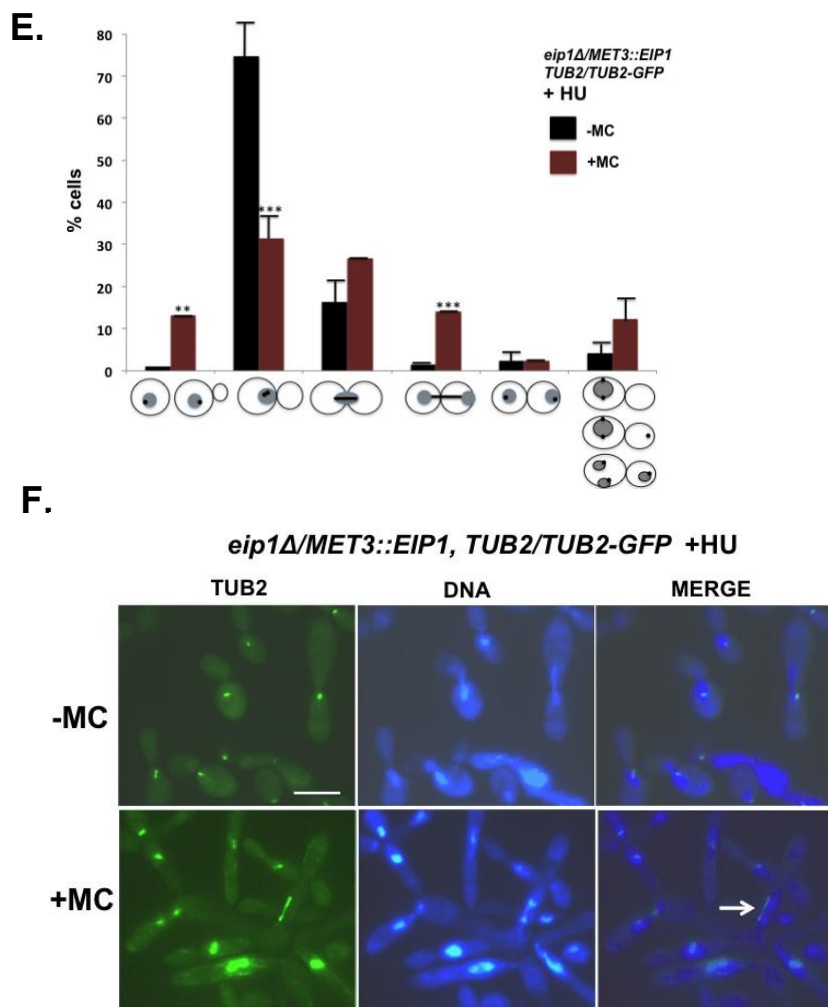
Figure 2.8. Eip1p is enriched in response to MMS or HU treatment, and its depletion permits cells to escape an MMS or HU-induced metaphase block.

(A, B) Strain SS22 (*eip1::URA3/EIP1-MYC-HIS1*) was incubated in the presence or absence of 0.02% MMS or 200 mM HU for 5 h, collected and processed for Western blotting. Treated (+) and untreated (-) samples (30, 10 or 5 μg) were loaded onto a 10% SDS gel. Blots were incubated with anti-MYC antibody, stripped then incubated in anti-pSTAIRE antibody. Adjusted relative densities (A.R.D) of Eip1p-MYC bands were obtained using lanes of untreated samples as a reference for each amount of protein loaded. **(**C, D) Strain SS38 (*TUB2-GFP-ARG4/TUB2, eip1::URA3/MET3::EIP1-HIS1*) was incubated in inducing (-MC) or repressing (+MC) medium

for 2.5 h, transferred to fresh –MC or +MC medium, respectively, containing 0.02% MMS and incubated for 5 h. Cells were fixed and stained with DAPI. Proportions of cells showing different patterns of Tub2p-GFP associated with DAPI staining and cell bud stage were quantified. Tub2p-GFP appeared as a small spot associated with DNA in unbudded or small-budded cells, representing a spindle pole body of G1/early S phase cells, a more intense spot in larger-budded cells with DNA confined to the mother cell, reflecting S-G2/M phase cells, a short rod associated with a single mass of DNA, representative of a metaphase or early anaphase spindle (arrowhead in D), an elongated bar with separated DNA masses at the ends, reflecting late anaphase (arrow in D), or 2 separate spindle pole bodies associated with segregated DNA in large-budded cells, reflecting exit from mitosis. Abnormal organizations including two spindle pole bodies per DNA mass, or multiple DNA masses within one cell compartment were also observed. Error bars represent s.d. from the mean of biological duplicates. Sample sizes included at least 140 cells. Significance was determined using the Fisher Exact Test, 2-tailed, with $p<0.05$ (*), $p<0.01$ (**), and $p<0.001$(***). (E.F) Strain SS38 was incubated and analyzed as described in (C, D), with the exception of using 200 mM HU. Error bars represent s.d. from the mean of biological duplicates. Sample sizes included at least 80 cells. Significance was determined using the Fisher Exact Test, 2-tailed, with $p<0.05$ (*), $p<0.01$ (**), and $p<0.001$(***). Bars: 10 μm.

2.4.10 The cohesin homologue Mcd1p/Scc1p is reduced upon depletion of Eip1p.

Separase functions in part through cleaving the cohesin subunit Mcd1p/Scc1p for sister chromatid separation (Kumar, 2017). The cohesin complex has not been investigated in *C. albicans,* but *MCD1/SCC1* (*ORF19.7634*) is 34% identical to its homologue in *S. cerevisiae* (http://www.candidagenome.org/). If Eip1p is a securin that regulates separase, then modulation of Eip1p may influence the separase target Mcd1p. To investigate this, Mcd1p was tagged with TAP in an *EIP1*-conditional strain, cells were incubated in inducing or repressing medium for set times, and the levels of Mcd1p were determined by Western blotting. When Eip1p was depleted, Mcd1p was moderately reduced (Figure 2.9A), consistent with Eip1p having an inhibitory effect on separase. We next determined the levels of Mcd1p in Eip1p-depleted cells exposed to MMS. Since MMS arrests cells in early mitosis, and depletion of Eip1p under these conditions permits many cells to escape the arrest, we reasoned that Mcd1p should also be reduced. The *EIP1*-conditional strain carrying a TAP-tagged copy of *MCD1* was incubated in inducing or repressing medium for 2.5 h, transferred to fresh media containing 0.02% MMS or 200 mM HU, incubated for 5 h, then fixed, and stained with DAPI. Western blotting demonstrated that after 5 h of Eip1p depletion in the presence of MMS, Mcd1p was significantly reduced (Figure 2.9B). The data demonstrate that Eip1p can impact the levels of Mcd1p, a homologue of a cohesin subunit and target of separase, and support the model that Eip1p may function as a securin in *C. albicans.*

A.
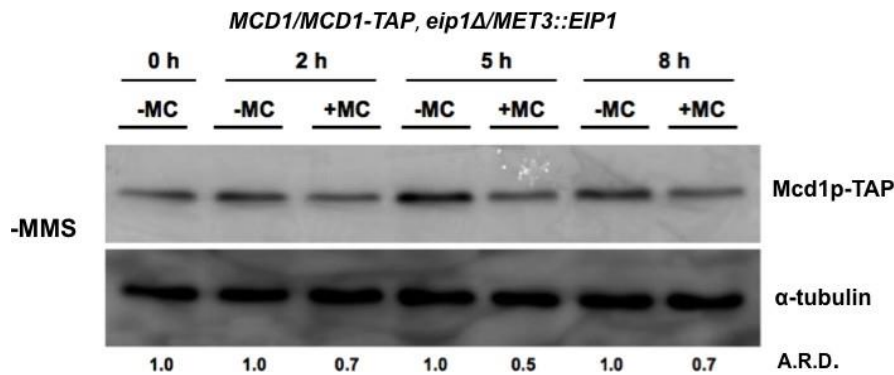
B.
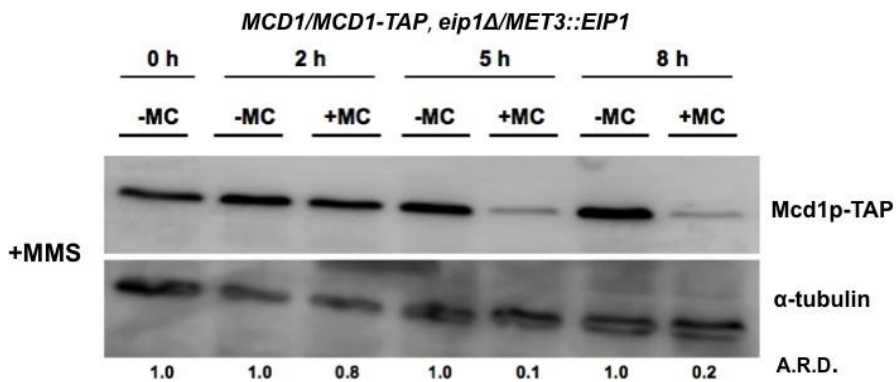
Figure 2.9. Cohesin subunit Mcd1p is reduced when Eip1p is depleted.

(A) Strain SS84 (*MCD1-TAP-ARG4/MCD, eip1::URA3/MET3::EIP1-HIS1*) was incubated in inducing (-MC) or repressing (+MC) medium. Samples were collected at set times and processed for Western blot analysis. Blots were incubated with anti-TAP and anti-α-tubulin antibodies. Adjusted relative densities (A.R.D) of Mcd1p-TAP bands were obtained using lanes from samples incubated in -MC medium as a reference for each time point. (B) Strain SS84 was incubated in -MC or +MC medium for 2.5 h, diluted into fresh –MC or +MC medium containing 0.02% MMS and incubated for set times. Western blotting analysis was performed as described in (A).

2.5 Discussion

Proper chromosome segregation at the metaphase-to-anaphase transition is critical for maintaining genomic stability, and is dependent on the highly conserved cohesin protease, separase. Securins are key regulators of separase, yet to date have only been identified in select model yeast, worms, flies, mice and humans, due to divergence in sequence (Moschou Bozhkov, 2012). *C. albicans* is a critical fungal pathogen of humans, and a deeper understanding of the regulation of its proliferation will be important for devising new strategies to treat infection. Through characterizing the *C. albicans* separase homologue Esp1p, we identified Eip1p, a *Candida*-specific separase-interacting protein that is important for growth and a candidate new securin. Our results provide an approach for identifying these divergent proteins, reveal new insights on mitotic regulation in fungi, and identify a potential novel target for anti-fungal therapeutics.

Since securins are difficult to identify with sequence-based homology searches, we reasoned that a functional homologue in *C. albicans* may be revealed by determining the interacting proteins of the separase homologue, Esp1p. However, Esp1p first required characterization since its functions were not clear, other than being essential for yeast growth (O'Meara et al., 2015). Here, we provide the first demonstration that *C. albicans* Esp1p is important for chromosome segregation. Esp1p-depleted cells were large-budded with an unsegregated DNA mass. Many contained short spindles characteristic of G2/M or early anaphase, but few elongated late anaphase spindles. Finally, some cells contained extra spindle pole bodies within a single mass of DNA, consistent with continuation of the cell cycle and similar to the situation with Esp1p-depleted *S. cerevisiae* cells (Baum et al., 1988; McGrew et al., 1992*)*. We also provide the first picture of putative Esp1p-interacting proteins in *C. albicans*. Cdc14p was one of the most enriched factors. Consistently, a recent screen for Cdc14p physical interactors in *C. albicans* identified Esp1p (Kaneva et al., 2019). Esp1p in *S. cerevisiae* functions with Cdc5p, Slk19p and PP2A$_{Cdc55}$ as part of the FEAR pathway that activates partial release of the phosphatase Cdc14p from the nucleolus. However, Esp1p and Cdc14p in *S. cerevisiae* have been reported to interact in a genetic rather than physical manner (https://www.yeastgenome.org/analyze), and homologues of Cdc5p, Slk19p and PP2A$_{Cdc55}$ did

not co-purify with Esp1p in *C. albicans*. Whether these differences reflect technical issues and/or diverse functional relationships remains to be determined. Notably, an equivalent FEAR pathway has not been identified in *C. albicans*. Collectively, the data are consistent with *C. albicans* Esp1p acting as a separase at the metaphase- to-anaphase transition. Given the diverse roles of separases (Kumar, 2017), Esp1p may have additional functions. Consistently, histones and histone deacetylase complex factors co-purified with Esp1p from exponential phase *C. albicans* cells (data not shown), suggesting possible roles in nucleosome organization and gene expression.

Among the proteins that interact with Esp1p, Eip1p represents a candidate divergent securin based on several features. First, it was one of the most enriched Esp1p-interacting proteins and unique in sequence. Second, its predicted 3D structure shares at least some similarity with securin Pds1p from *S. cerevisiae*. Third, Eip1p contains putative KEN and Destruction Boxes, and is turned over in mitosis in part through a Cdc20p-dependent manner, based on significant reduction in Eip1p during mitotic arrest induced by depletion of Cdc5p but not Cdc20p, similar to Pds1p (Charles et al., 1998; Hilioti et al., 2001). Fourth, Eip1p is important for chromosome segregation. Chromosome mis-segregation events in Eip1p-depleted cells were pleiotropic, and resulted in abnormal ploidy in some cases. Fifth, Eip1p is enriched in response to DNA damage or replication stress, and its absence permits a proportion of MMS or HU-treated cells to escape an early mitotic arrest, consistent with a role in blocking anaphase. *S. cerevisiae* Pds1p is also stabilized in response to HU or MMS, but this is not sufficient to block cell cycle progression; *pds1Δ* cells remain arrested due to Swe1p and Rad53p-mediated down-regulation of mitotic CDK activity (Palou et al,. 2015, 2017). Intriguingly, absence of Rad53p in *C. albicans* allows progression through an MMS-induced G2/M block (Shi et al., 2007), unlike the situation in *S. cerevisiae* (Palou et al., 2015), underscoring differences in the mechanisms governing mitotic progression between the two organisms. Finally, Eip1p modulates the levels of Mcd1p/Scc1p, a homologue of the separase target cohesin. Collectively, the data support the hypothesis that Eip1p functions as a securin-like protein. In order to confirm whether Eip1p shares additional traits of securins, investigations of its cell cycle-regulated abundance, functionality of its putative KEN and Destruction boxes, and its ability to block mitosis when in a non-degradable form should be explored.

Eip1p-depleted cells demonstrated other phenotypes that were distinct and may reflect additional functions. For example, the presence of misoriented spindles, a stretched and misoriented DNA mass in the mother cell that subsequently reoriented and segregated to the daughter cell, or two separate DNA masses within one cell compartment, imply a role for Eip1p in spindle orientation. Intriguingly, similar phenotypes were reported for mutants of Kar9p in *S. cerevisiae* (Miller and Rose, 1998) and dynein in *C. albicans* (Finley et al., 2008). Kar9p in *S. cerevisiae* mediates a connection between the plus end of astral microtubules associated with one spindle pole body and type V myosin on cortical actin cables. Coupled with depolymerization of the microtubules at the cortex, this moves the nucleus to the bud neck. The spindle oscillates across the neck via dynein acting on astral microtubules, and subsequent spindle elongation at anaphase partitions the DNA between mother and daughter cells (Gladfelter and Berman, 2009). Thus, Eip1p may impact spindle orientation through a mechanism affecting cortical positioning cues, microtubule dynamics/integrity or associated motors. Consistently, some abnormalities in microtubules and spindles were observed in Eip1p-depleted cells, as well as random oscillations of elongated spindles, and abnormal movements of nuclei, at times from mother cell to bud and back. The latter, particularly reverse movement of the post-mitotic nucleus back to the mother cell, is highly unusual for yeast and the mechanisms remain unclear. In hyphae, retrograde movement of a daughter nucleus to the mother cell after division in the germ tube is accomplished by spindle elongation, but a slower and unknown mechanism is required after the spindle disassembles (Finley and Berman, 2005). Another distinct phenotype included maintenance of elongated spindles. Where spindles were confined to the mother cell, it is possible that the spindle orientation checkpoint (SPOC) was activated by spindle disorientation and/or cytoplasmic microtubule defects, which delays mitotic exit and spindle disassembly (Finley et al., 2008; Caydasi et al., 2010). Down-regulation of some MEN factors in *S. cerevisiae* can also impair spindle orientation through affecting Kar9p localization (Hotz et al., 2012). However, maintained spindles in other Eip1p-depleted cells spanned the mother and daughter cells, reminiscent of spindle disassembly or MEN pathway mutants (Woodruff et al., 2010; Weiss 2012). In *C. albicans,* these pathways are not well defined (Bates, 2018). Further, *C. albicans* homologues of some *S. cerevisiae* MEN factors, including Dbf2p and Cdc14p, have prominent

functions in additional processes (Clemente-Blanco et al., 2006; González-Novo et al., 2009). Intriguingly, Dbf2p shares several phenotypes with Eip1p (González-Novo et al., 2009). *S. cerevisiae, pds1Δ* cells did not demonstrate a spindle maintenance phenotype. Rather, some cells were multinucleate, consistent with precocious mitotic exit due to the positive role for separase in this process, and inhibition by Pds1p (Hatano et al., 2016). Although two DNA masses were also present in some Eip1p-depleted cells, they were often connected by a spindle. Coupled with other microtubule-dependent processes affected, we propose that maintenance of elongated spindles in a proportion of Eip1p-depleted cells may be due to an impact on spindle disassembly mechanics, as opposed to Eip1p playing some positive role in the mitotic exit pathway. The additional phenotypes involving spindle behavior and/or microtubules in Eip1p-depleted cells may be indirect effects of deregulated separase, since separases are important for a variety of spindle-related processes (Kumar, 2017). Alternatively, we cannot rule out the possibility that they represent separase-independent functions of Eip1p. Consistently, the securin Pttg1p has several roles, including a separase-independent function in microtubule nucleation (Moreno-Mateos et al., 2011). Taken together, we propose that Eip1p may function as a securin that regulates separase for chromosome segregation, and may have additional roles that impact spindle orientation, disassembly and/or microtubule function. In this way, Eip1p could coordinate multiple aspects of mitotic progression.

Chromosome segregation and cell division could take place in many cells lacking Eip1p, suggesting that Eip1p may not be immediately essential for these processes. While it is possible that trace amounts of Eip1p were present, or that deletion strains contained secondary mutations that permitted growth, it is notable that when *EIP1* was repressed, diverse phenotypes were observed within groups of closely-associated cells. In addition, repressing *EIP1* with the *TET* vs. *MET3* promoter produced similar effects, *eip1Δ/Δ* cells from independent transformations resembled cells depleted of Eip1p, and depletion of Esp1p using the *TET* or *MET3* promoter resulted in more severe and homogeneous effects on growth and chromosome segregation than depletion of Eip1p. We propose that cells lacking Eip1p variably accumulate defects in chromosome segregation, which can lead to a loss in viability, somewhat similar to the situation with *EST* mutants in *S. cerevisiae* (Lundblad and Szostak, 1989). Where securins are essential,

the null phenotype resembles that of separase mutants, due to the negative and positive regulation of separase by securin (Funabiki et al., 1996; Hellmuth et al., 2015). If securin is not essential, separase requires additional negative regulation. In metazoans, CDK/CyclinB phosphorylation serves this role (Hellmuth et al., 2015). In *S. cerevisiae*, Slk19p and PP2A$_{Cdc55}$ act redundantly with Pds1p to negatively regulate Esp1p (Lianga et al., 2018). *C. albicans* has homologues of Slk19p and Cdc55p, but they are not characterized. Since several mitotic factors show variations in function in *C. albicans*, different proteins could contribute to separase regulation. Eip1p may be even more critical for chromosome segregation under specific conditions, including DNA damage or replication stress caused by MMS or HU treatment, respectively.

In summary, we identified a separase binding protein, Eip1p, with functions that suggest it is a new candidate securin. Our work provides an approach for identifying divergent securins, and expands our understanding of the factors involved in regulating the metaphase-to-anaphase transition in eukaryotic cells. Given its importance in cell division, and lack of a sequence homologue in humans, Eip1p also represents a candidate target for approaches aimed at controlling growth of *C. albicans*. Determining the full range of functions and regulation of Eip1p and separase in *C. albicans* will provide additional important insights on the circuitry controlling fungal cell proliferation and diversity in eukaryotic mitotic networks.

2.6 Supplemental Figures and Tables

Table S2.1 Strains used in this study.

Strain	Genotype	Source
BH440	BWP17 (pBS-Ca*HIS1*, pBS-Ca*URA3*)	Hussein et al., 2011
BWP17	*ura3:imm434/ura3:imm434, his1::hisG/his1::hisG arg4::hisG/arg4::hisG*	Wilson et al.,1999
AG153	*MET3::CDC20-ARG4/cdc20::URA3, CLB/CLB2-HA-HIS1*	Chou et al., 2011
AG500	*cdc5::URA3/MET3::CDC5-HIS1*	Glory, 2017
AG636	*ESP1/ESP1-TAP-URA3*	This study
HCCA109	*cdc20::URA3/MET3::CDC20-HIS1*	Chou et al., 2011
HCCA23	*cdc20::URA3/MET3::CDC20-HIS1*	Chou et al., 2011
SS1	*esp1::HIS1/ESP1-TAP-URA3*	This study
SS3	*ESP1/ESP1-TAP-ARG4, cdc20::URA3/MET3::CDC20-HIS1*	This study
SS10	*eip1::URA3/EIP1*	This study
SS16	*ESP1/ESP1-HA-URA3*	This study
SS20	*esp1::URA3/ESP1*	This study
SS22	*eip1::URA3/EIP1-MYC-HIS1*	This study
SS25	*eip1::URA3/MET3::EIP1-HIS1*	This study
SS29	*EIP1-MYC-HIS1/EIP1, ESP1-HA-URA3/ESP1*	This study
SS35	*esp1::URA3/MET3::ESP1-HIS1*	This study

SS37	*TUB2-GFP-ARG4/TUB2, esp1::URA3/MET3::ESP1-HIS1*	This study
SS38	*TUB2-GFP-ARG4/TUB2, eip1::URA3/MET3::EIP1-HIS1*	This study
SS40	*eip1::URA3/EIP1-TAP-ARG4*	This study
SS41	*EIP1/EIP1-TAP-ARG4, cdc20::URA3/MET3::CDC20- HIS1*	This study
SS43	*EIP1/EIP1-TAP-URA3, cdc5::hisG/MET3::CDC5-ARG4*	This study
SS44	*HTB1/HTB1-GFP-ARG4, eip1::URA3/MET3::EIP1-HIS1*	This study
SS63-65	*eip1::URA3/eip1::HIS1*	This study
SS86	*MCD1/MCD1-TAP-ARG4, eip1::URA3/MET3::EIP1-HIS1*	This study

Table S2.2. Plasmids used in this study.

Plasmids	Description	Source
pFA-GFP-Ca*ARG4*	pFunctional Analysis Casette-GFP-ARG4	Lavoie et al., 2008
pMG2093	pFA6a-13myc-TRP1 ligated into pFA-GFP-HIS1	Bensen et al., 2005
pFA-HA-Ca*URA3*	pFunctional Analysis Casette-HA-URA3	Lavoie et al., 2008
pFA-TAP-Ca*URA3*	pFunctional Analysis Casette-TAP-URA3	Lavoie et al., 2008
pFA-TAP-Ca*ARG4*	pFunctional Analysis Casette-TAP-ARG4	Lavoie et al., 2008
pFA-*MET3*-Ca*HIS1*	*MET3* promotor-Ca*HIS1*	Gola et al., 2003
pBS-Ca*URA3*	pBluescript-Ca*URA3*	A.J.P Brown
pBS-Ca*HIS1*	pBluescript-Ca*HIS1*	Chou et al., 2011

Table S2.3. Oligonucleotides used in this study.

Oligonucleotide	Sequence in 5'-3' direction	Source
AG3R	GCG GTT GGC TGC TGA GAC GG	Chou et al., 2011
AG4F	GGT CGA CGG ATC CCC GGG TTA TAC CCA TAC GAT GTT CCT GAC	Chou et al., 2011
AG4R	TCG ATG AAT TCG AGC TCG TT	Chou et al., 2011
AG103F	GGA TTT GAC TAA TTG TGT TGT TCA AAG TCG AAG TAA ATG TAC TTT GAA ATA CTT GAA TGG ATC AGC ACC TGT GGT TTA TGG TCT ACC AAT GTA TTT AAA AGG TCG ACG GAT CCC CGG GTT	This study
AG103R	AGT GAT TGG GTG CAA AAT TTG TTC ATA ACA AAC CAA ACA ATA CAA AAT CAA GAT CCA AAT TAT GCT CTT TTT CTT ATT ATT AAA ATA TAT AAA CTT ATA TTC GAT GAA TTC GAG CTC GTT	This study
AG104F	CCC AGT GGT GAT TTA ATT CG	This study
AG104R	GGC TGT AGA TCA TTC AGT CC	This study
CB135F	CAA TAC CAA GAA GCT AGT ATT GAT GAA GAA GAA TTA GAA TAT GCC GAT GAA ATC CCA TTA GAA GAT GCC GCC ATG GCT GGC GCA GGT GCT TC	This study
CB135R	ATA TTG TGC CGA TAA ATA ATA AAA GGG TAT AAT CAT TAA CTA AAC CAA AAA AAA CCA TAA TTA TAT TAG AAG TGA ACA AAG ATA TCA TCG ATG AAT TCG A	This study
SS1F	GTT ATT GCT AAA AGA CAA GCT TTG GAA CGT	This study

SS1R	GC TGA ATC AAA CTG TAA TGA AAT ACA GAT	This study
SS2F	TAA TGT TGG CAT TTT CTG ATG GAA TTG TTG	This study
SS2R	TGC ACA GTA TGG ATT GCT AGT CCT AGA GAA	This study
SS3F	ATC TGT ATT TCA TTA CAG TTT GAT TCA GCC/TAT AGG GCG AAT GGG AGC TC	This study
SS3R	CAA CAA TTC CAT CAG AAA ATG CCA ACA TTA/GAC GGT ATC GAT AAG CTT GA	This study
SS10F	GGA ACC ATT AAG AGA GCA TA	This study
SS18F	AAT ACC AAT TAT TGA AGG TAT TGA TGA GGA AAT TGG TTT AAC TAG CGA TGA TTT GGA TAA TTT ATT AGG AGG TGG TGG TCG ATC CCC CGG GTT AAT TAA	This study
SS18R	AGT ATG AAC AAC AGG GGT ACG AGC AAT CAT GTG CCC AAC AAT AAT ACC ATG TAA ATA CTC AAT ATA TGAA	This study
SS19F	GAA CCA TTA AGA GAG CAT AAA TTG GGT AAG	This study
SS19R	AAC TCA TTG TAA GCT AAT GAA GGG AGT AA	This study
SS20F	ATG GAT AAC TCG TTG GAT CAA AAA CTA TTG	This study
SS20R	TGG AAA CAT ATT GGG CTA TCC ATT GTA AAA	This study
SS21F	TTA CTC CCT TCA TTA GCT TAC AAT TGA GTT GGA TCC TGG AGG ATG AGG AG	This study
SS21R	CAA TAG TTT TTG ATC AAC GA GTT ATC CAT CAT GTT TTC TGG GGA GGG TA	This study
SS22F	CTG TTT AAT CTG AAA ATC AAA TAC CTC CAT	This study
SS22R	AAT CTA CAC AGC GCG TAG CTC CCA ACC CCC	This study

67

SS23F	GAG TAT TTA CAT GGT ATT ATT GTT GGG CAC	This study
SS23R	CAT ATT GGA ATA CAA ATG CAA ACC ACA TAA	This study
SS24F	GGG GGT TGG GAG CTA CGC GCT GTG TAG ATT TAT AGG GCG AAT TGG AGC TC	This study
SS24R	GTG CCC AAC AAT AAT ACC ATG TAA ATA CTC GAC GGT ATC GAT AAG CTT GA	This study
SS25F	GGG GGC TTC ATT ATC TAT TT	This study
SS25R	GAG AAT CCG ATC AAT TTC CA	This study
SS26F	CGA TGG AGA CAT AAG TTT CT	This study
SS27F	GTC GAC CAC CAA GTG GTG ACA CTT TAA ATG	This study
SS27R	TTC CTC ATT TCT CCT TTT AGT GGT TCA ACC	This study
SS28F	ATG TCA AGT CAT ATA TTC AAA GAT ATT CAA	This study
SS28R	TTG AGT GGC TTA GT TAA TGA ATC CGT AAA	This study
SS29F	GGT TGA ACC ACT AAA AGG AGA AAT GAG GAA GGA TCC TGG AGG ATG AGG AG	This study
SS29R	TTG AAT ATC TTT GAA TAT ATG ACT TGA CAT CAT GTT TTC TGG GGA GGG TA	This study
SS33F	GGA CTT GAA GAT GAA GTA ATG TGT TGG AGA AAT ACC AAT TAT TGA AGG TAT TGA TGA GGA AAT TGG TTT AAC TAG CGA TGA TTT GGA TAA TTT ATT AGG AGG TCG ACG GAT CCC GGG TT	This study
SS33R	ATC AGT TAC CCA AGT ACA ATC AGG ATA GAA AGT ATG AAC AAC AGG GGT ACG AGC AAT CAT GTG CCC AAC AAT AAT ACC ATG TAA ATA CTC AAT ATA TGA ATC GAT GAA TTC GAG CTC GTT	This study
SS37F	AAT CCA AAC TGC TGT TAG ATT AAT TTT GCC AGG TGA ATT GGC CAA ACA TGC CGT TTC CGA AGG TAC CAG AGC CGT TAC AAA ATA CTC ATC TGC TTC TAG TGG TGC TGG CGC AGG TGC TTC	This study

SS37R	GGT AAT AAT AGA AAC ATA ATA CTA TAA TAT AAT AAC GAA CTA AAG TAC AAA AAA AAG TGG GCA ACT AAA AAT ACA ATT GGG AGA CAA TAC AAG ATC CAT CCC GCA TAG GCC ACT AGT GGA	This study
SS47F	AAC TAA TAA TTG CAT TTC TTT AGG TCA AAT CCC ACA AGA AAC AAC AAT TGC TGG AGA TAT CAG CAT CAC TTC AAG AGA CAG ATT ATT TAG TCA GTT TGT AGG TCG ACG GAT CCC CGG GTT	This study
SS47R	ATA TCT GGG ATT TGA GCA AGA AGA TAT ATT CTC CTA TCA CCA CCA TAA TGG AAT CTG TCG ATA AAA TTG ATG ATA TTG CCT TTA ATG AAA CTG GTG ACA CTC GAT GAA TTC GAG CTC GTT	This study
SS48F	TTA CAC ACA CAC GGC AAG AG	This study
SS48R	TGT ACA TGA GGA CTG TCT AT	This study
CaHIS1F	CCT GCA GCT GAT ATC CCA GT	Chou et al., 2011
CaHIS1R	ACT GGG ATA TCA GCT GCA GG	Chou et al., 2011
CaURA3F	GGT AAT ACC GTG AAG AAA CA	Chou et al., 2011
CaURA3R	TTC AAA TAA GCA TTC CAA CC	Chou et al., 2011
CaARG4F	ACT ATG GAT ATG TTG GCT ACT	Glory, 2017

Table S2.4 Orbitrap LC/MS analysis of putative Esp1p-interacting factors in *CDC20*-depleted cells[1]

PROTEIN ID	Number of Peptides[2,3]	ORF	Identified Proteins	Frequency of hits[4]
CAL0004160	63	ESP1	Putative caspase-like cysteine protease; mutation confers increased sensitivity to nocodazole; periodic mRNA expression, peak at cell-cycle S/G2 phase; mRNA binds She3	1
CAL0005886	24	CDC14	Tyrosine-protein phosphatase CDC14 OS=*Candida albicans* (strain SC5314)	1
CAL0003715	11	Orf19.955	Uncharacterized ORF	1
CAL0000006	8	HSP70	Putative hsp70 chaperone; role in entry into host cells; heat-shock, amphotericin B, cadmium, ketoconazole-induced; surface localized in yeast and hyphae; antigenic in host; farnesol-	1
CAL0005977	6	CDC19	Pyruvate kinase at yeast cell surface; Gcn4/Hog1/GlcNAc regulated; Hap43/polystyrene adherence induced; repressed by phagocytosis/farnesol; hyphal growth role; stationary phase	1
CAL0004558	4	TEF1	Translation elongation factor 1-alpha; at cell surface; binds human plasminogen; macrophage/pseudohyphal-induced; induced in RHE model of oral candidiasis, in clinical oral candidiasis isolates; possibly essential; Spider biofilm repressed	1
CAL0001571	4	ACT1	Actin; gene has intron; transcript regulated by growth phase, starvation; at polarized growth site in budding and hyphal cells; required for wild-type Cdc42 localization; unprocessed N terminus; Hap43-induced; Spider biofilm repressed	1
CAL0000121	4	DEF1	RNA polymerase II regulator; role in filamentation, epithelial cell escape, dissemination in RHE model; induced by fluconazole, high cell density; Efg1/hyphal regulated; role in adhesion,	1
CAL0003176	3	ADH1	lcohol dehydrogenase; oxidizes ethanol to acetaldehyde; at yeast cell surface; immunogenic in humans/mice; complements *S. cerevisiae* adh1 adh2 adh3 mutant; fluconazole, farnesol-induced; flow model biofilm induced; Spider biofilm repressed	1
CAL0001672	3	Orf19.1840	Predicted lipid-binding ER protein; involved in ER-plasma membrane tethering; Spider biofilm induced	1
CAL0003655	3	PET9	Mitochondrial ADP/ATP carrier protein involved in ATP biosynthesis; possible lipid raft component; 3 predicted transmembrane helices; flucytosine induced; ketoconazole-induced; downregulated by Efg1p	1

CAL0001016	2	Orf19.4246	Ortholog(s) have protein anchor activity, role in COPII vesicle coating, protein localization to endoplasmic reticulum exit site and ER to Golgi transport vesicle membrane, endoplasmic	1
CAL0004511	2	TUB1	Alpha-tubulin; gene has intron; complements cold-sensitivity of *S. cerevisiae* tub1 mutant; *C. albicans* has single alpha-tubulin gene, whereas *S. cerevisiae* has two (TUB1, TUB3); farnesol-upregulated in biofilm; sumoylation target	1
CAL0006245	2	Orf19.5579	Protein with a predicted double-strand break repair domain; Hap43-repressed gene	1
CAL0001878	2	BN14	Protein required for wild-type cell wall chitin distribution, morphology, hyphal growth; not essential; similar to *S. cerevisiae* Bni4p (targeting subunit for Glc7p phosphatase, involved in bud-	1
CAL0004607	2	BGL2	Putative glucanase; induced during cell wall regeneration	1
CAL0005867	2	RPSA8	Small 40S ribosomal subunit protein; induced by ciclopirox olamine; repressed upon phagocytosis by murine macrophage; 5'-UTR intron; Hap43-induced; Spider biofilm repressed	1
CAL0003729	2	Orf19.4657	Ortholog(s) have phosphoprotein phosphatase activity, role in negative regulation of phospholipid biosynthetic process, nuclear envelope organization and Nem1-Spo7 phosphatase complex, integral to membrane, mitochondrion localization	1
CAL0005797	2	ATP1	ATP synthase alpha subunit; antigenic in human/mouse; at hyphal surface; ciclopirox, ketoconazole, flucytosine induced; Efg1, caspofungin repressed; may be essential; sumoylation target; stationary phase-enriched; Spider biofilm repressed	1
CAL0006292	2	POL5	Putative DNA Polymerase phi; F-12/CO2 early biofilm induced	1
CAL0002073	2	CTA3	Protein similar to *S. cerevisiae* Ede1p, which is involved in endocytosis; activates transcription in 1-hybrid assay in *S. cerevisiae*	1

[1]330 mg protein extracts from 4 L cultures of strain SS3 (*ESP1/ESP1-TAP-ARG4, cdc20::URA3/MET3::CDC20-HIS1*) and AG153(*MET3::CDC20-ARG4/cdc20::URA3, CLB2-HA-HIS1*) incubated in +MC medium until reaching an O.D.600nm of 0.4 were subjected totandem affinity purification. Elutions were TCA-precipitated and run just into the resolving portion of an SDS PAGE gel. The compressed bands were stained with Coomasie blue, cut from the gel, and analysed using an LTQ-Orbitrap Elite with nano-ESI.
[2]Peptides less than 2 were excluded from the results.
[3]Peptides identified in both the tagged strain and the untagged control strain were excluded from the table.
[4]Number of times indicated proteins were purified over total number of two affinity purification repeats.

A.

esp1Δ/TET::ESP1

- DOX   + DOX

B.

esp1Δ/TET::ESP1

-DOX   +DOX

DIC

DAPI

Figure S2.1. Depletion of *ESP1* with the *TET* promoter impairs growth and chromosome segregation.

(A)GRACE strain *esp1::URA3/TET::ESP1-HIS1* was streaked onto YPD plates with (+DOX) or without (-DOX) 100 µg/ml doxycycline and incubated for 24 h at 30°C. (B) Cells of the same strain were incubated in liquid YPD medium with or without 100 µg/ml doxycycline for 8 h, fixed and stained with DAPI. Bar: 10 µm.
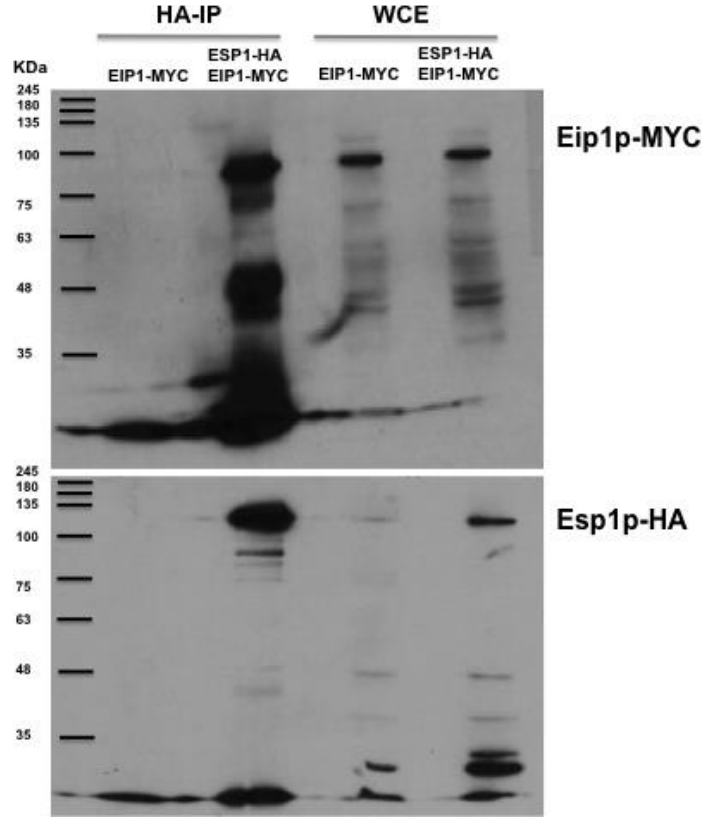
Figure S2.2. Eip1p-MYC co-purifies with Esp1p-HA.

Western blots of whole cell extracts (WCE) and immune-precipitates (HA-IP) of strains SS22 (*eip1::URA3/EIP1-MYC-HIS1*) and SS29 (*EIP1/EIP1-MYC-HIS1, ESP1/ESP1-HA-URA3*), using anti-HA agarose (HA-IP). Blots were incubated with anti-MYC antibody, stripped, then incubated with anti-HA antibody.
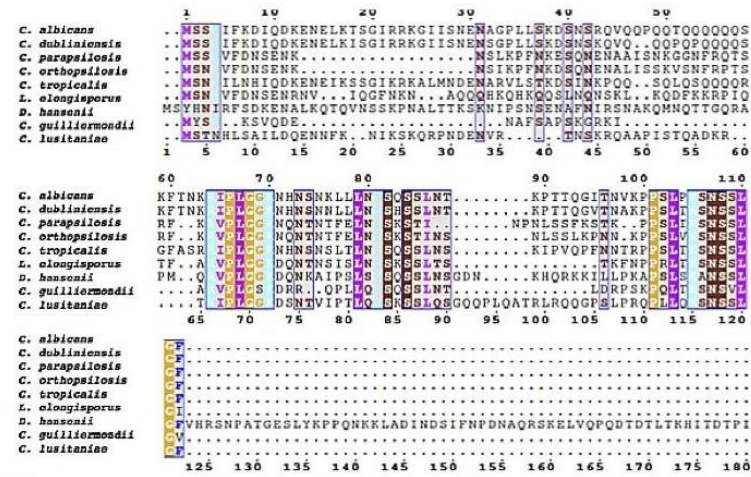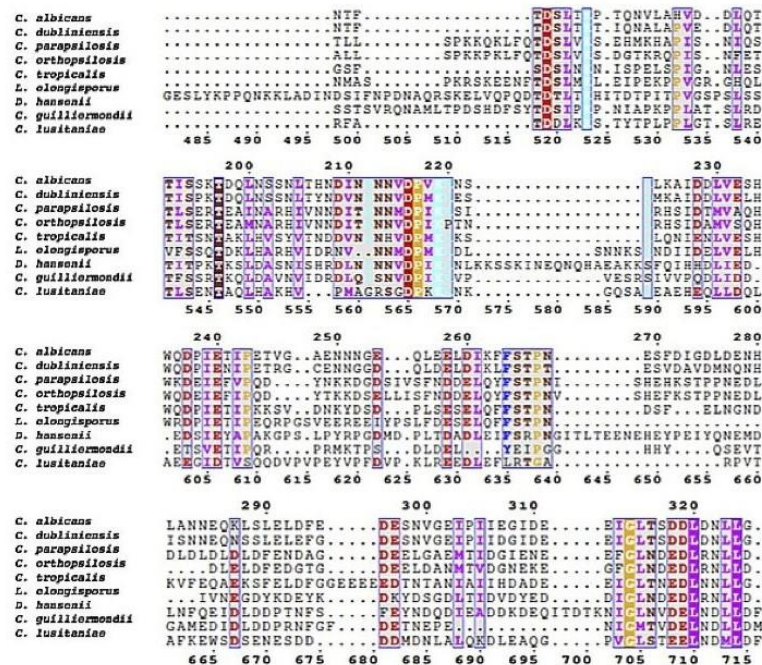
Figure S2.3. Comparison of Eip1p/Orf19.955p amino acid sequence with homologues in other *Candida* species. (A) Alignment was obtained from Candida Genome Database (CGD: http://www.candidagenome.org). Colors represent >80% identity. Hydrophobic (A, I, L, M, V), aromatic (F, W, Y), polar (N, Q, S, T), negative charge (D, E), positive charge (H, K, R),

backbone change (G, P) and Cysteine (C) are highlighted. (B) Identity (%) across amino acid sequence, obtained from CGD.
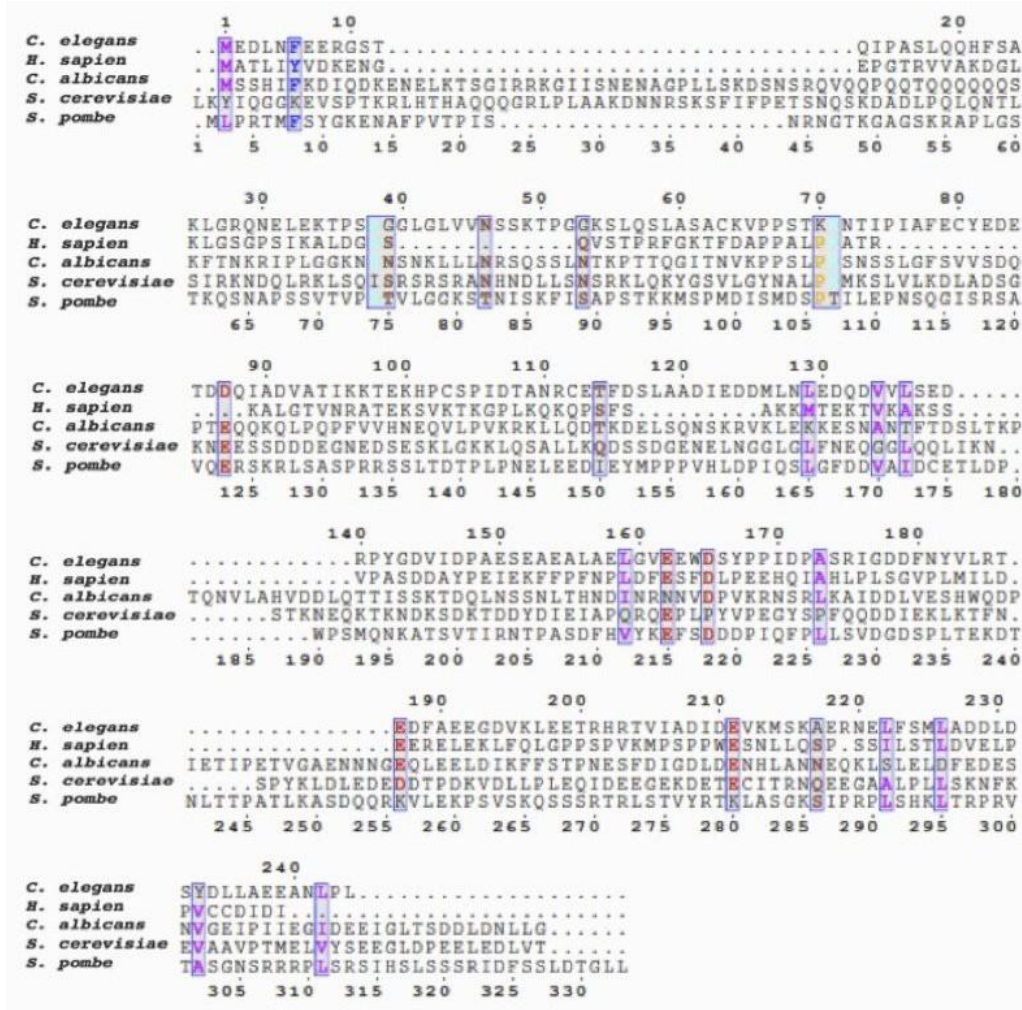
Figure S2.4. Comparative analysis of Eip1p amino acid sequence with securins.
Sequences of Pds1p (*S. cerevisiae*), Cut2p (*S. pombe*), IFY-1 (*C. elegans*), and PTTG1 (*H. sapiens*) were aligned with ClustalW (Larkin et al., 2007), and further analyzed with ESPript software (Robert et al., 2014). Parameters included sequence similarity (% similarity), alignment output layout (flashy, portrait), and a global score of 0.7, as set by the program. Regions of similarity are designated by boxed amino acids.
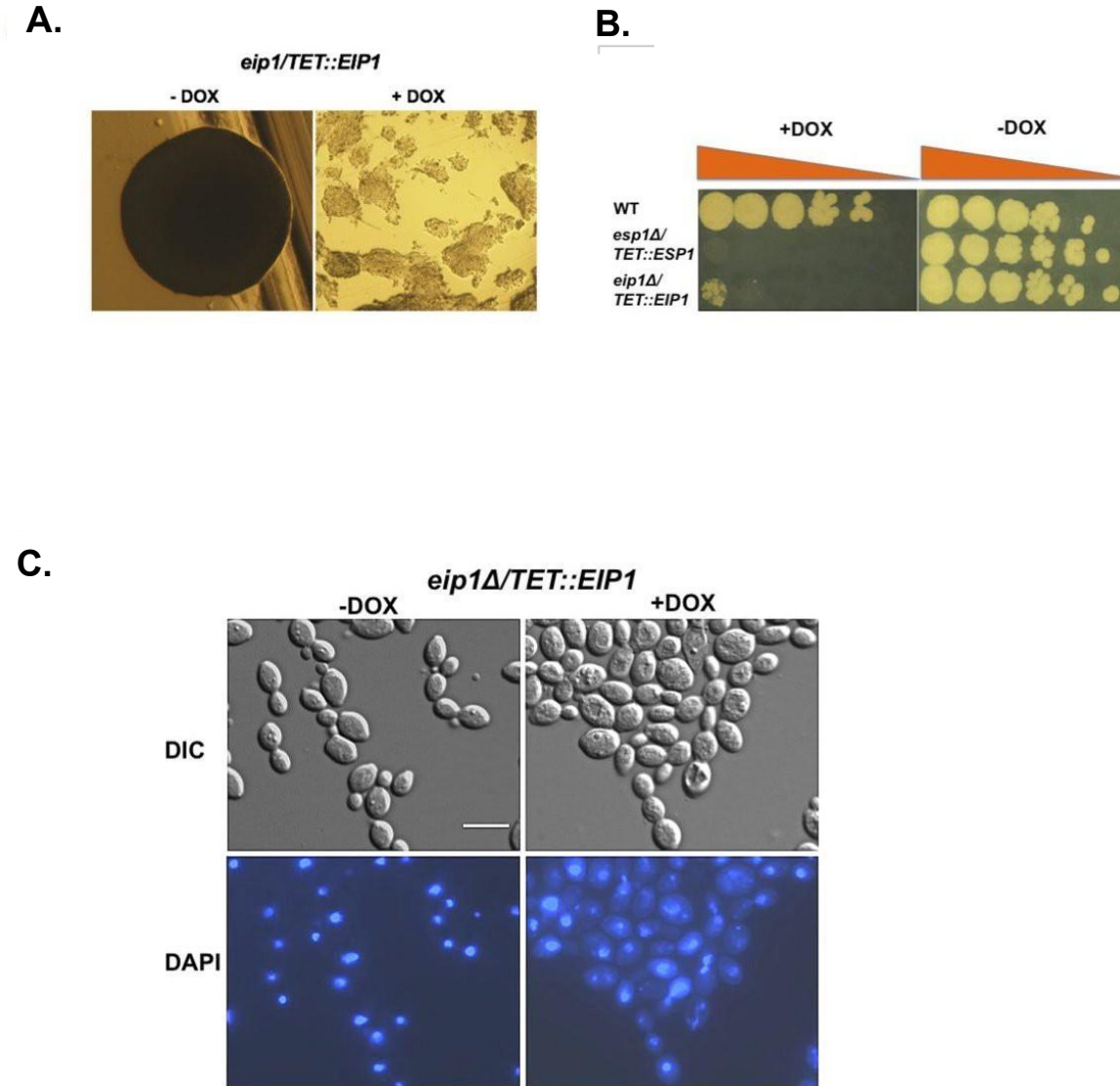
Figure S2.5. Depletion of *EIP1* with the *TET* promoter impairs growth and chromosome segregation in a similar manner as the *MET3* promoter.

(A) GRACE strain *orf19.955::URA3/TET::ORF19.955-HIS1* was plated on YPD medium with (+DOX) or without (-DOX) 100 µg/ml doxycycline and incubated at 30°C for 24 h. (B). Strains *orf19.955::URA3/TET::ORF19.955-HIS1, esp1::URA3/TET::ESP1-HIS1* and BH440 (*URA3+, HIS1+*) were serial diluted and incubated on solid YPD medium with or without doxycycline for 72 h. (C) Cells of strain *orf19.955::URA3/TET::ORF19.955-HIS1* were incubated in liquid YPD medium with or without doxycycline for 8 h, fixed and stained with DAPI. Bar: 10 µm.

A.
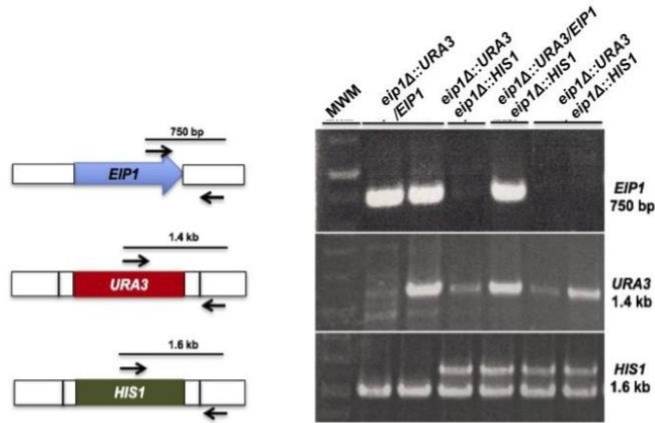
B.
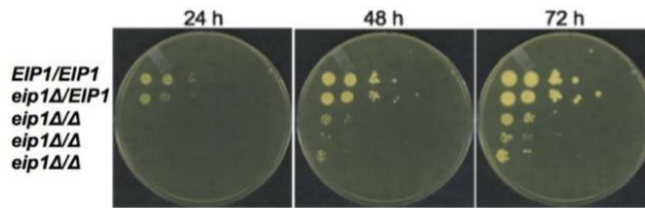
C.
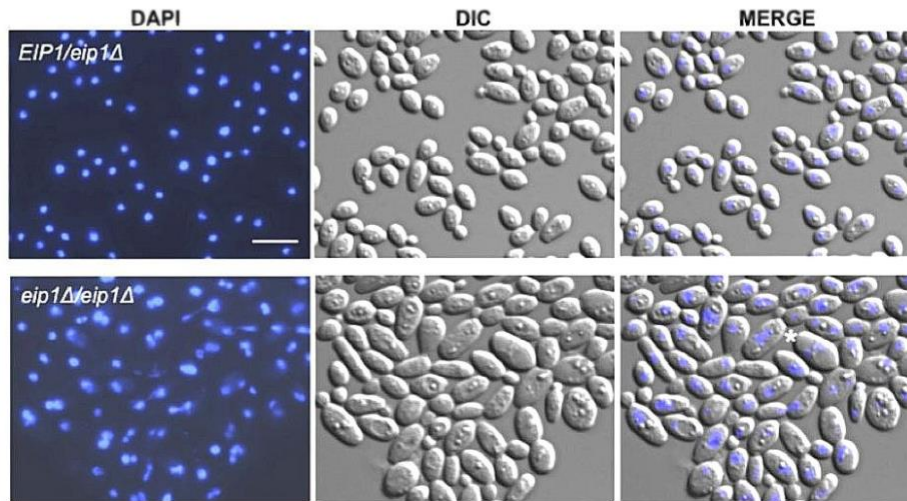
Figure S2.6. Cells deleted of Eip1p are viable but severely impaired in growth, and show defects in chromosome segregation.

(A)Map and gel showing PCR strategy to confirm replacement of alleles of *EIP1* with *URA3* and *HIS1* markers, and absence of the *EIP1* ORF. Strains BWP17 (*EIP1/EIP1*), SS11 (*eip1::URA3/EIP1*), a negative transformant (*eip1/EIP1*), and strains SS63-SS65

(*eip1::URA3/eip1::HIS1*) were screened with primer pairs CaURA3F and SS25R (1400 bp), CaHIS1F and SS25R (1600 bp), and SS25F and SS25R (750 bp). Lower bands in the *HIS1* integration confirmation gel are non-specific. (B) Serial dilutions of strains SC5314 (*EIP1/EIP1*), SS22 (*eip1::URA3/EIP1-MYC-HIS1*) and transformants SS63-65 (*eip1::URA3/eip1::HIS1*) were plated on YPD medium and incubated at 30°C for set times. (C) Strain SS63 (*eip1::URA3/eip1::HIS1*) was incubated in YPD medium containing uridine (50μg/μl) at 30°C for 7 h, fixed and stained with DAPI. Bar: 10μm.
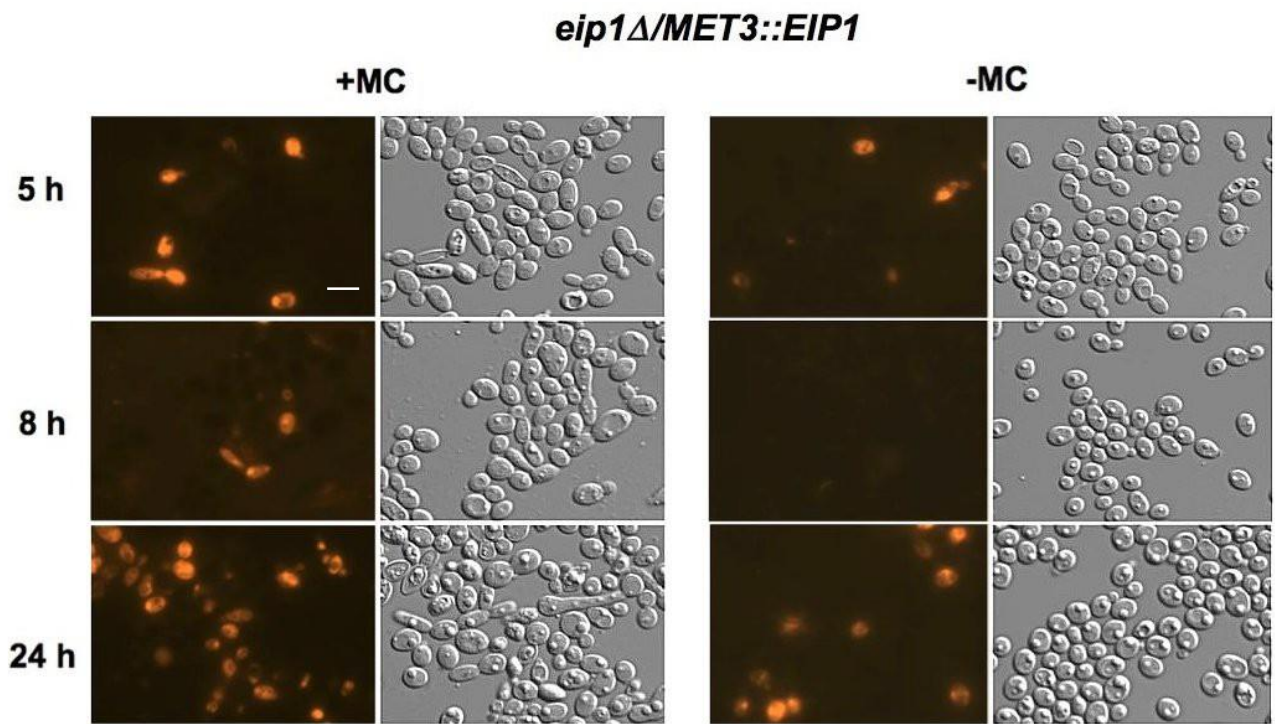
Figure S2.7: Eip1p-depleted cells show increased staining with propidium iodide over time. Strain SS25 (*eip1::URA3/MET3::EIP1-HIS1*) was incubated in inducing (-MC) or repressing (+MC) medium for indicated times, stained with propidium iodide and imaged immediately. Bar: 10 μm.

Chapter 3. Characterization of the APC/C subunit Cdc16p and Regulation of Eip1p during the Metaphase-to-Anaphase Transition in *Candida albicans*

All figures were contributed by Samantha Sparapani

3.1 Abstract

Securins are key regulators of the metaphase-to-anaphase transition and the conserved separase, and are present in most organisms including some yeast, flies, plants and humans. However, securins are divergent due to low sequence homology. We previously identified Eip1p as a securin-like protein in *C. albicans* and showed it to bind Esp1p, is important for chromosome segregation, is induced upon DNA damage, and its absence partially supresses a metaphase arrest induced by MMS or HU, suggesting a role in blocking anaphase. We also previously found that Eip1p depletion resulted in some novel phenotypes including misoriented spindles, spindles that failed to disassemble and a pleiotropic morphology consisting of chains of cells and pseudohyphae. In addition, all securins are regulated in part by APC/C$_{Cdc20p}$-mediated degradation. However, when Cdc20p was depleted, Eip1p was not significantly or consistently enriched, in contrast to other securins, which could be due to a heterogeneous Cdc20p-depleted phenotype, or alternative modes of regulation of Eip1p. In addition, APC/C composition and function is not well characterized in *C. albicans*. In this study, we provide the first characterization of the APC/C subunit Cdc16p in *C. albicans,* and address further the regulation of Eip1p during the metaphase-to-anaphase transition. We show that *C. albicans'* Cdc16p has conservation in function, where its depletion resulted in a metaphase arrest and enrichment of the mitotic cyclin Clb2p, consistent with Cdc16p in *S. cerevisiae*. We also demonstrate Eip1p enrichment in the absence of Cdc16p, clarifying the involvement of APC/C-mediated degradation and consistent with other securins. In order to address Eip1p mechanisms of action, affinity purification of Eip1p-TAP followed by mass spectrometry revealed several unique co-purifying proteins, including Cdc14p, the cohesin subunit Smc3p, several chromatin-associated factors including Smc3p, Spo69/Rec8p and Smc6p, RNA mediator proteins including Med1p, proteins involved in proteasome activity such as Apc3p, Rpn9p, and Ecm29p as well as filament-

associated factors, including Kem1p, Fab1p and Opi1p. Collectively, the data reveal that Cdc16p of *C. albicans* shows conserved features in the metaphase-to-anaphase transition, Eip1p is regulated in part in an APC/C-dependent manner, reinforcing the concept that it is a securin, and Eip1p may be linked to additional roles in other mitotic processes and possibly morphogenesis.

3.2 Introduction

The cell cycle is a series of phases regulated by a diversity of factors that function to maintain genomic stability and cell cycle progression. (Morgan, 2007). In most eukaryotes, G1 and G2 phases of the cell cycle are associated with cellular growth, while DNA is replicated during S phase and subsequently segregated to daughter cells during mitosis followed by cytokinesis. The metaphase-to-anaphase transition during mitosis is characterized by separation of sister chromatids that previously condensed and aligned at the equatorial plane of the cell on the mitotic spindle (Morgan, 2007). In most organisms including *Saccharomyces cerevisiae,* sister chromatids are held together prior to anaphase by the cohesin ring-like complex, which is comprised of several subunits including the Structural Maintenance of Chromosomes (SMC) proteins Smc1p and Smc3p, the kleisin subunit Mcd1p/Scc1p, and Scc3p (Mehta et al., 2013). In order for chromatids to segregate to opposite poles of the cell, the Mcd1p/Scc1p subunit must be cleaved. This is carried out by separase, a conserved cysteine protease (Kumar, 2017). In *S. cerevisiae*, depletion of the separase Esp1p results in cells arresting as large budded cells with a single unsegregated mass of DNA near the mother-bud neck (McGrew et al., 1992).

A major regulator of separase activity and the metaphase-to-anaphase transition is securin. Securins have been identified in *S. cerevisiae* (Pds1p), *S. pombe* (Cut2p), *C. elegans* (IFY-1), humans (PTTG1) and most recently *Arabidopsis* (Pans1p and Pand2p) (Yamamoto et al., 1996a; Funabiki et al., 1996; Kitigawa et al., 2002; Cromer et al., 2019). Securin regulates separase in several ways. It functions as an inhibitor, where it prevents separase activity until required at the onset of anaphase. Securin also acts as an activator for separase, where it aids in its localization to the nucleus and proper protein folding (Agarwal and Cohen-Fix, 2002; Hornig et al., 2002; Hellmuth et al., 2015). Securins are essential for growth in *S. pombe*, *D. melanogaster* and *C. elegans* (Funabiki et al., 1996; Stratmann and Lehner, 1996; Jäger et al., 2001; Kitigawa et al., 2002) but not in vertebrates (Hellmuth et al., 2015). In *S. cerevisiae*, *Δpds1* cells are viable at 24°C, although they demonstrate some growth defects and chromosome loss. At higher temperatures, however, *PDS1* becomes essential due to a temperature sensitive defect at G1/S that prevents normal spindle elongation and Esp1p from entering the nucleus (Yamamoto et al., 1996a; Jensen et al., 2001). Despite their importance in regulating the highly conserved

separase, securins are divergent proteins (Moschou and Bozhkov, 2002), and have yet to be identified in many organisms, including filamentous fungi for example.

Securin and the metaphase-to-anaphase transition are regulated in part by degradation mediated by the Anaphase Promoting Complex/Cyclosome (APC/C). The APC/C is a ubiquitin ligase system that functions during M to G1 phase and targets proteins for destruction through assembling a chain of ubiquitin tags on substrates (McLean et al., 2011). Such tags are recognized by the 26S proteasome and destroyed at the appropriate time. The APC/C is a large complex composed of 11 to 13 subunits (Barford, 2011). In *S. cerevisiae*, a catalytic domain consists of the cullin subunit Apc2p and the RING H2 domain subunit Apc11p, which are responsible for binding the E2-ubiquitin conjugate, as well as APC core components such as Cdc16p, Cdc27p and Cdc23p, for example (Peters, 2006; Barford, 2011; McClean et al., 2011). The non-catalytic core subunits act as scaffold and stabilizing factors, many of which contain the tetratricopeptide repeat (TPR) motif, a 34 amino acids region that acts to anchor proteins during complex formation and interactions (Barford, 2011). The APC/C complex acts to target several mitotic-specific proteins for degradation. Several subunits, including Cdc16p, Cdc23p and Cdc27p of *S. cerevisiae*, for example, are essential; temperature-sensitive mutants arrest as large-budded cells that contain a large mass of DNA lying either at or through the bud neck, and demonstrate chromosome loss (Lamb et al., 1994; Heichman and Roberts, 1996). APC/C activity is regulated by two cofactors; Cdc20p and Cdh1p (Morgan, 2007). During the early stages of mitosis, Cdc20p binds Cdc23p and Cdc26p through its N-terminus, anchoring it to the APC/C and directing APC/C activity towards mitotic proteins such as the cyclin Clb2p and securin, for example (Acquaviva and Pines, 2006; Barford, 2011; Qiao et al., 2016). In *S. cerevisiae*, *CDC20* mutants arrest in metaphase with elevated Clb2p and Pds1p levels (Cohen-fix et al., 1996), similar to the situation with absence of Cdc16p (Irniger and Nasmyth, 1997). Simultaneous absence of the securin *PDS1* in the *CDC20* mutant background results in a telophase arrest, suggesting that Cdc20p is important for mitotic exit, in addition to the metaphase-to-anaphase transition (Lim et al., 1998). Later in the mitotic cycle, the APC/C falls under control of Cdh1p. Cdh1p also binds Cdc23p and Cdc26p and assists the APC/C in targeting additional mitotic regulators such as the polo-like kinase Cdc5p, the remainder of Clb2p, securin, as well as Cdc20p

for degradation, permitting mitotic exit (Lianga et al., 2018). In *S. cerevisiae*, APC/C subunits and cofactors are regulated in part by phosphorylation by the CDK complex Cdc28p/Clb2p. Phosphorylation of Cdc16p and Cdc23p during anaphase help with the stabilization and binding of Cdc20p (Acquaviva and Pines, 2006). Phosphorylation of Cdh1p keeps the cofactor inactive until late mitosis (Harkness, 2018). In order for Cdh1p to become active later in mitosis, it must be dephosphorylated by the phosphatase Cdc14p (Jaspersen et al., 1999), which is under control of the Fourteen Early Anaphase Release (FEAR) and Mitotic Exit Network (MEN) pathways (Weiss, 2012).

  C. *albicans* is a diploid ascomycete that exists in many morphological forms including yeast, pseudohyphal, hyphal or chlamydospore cells, and is one of the most common opportunistic fungal pathogens of humans (Berman, 2012). It can exist as a commensal in the gastrointestinal and urogenital tracts and can also be responsible for causing both invasive and systemic infections. Systemic infections have been associated with mortality rates reaching 50% (da Silva Dantas et al., 2016). Identification of novel proteins as potential drug targets and the development of drug therapies is crucial given the increase in drug resistance and limitations in available treatments (O'Meara et al., 2015). For this, a thorough understanding of the basic biology of the organism and the mechanisms governing resistance in *C. albicans* is important (Sellam and Whiteway, 2016).

  Proper segregation of chromosomes and progression through mitosis is critical for survival and virulence in *C. albicans*. For example, changes in ploidy can be induced by stress, which is thought to contribute to diversity given the lack of a sexual cycle (Selmecki et al., 2010). However, the networks responsible for regulating these processes are not well defined. In addition, certain key players that have been explored show conserved as well as variations in function. For example, *C. albicans* homologues of the APC/C cofactors Cdc20p and Cdh1p are conserved in regulating anaphase onset, telophase, and mitotic exit through targeting the mitotic cyclin Clb2p and the polo kinase Cdc5p for degradation (Chou et al., 2011). However, Cdc20p depletion resulted in filamentation, in contrast to the large doublets formed from Cdc20p depletion in *S. cerevisiae* (Lim et al., 1998). In addition, *cdh1Δ/Δ* cells showed a pleiotropic phenotype and were enlarged, in contrast to the situation in *S. cerevisiae,* where cells were

significantly reduced in size due to a role for Cdh1p in repressing START (Jorgensen and Tyers, 2004). The cysteine protease separase (Esp1p) has also been characterized in *C. albicans*, and shows conservation in regulating chromosome segregation, but its depletion results in filamentous cells (Sparapani and Bachewich, 2019), in contrast to the large-budded phenotype of *esp1Δ* cells in *S. cerevisiae* (McGrew et al., 1992).

Recently, a novel separase-interacting factor specific to *Candida* species, Eip1p, was identified in *C. albicans* (Sparapani and Bachewich, 2019) and represents a candidate new securin. Eip1p contains KEN and D-box sequences that are normally recognized by the APC/C, similar to other securins, as well as conservation in part of its three-dimensional structure compared to the securin Pds1p (Sparapani and Bachewich, 2019). In addition, Eip1p is important for proper growth and chromosome segregation, and its levels are enriched in the presence of DNA damaging agents including MMS and HU, consistent with Pds1p in *S. cerevisiae* (Palou et al., 2015; Sparapani and Bachewich, 2019). Further, depleting Eip1p from cells arrested in metaphase during MMS or HU treatment results in a partial escape and progression to later mitotic phases, suggesting that it acts as an anaphase inhibitor. Eip1p is regulated in part by degradation, similar to other securins, since its levels were drastically reduced when cells were blocked in mitosis through depletion of the polo-like kinase Cdc5p, but not during absence of the APC/C cofactor Cdc20p. Although this suggests that Eip1p degradation may be mediated by APC/C$_{Cdc20p}$, Eip1p levels were not significantly enriched when Cdc20p was depleted, unlike other securins such as Pds1p. While this may be due to variability in the mitotic arrest point of Cdc20p- depleted cells of *C. albicans* (Chou et al., 2011; Sparapani and Bachewich, 2019), it is alternatively possible that regulated degradation of Eip1p during mitosis involves additional or other mechanisms. For example, degradation of residual Pds1p near the end of mitosis and into G1 phase requires the APC/C cofactor Cdh1p in *S. cerevisiae* (Hatano et al., 2016). In addition, turnover of Ndd1p, a transcriptional activator of the mitotic gene cluster in *S. cerevisiae*, requires the Skp, Cullin, F-box (SCF)-containing ubiquitin ligase system as well as the APC/C$_{Cdh1p}$ complex during mitosis and G1 phase (Edenberg et al., 2015; Sajman et al., 2015). In addition to showing many features and functions consistent with other securins, a proportion of Eip1p-depleted cells demonstrated some distinct traits including misoriented spindles, maintenance of

elongated spindles, and abnormal nuclear movements (Sparapani and Bachewich, 2019). This suggests the possibility that Eip1p has additional, separase-independent roles, similar to the securin Pttg1p in mammals that is important for microtubule nucleation (Moreno-Mateos et al., 2011).

In order to gain further insight on the regulation and functions of Eip1p, a new candidate securin, we explored the role of the APC/C in mediating degradation of Eip1p, and the identity of Eip1p-interacting proteins. Through investigating the influence of Cdc16p on Eip1p levels, we provide the first characterization of an APC/C core component in *C. albicans*, and show that it is essential for growth, metaphase progression and degradation of the mitotic cyclin Clb2p. We further show that Cdc16p is required for Eip1p degradation, thus confirming the involvement of the APC/C in regulating Eip1p. Affinity purification of Eip1p followed by mass spectrometry revealed homologues of cohesin subunit Smc3p, the structural maintenance of chromosomes factor Smc6p that is involved in DNA double-strand breaks by homologous recombination, APC/C subunit Apc3p/Cdc23p, as well as the phosphatase Cdc14p. These physical interactions have not been reported with Pds1p in *S. cerevisiae*, however the securin Pttg1p has been shown to interact with Apc3p in humans (Kraft et al., 2003). Overall, the results provide additional support that Eip1p is regulated in part in a manner similar to other securins, consistent with it being a new member of the securin family, and imply some potential novel mechanisms of action in influencing cohesin stability and mitotic progression.

3.3 Materials and Methods

3.3.1 Strains, oligonucleotides, plasmids, culture conditions

Strains, oligonucleotides and plasmids used in this study are listed in Tables S3.1-3.3, respectively. Strains were cultured in rich media (YPD) containing 1.0% yeast extract, 2.0% peptone, 2.0% glucose and 50 g/ml of uridine (Bensen et al., 2002). For strains under control of the *TET* promoter, 100μg/mL doxycycline was added for promoter repression (Lavoie et al., 2008). Alternatively, strains containing genes under control of the *MET3* promoter were incubated in synthetic defined (SD) yeast culture medium containing 0.67% of yeast nitrogen base, 2.0% dextrose, amino acid supplements (2.0 g adenine, 2.5 g uridine, 2.0 g tryptophan, 1.0 g histidine, 1.0 g arginine, 1.5 g tyrosine, 1.5 g isoleucine, 7.45 g valine, 1.5 g lysine, 2.5 g phenylalanine, 5.0 g glutamic acid, 10.0 g threonine and 3.0 g leucine per 50 L) that either lacked methionine and cysteine for promoter induction (-MC), or contained 2.5 mM methionine and cysteine for promoter repression (Care et al., 1999). For phenotype and Western blot assays, cells from plates were mixed in small volumes of inducing medium, from which large dilutions were made and cultured overnight. Cultures in low exponential phase were then collected and diluted to an O.D.$_{600nm}$ of 0.1 or 0.2, respectively, in fresh inducing or repressing medium, and incubated for indicated time points. For affinity purification of Eip1p-TAP from *CDC20* or *CDC16*-conditional strains, cells were prepared in the same way with the exception of diluting to an O.D.$_{600nm}$ of 0.1 in repressing medium and collecting at a final O.D.$_{600nm}$ of 0.4. For affinity purification of Eip1-TAP from exponential phase cells, strains were directly inoculated into YPD medium, cultured overnight, diluted into fresh YPD medium to an O.D.$_{600nm}$ of 0.1 and incubated until reaching an O.D.$_{600nm}$ of 0.8-1.0. All experiments were performed at 30°C, and repeated at least two times.

3.3.2 Strain Construction

In order to construct a strain carrying a single copy of *CDC16* under control of the *MET3* promoter and a copy of *EIP1* tagged at the C-terminus with the TAP epitope (Protein A and Calmodulin binding protein separated by a tobacco etch virus (TEV) protease cleavage site) (Lavoie et al., 2008), the *TAP-ARG4* cassette was amplified from plasmid pFA-*TAP-ARG4* with

primers SS33F and SS33R, and transformed into strain BWP17. The resulting strain SS58 was confirmed by PCR with primer pair CaARG4F and SS25R (Figure S3.1). One copy of *CDC16* was next placed under control of the *MET3* promoter. Primer pairs SS43F, SS43R and SS44F, SS44R were used to amplify fragments lying upstream and downstream of the *CDC16* START codon, respectively, while primers SS45F and SS45R amplified a *HIS1-MET3* fragment from plasmid pFA-*MET3*-Ca*HIS1* (Gola et al., 2003). The three fragments were combined in a fusion PCR with primers SS43F and SS44R. The final construct was transformed into strain SS58 resulting in strain SS71 (*EIP1/EIP1-TAP-ARG4, CDC16/MET3::CDC16-HIS1*). Correct integration was confirmed using PCR with primer pair SS43F and CaHIS1R. To replace the second copy of *CDC16* with the *URA3* marker, primer pairs SS40F, SS40R and SS41F, SS41R were used to amplify sequences lying upstream of the START or downstream from the STOP codon of *CDC16*, respectively, and primers SS42F and SS42R were used to amplify *URA3* from plasmid pBS-Ca*URA3* (Chou et al., 2011). A fusion PCR was conducted using primer pair SS40F and SS41R and the product was transformed into strain SS71 resulting in strain SS75 (*EIP1/EIP1-TAP-ARG4, cdc16::URA3/MET3::CDC16-HIS1*). Correct integration was confirmed using PCR with primer pair SS46F and CaURA3R (Figure S3.2).

To create a strain carrying a single copy of *CLB2* tagged at the C-terminus with the TAP epitope in a *CDC16* conditional background, a copy of *CDC16* was placed under control of the *MET3* promoter and a second copy of *CDC16* was replaced with the *URA3* cassette as described above to generate strain SS82 (*cdc16::URA3/MET3::CDC16-HIS1*). Next, the *TAP-ARG4* cassette was amplified from plasmid pFA-*TAP-ARG4* with primers AG5F and AG5R, and transformed into strain SS82 (*cdc16::URA3/MET3::CDC16-HIS1*) resulting in strain SS87 (*CLB2/CLB2-TAP-ARG4, cdc16::URA3/MET3::CDC16-HIS1*). Correct integration was confirmed using primers CaARG4F and AG6R (Figure S3.3).

In order to create a strain carrying a copy of *EIP1* tagged at the C-terminus with the HA epitope and *CDC14* tagged with MYC, *HA-ARG4*-was amplified from plasmid pFA-*HA-ARG4* with primers SS33F and SS33R, and transformed into strain BWP17, resulting in strain SS88 (*EIP1/EIP1-HA-ARG4*). Proper integration of the construct was determined using PCR with primers CaARG4F and SS25R (Figure S3.4). Next, a *MYC-HIS1* cassette was amplified from

plasmid pMG2093 (Bensen et al., 2005) with oligonucleotides SS53F and SS53R. The resulting construct was transformed into strain SS88 resulting in strain SS91 (*EIP1/EIP1-HA-ARG4, CDC14/CDC14-MYC-HIS1*). Proper integration was confirmed by PCR using primers CaHIS1F and SS54R.

3.3.3 Protein extraction, Western blotting, Affinity purification

In order to measure the levels of Eip1p or Clb2p in response to manipulation of Cdc16p, cells from strains SS75 and SS87 were collected as indicated above. Protein extracts were prepared using HK buffer according to Liu et al., 2010, and protein was extracted and quantified using the Bradford assay (Bio-Rad, Mississauga). Western blots were completed and quantified as previously described (Sparapani and Bachewich, 2019). Affinity purifications were carried out according to Rigaut et al. 1999 and Liu et al. 2010, as described in Sparapani and Bachewich (2019). For purification of Eip1p-TAP from exponential-phase, *CDC20*-conditional or *CDC16*-conditional cells, 350 mg of protein from strains BWP17 and SS40, 526 mg of protein from strains AG153 and SS41, or 419 mg of protein from strains SS82 and SS75 were utilized, respectively.

3.3.4 Cell imaging

In order to visualize DNA, cells were fixed in fresh 70% ethanol for 20 min, washed with sterile water, incubated in 1.0 µg/ml of 4′, 6′-diamidino-2-phenylindole dihydrochloride (DAPI; Sigma-Aldrich) for 20 min, washed twice with sterile water, and mounted on slides. Cells were imaged on a LeicaDM6000B microscope (Leica Microsystems Canada Inc., Richmond Hill, ON, Canada) equipped with a Hamamatsu-ORCA ER camera (Hamamatsu Photonics, Hamamatsu City, Japan) and the HCX PL APO 100x NA 1.40-0 oil or HCX PLFLUO TAR 100x NA 1.30-0.6 oil objectives. Differential Interference Contrast (DIC) optics, or epifluorescence with DAPI (460nm) filters were utilized. Images were captured with Volocity software (Improvision Inc., Perkin-Elmer, Waltham, MA).

3.3.5 *Bioinformatic Analysis*

Comparative analysis of the amino acid sequence of *CDC16* began with the alignment of its sequence alongside the sequences of Cdc16p (*S. cerevisiae*), Cut9p (*S. pombe*), EMB-25 (*C. elegans*), and CDC16 (*H. sapiens*) using ClustalW (Larkin et al., 2007). Aligned sequences obtained from ClustalW were further analyzed using ESPript software (Robert et al., 2014). Parameters used included sequence similarity (% similarity), alignment output layout (flashy, portrait), and a global score of 0.7, as set by the program. Three dimensional protein simulation was generated using the Protein Homology/Analogy Recognition Engine V 2.0 (PHYRE 2.0). The Cdc16 amino acid sequence was downloaded from the Candida Genome Database (http://www.candidagenome.org) and entered into PHYRE2.

3.4 Results

3.4.1 *C. albicans* contains homologues of the APC complex components, including *CDC16*

If the APC/C functions in *C. albicans* similar to the situation in *S. cerevisiae*, and is critical for mediating Eip1p turnover during mitosis, as with other securins, we hypothesize that the levels of Eip1p should be significantly enhanced when APC/C activity is downregulated, and that lack of strong or consistent enrichment when Cdc20p was depleted is due to variability in the arrest phenotype. In order to investigate this, we first characterized the APC/C and its components in *C. albicans*. The APC/C in *S. cerevisiae* contains 13 core subunits (Table 3.1), some of which are present in two copies (Barford, 2011). These include catalytic subunits Apc1p, Apc2p and Apc11p, scaffold factors Apc4p and Apc5p, Cdc16p, Cdc23p, Cdc27p, stabilizing factors Apc9p, Cdc26p, and Apc13p, as well as the Cdc27p stabilizing factor Apc10p and Mnd2p (Acquaviva and Pines, 2006). In comparison, *C. albicans* contains homologues of the catalytic, scaffolding and stabilizing subunits except for Apc9p and Mnd2p, a subunit that prevents premature degradation of sister chromatid during meiosis (Acquaviva and Pines, 2006). Sequence similarity between each of the APC/C subunits in *C. albicans* and their homologues in *S. cerevisiae* ranges between 20% and 50% with subunits Cdc16p and Cdc27p containing 49% sequence similarity (https://blast.ncbi.nlm.nih.gov/Blast.cgi).

Table. 3.1 Comparison of homologues of APC/C subunits[1]

Subunits (*S. cerevisiae*)	*Homo sapien*	*C. albicans*	Function in *S. cerevisiae*	Function in *C. albicans*	Essential in *C. albicans*[2]	Filamentation in *C. albicans*
Apc1	Anapc1	Apc1	Scaffolding	Uncharacterized, putative APC/C subunit	No	None
Apc2	Anapc2	Apc2	Catalytic	Uncharacterized, putative APC/C catalytic subunit	No	None
Cdc16	Anapc6	Cdc16	Scaffolding	Uncharacterized	Yes	Yes
Cdc27	Anapc3	Cdc27	Cdh1 binding	Uncharacterized, putative ubiquitin-ligase	No	None
-	Anapc7	-	Cdh1 binding	-	Yes	-
Apc4	Anapc4	orf19.5692	Scaffolding	Uncharacterized, putative APC/C catalytic subunit	No	Yes
Apc5	Anapc5	Apc5	Scaffolding	Uncharacterized, putative APC/C catalytic subunit, role in chromatin assembly	No	No
Apc9	-	-	Cdc27 stabilizing	-	-	-
Cdc23	Anapc8	Cdc23	Scaffolding	Uncharacterized, putative APC/C subunit	Yes	Yes
Apc10	Anapc10	Apc10/Doc1	Substrate recognition	Uncharacterized, putative APC/C catalytic subunit, role in chromatin assembly	-	NA
Apc11	Apc11	Apc11	Catalytic RING	Uncharacterized, putative APC/C catalytic subunit, role in APC/C localization	Yes	Yes
Cdc26	Cdc26	orf19.3471	Cdc16 stabilizing	Uncharacterized	Yes	Yes
Apc13	Apc13	-	Cdc26 stabilizing	-	-	-
Mnd2	-	-	Prevents premature sister chromosome segregation during meiosis	-	-	-

[1]Homologues of the APC/C subunits in *S. cerevisiae* and humans as well as their function were obtained from Barford, 2011.
[2]Essentiality assays were referenced from O'Meara et al., 2015.

In order to initiate a characterization of APC/C function in *C. albicans*, we focused on the subunit homologue Cdc16p. Cdc16p is part of a stabilization complex with Cdc23p and Cdc27p which help bind the cofactors Cdc20p and Cdh1p to the APC/C during mitosis (Acquaviva and Pines, 2006). Depletion of Cdc16p prevents APC/C activity in *S. cerevisiae*, resulting in a mitotic block and elevated levels of the mitotic cyclin Clb2p and the securin Pds1p (Cohen-Fix et al., 1996; Irniger and Nasmyth, 1997), and is essential in *C. albicans* (O'Meara et al., 2015). *C. albicans CDC16* encodes a protein of 785 amino acids and a predicted molecular weight of 89

kDa (http://www.candidagenome.org). A BLAST search of the *CDC16* sequence against all known organisms (http://blast.ncbi.nlm.nih.gov/Blast.cgi) or against fungi alone (http://www.yeastgenome.org) revealed homologues that were present in other fungi including most *Candida* species as well as in *S. pombe* (Cut9p), and humans (Cdc16p) (Figure 3.1). APC/C subunits including Cdc16p are well conserved, since all contain several TPR motifs (Figure 3.1 A,B) (Barford, 2011). Moreover, sequence alignment between Cdc16p in *C. albicans* and Cut9p or between *C. albicans* Cdc26p and Cdc16p in humans revealed 46% and 33% identity, respectively. In order to explore the *CDC16* sequence further, a 3D structure analysis comparison using the program Phyre2 Protein Folder was performed. Intriguingly, the results demonstrated 100% confidence in alignment at a specific region with Cut9p, and some similarity in the predicted 3D structure based on this alignment (Figure 3.1C). Thus, Cdc16p in *C. albicans* shows conservation at the sequence level as well as in its protein structure compared to the APC/C subunit in other organisms including yeast.

A.

B.

Cdc16p (785aa)

MTTNQSINTTTTTTTTTTTTTTTTTTTTTSSTQSISPFVPYHPNTHIFIMVQNQKTPNHNNST
LYISPVVNKKNDLMYVTPPNPTTVTTNKLLETPGSNKSTSTSTSSFFHFDRASNHTLHDR
VTDNNLLDDPLTPVDKLRLWRHDAIMQHQYKTAEFIGDKILELTNDDANDAFWLGQVYF
N QGNYLRCKNLLTSNINYQNSISCRYLAGYSLIKLEMWDDALDLIGETNPFKNNNDSGSSS
TTTTTDGGIKLESSMCYLRGLIYANQNNFERAKECYKEACIVDVKCYEAFNELIMNNLMT
PNEEWEFVTQLNFRDNLDDTNNDELIKLLYMTKLSKYLNPDKFNESEHILKEEYELYDN
CDLMLSRADYLYIQCNFDECLNLCERILNKDEYNFDVLPNYLSCLYELGGKNKLFLKAHQ
LAELHPINPMTWLAIGTYYLSINKMVEARKFFSKATLLNPNFGNGWIGFAHTFAAEGEHE
QAISAYAFAARLFPGTHLPNLFLGMQHLQMNNLNLSEEYLLASYHICNSDPLLLNELGVI
NFHKNQFDKAEFFLQEALNAAKNLNSDSKTWISIHANLGHVYRRANQPYKALDCFNQVL
KISNKNDANILSAIGLIHLRLQNIFQAIEFLHDALAISPLDPIASDLLKRALEANKENQEIFSTT
EKLFQLNLPIERRKYESSRLAKQQRQSRCSISGGGGGGGGGEENTKNIVTPLTTKIRDRHINV
GNSSIDPVLFVNDPTGKNEDIQDDGEPEGEGDDVTLLAQELQNGEASSDDEDVMDIESD

Motif	**Consensus Sequence**
Tetratricopeptide repeat (TPR)	-X-X-W-LG-Y-A-F-A-P-X-X-

C.

94

Figure 3.1. Bioinformatic analyses of Cdc16p in *C. albicans*

(A) Comparative analysis of amino acid sequences of Cdc16p homologues from *C. albicans* (Cdc16p), *S. cerevisiae* (Cdc16p), *H. sapiens* (CDC16), *S. pombe* (Cut9p) and *C. elegans* (EMB- 27). TPR repeat domains are highlighted in brown and regions of disorder are highlighted in black. Amino acid sequences were obtained from the Saccharomyces Genome Database (https://www.yeastgenome.org), Candida Genome Database (http://www.candidagenome.org), WormBase (https://www.wormbase.org/#012-34-5), Pombase (https://www.pombase.org) and UniProt (https://www.uniprot.org), respectively. Sequences were analyzed with InterPro (https://www.ebi.ac.uk/interpro/) and information in Bachmann et al., 2016. (B) Cdc16p amino acid sequence (Candida Genome Data base; http://www.candidagenome.org), with TPR motifs indicated. (C) 3D protein simulation using PHYRE 2.0, demonstrating some similarity at a specific region with Cut9p from *S. pombe*. Bottom portion represents the region of amino acid sequence homology between the template strain (Cut9p) and query strain (Cdc16p). Green coils and blue arrows represent regions of helices and pleated sheet arrangements, respectively. Polar properties of the protein sequences are shown in colored amino acids. Secondary structures are represented by the number of "G" and "T" segments present, where G indicates a 3-turn -helix and T represents a hydrogen-bonded turn.

3.4.2 Depletion of Cdc16p results in growth inhibition and filamentation

The APC component *CDC16* is essential in *S. cerevisiae* and its depletion results in large-budded cells containing a large mass of DNA lying either near or through the budneck (Lamb et al., 1994; Heichman and Robert, 1996). A phenotypic screen of a set of *C. albicans* strains under control of the *TET* promoter demonstrated that *ORF19.1792* (*CDC16*) was also essential for growth, and its depletion resulted in strong growth defects as well as some filamentation (O'Meara et al., 2015). However, the functions of Cdc16p and any role in regulating mitosis were not determined. In order to characterize Cdc16p function, we created a strain where one copy of *CDC16* was deleted and the second copy was placed under control of the *MET3* promoter. Cells were incubated in inducing (-MC) or repressing (+MC) medium for 5 or 8 h, and fixed. In repressing medium, cells lacking Cdc16p were predominantly large-budded by 5 h, but more filamentous by 8 h (Figure 3.2). Intriguingly, of the elongated cells, 12% demonstrated an enlarged daughter cell from which emanated a filament, suggesting enhanced isometric growth of the bud followed by formation of a polarized outgrowth (Figure 3.2). In contrast, normal yeast-form cells were observed under inducing conditions, and in a wild-type control strain in both media (Figure 3.2). Similar results were observed when *CDC16* was repressed with the *TET* promoter using doxycycline (Figure 3.3), in agreement with previous results (O'Meara et al., 2015). Thus, absence of Cdc16p in *C. albicans* results in a block in yeast cell proliferation, followed by filamentous growth.
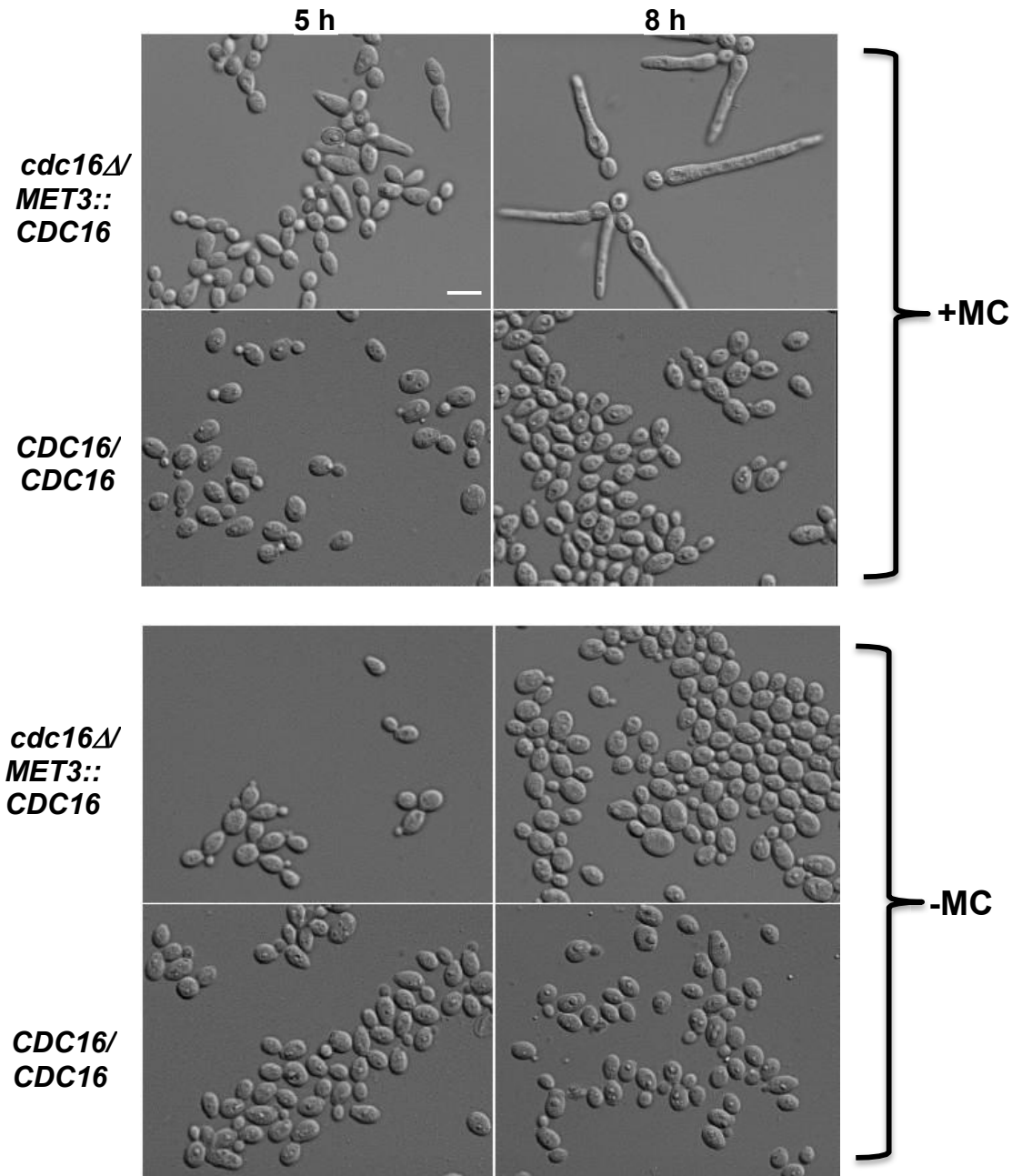
Figure 3.2. Depletion of Cdc16p results in elongated filaments.

Overnight strains of BWP17 (*CDC16/CDC16*) and SS75 (*cdc16::URA3/MET3::CDC16-HIS1, EIP1/EIP1-TAP-ARG4*) were diluted into liquid –MC or +MC medium and incubated at 30°C for 5 h or 8 h. Bar: 10μm.
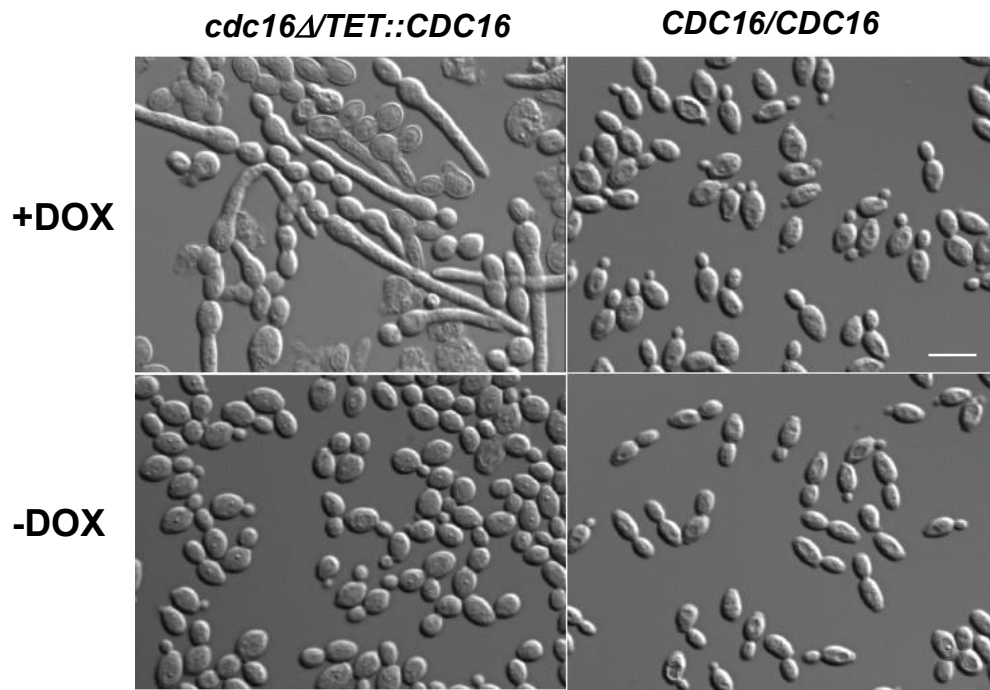
Figure 3.3. Depletion of Cdc16p by the *TET* promoter shows filamentous growth.
Overnight strains of strains BWP17 (*CDC16/CDC16)* and GRACE strain
cdc16::URA3/TET::CDC16-HIS1 were diluted into liquid YPD medium with or without 100
µg/mL doxycycline and incubated at 30°C for 8 h. Bar: 10µm.

3.4.3 Depletion of Cdc16p results in an early mitotic arrest

In *S. cerevisiae*, temperature-sensitive mutants of *CDC16* grown at restrictive temperature were blocked in mitosis with high levels of the mitotic cyclin Clb2p. Cells were large-budded with either a single mass of DNA on one side of the bud neck (64%), or showed segregated DNA through the bud-neck and into the daughter cell (20%) (Palmer et al., 1989; Heichman and Roberts, 1996). In order to determine if *C. albicans* Cdc16p is required for mitotic progression, the conditional *CDC16* and control strains were incubated in inducing (-MC) or repressing (+MC) medium for 5 or 8 h, fixed and stained with DAPI. Wild-type cells grown in both media or conditional *CDC16* cells grown in inducing medium demonstrated normal distributions of yeast cells, with approximately 30 % in mitosis, based on being large-budded and containing a single mass of DNA (Figure 3.4; Table 3.2). In contrast, approximately 55% of cells depleted of Cdc16p were in this form (Figure 3.4; Table 3.2). After 8 h of *CDC16* depletion, approximately 68% of cells contained a single mass of DNA compared to 39% in inducing medium (Figure 3.4; Table 3.3). Thus, *C. albicans'* Cdc16p is critical for mitotic progression, and possibly the transition from metaphase to anaphase.
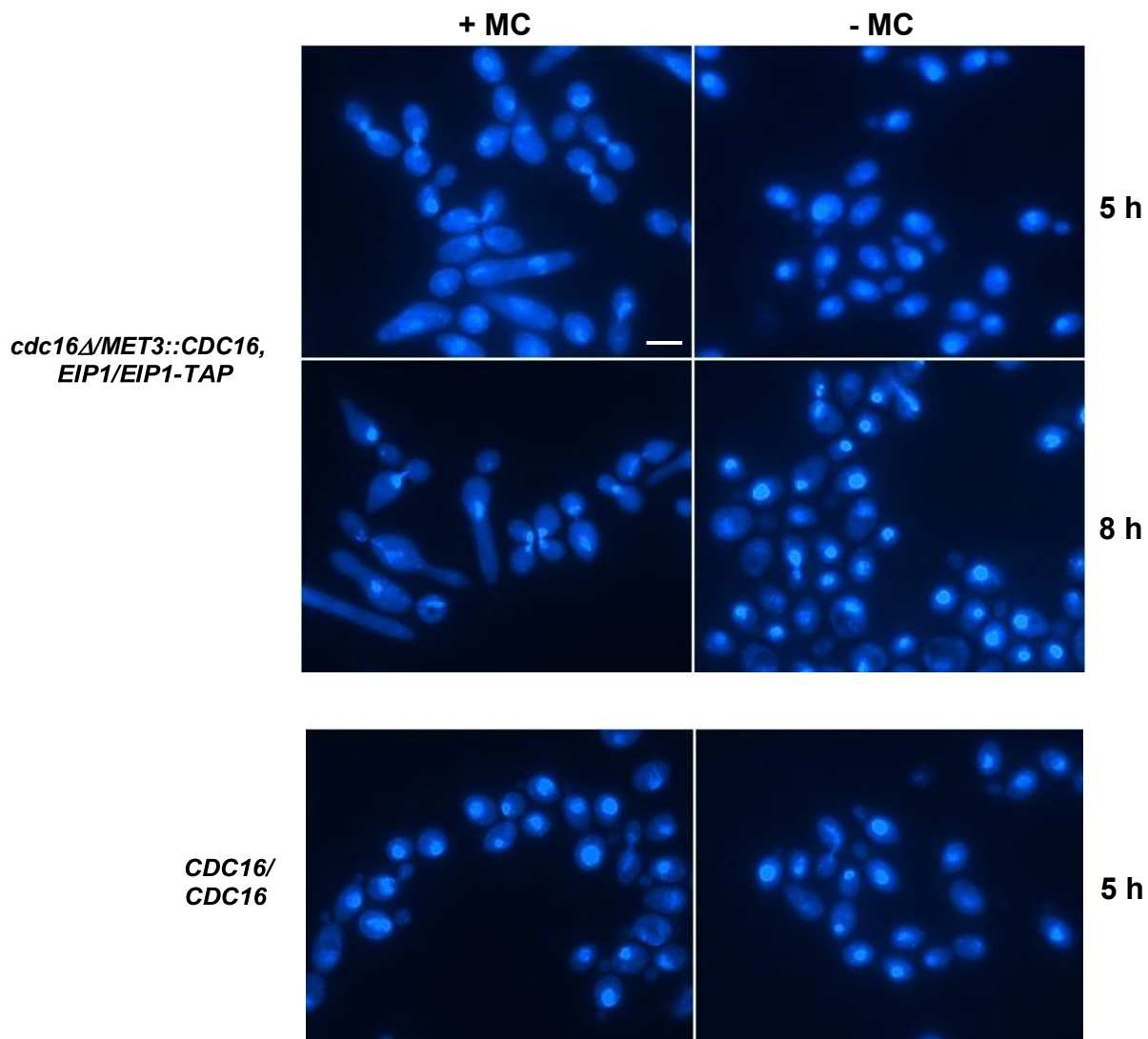
Figure 3.4. Absence of Cdc16p results in an early mitotic arrest.

Strains SS75 (*cdc16::URA3/MET3::CDC16-HIS1, EIP1/EIP1-TAP-ARG4,*) and BWP17 (*CDC16/CDC16*) were incubated in inducing (-MC) or repressing (+MC) medium for 5 or 8 h, fixed and stained with DAPI. Bar: 10μm.

Table 3.2. Number and distribution of nuclei in Cdc16p-depleted cells after 5 h[1].
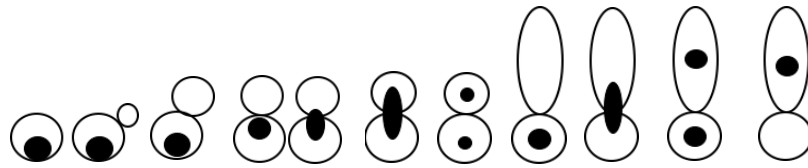
+MC									
cdc16/MET3::CDC16, EIP1/EIP1-TAP (n=225)	4.4	12	20	23	30	0.4	2.9	5.4	3.9
CDC16/CDC16 (n=251)	51	21	4.4	8.0	15	0	0	0	0.3
-MC									
cdc16/MET3::CDC16, EIP1/E (n=218)	71	17	4.6	5.0	3.2	0	0	0	0
CDC16/CDC16 (n=221)	65	22	4.5	4.5	4.1	0	0	0	0

[1]Percentage of cells showing the indicated patterns. Strains SS75 (*cdc16::URA3/MET3::CDC16-HIS1, EIP1/EIP1-TAP-ARG4*) and BWP17 (*CDC16/CDC16*) were incubated in +MC or –MC medium for 5 h, fixed, and stained with DAPI.

Table 3.3. Number and distribution of nuclei in Cdc16p-depleted cells after 8 h[1].
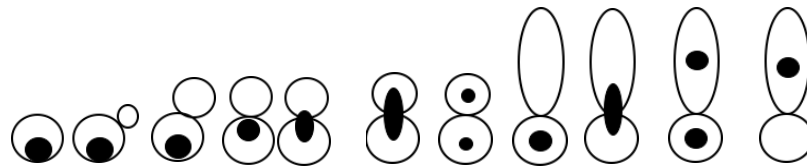
+MC									
EIP1/EIP1-TAP, cdc16/MET3::CDC16 (n=217)	2.5	2.5	12	8.4	18	2.5	7.4	11	35
CDC16/CDC16 (n=241)	58	22	5.4	3.1	12	0	0.4	0	0
-MC									
EIP1/EIP1-TAP, cdc16/MET3::CDC16 (n=200)	41	28	5.0	6.5	20	0	0	0	0
CDC16/CDC16 (n=210)	78	7.6	3.3	3.3	6.6	0.5	0	0	0

[1]Percentage of cells showing the indicated patterns. Strains SS75 (*cdc16::URA3/MET3::CDC16-HIS1, EIP1/EIP1-TAP-ARG4*) and BWP17 (*CDC16/CDC16*) were incubated in +MC or –MC medium for 8 h, fixed, and stained with DAPI.

Previous work in *C. albicans* demonstrated that Cdc20p is important for the metaphase-to-anaphase transition and mitotic exit (Chou et al., 2011). Depletion of Cdc20p with the *MET3* promoter resulted in cells initially containing a single mass of DNA, similar to depletion of Cdc16p. However, at later stages, most cells contained 2 DNA masses within a filament connected by an elongated spindle, unlike Cdc16p-depleted cells, indicating progression through metaphase and a block at late anaphase. This phenotype could be due to general promoter leakiness, the possibility that only trace amounts of Cdc20p are required for progression through metaphase, or that Cdc20p is important, but not essential, for the metaphase-to-anaphase transition. Indeed, the previous study employed a lower concentration of methionine and cysteine for repressing the *MET3* promoter (2.5 mM, 0.5mM, respectively) than that used in the current study with the conditional *CDC16* strain (2.5mM for both amino acids). In order to explore this further and directly compare the phenotypes of cells depleted of Cdc20p vs. Cdc16p, the conditional *CDC20* strain was incubated in inducing (-MC) or repressing medium (+MC; 2.5 mM methionine and cysteine) for 5 or 8 h, fixed and stained with DAPI. After 5 h of repression, approximately 44% of Cdc20p-depleted cells were large-budded or elongated and contained a single mass of DNA, compared to 43% with two nuclei (Table 3.4). By 8 h of repression, 36% of large-budded or elongated cells contained a single nucleus, compared to cells over 50% with two masses of DNA (Table 3.5), in agreement with the previous study (Chou et al., 2011). The results demonstrate that repressing *CDC16* results in a stronger block in early mitosis compared to repressing *CDC20* (Table 3.2). Thus, Cdc16p may be critical for metaphase progression, and either trace amounts of Cdc20p are required, or Cdc20p may not be essential for the process.

Table 3.4. Number and distribution of nuclei in Cdc20p-depleted cells after 5 h[1].

+MC									
EIP1/EIP1-TAP, cdc20/MET3::CDC20 (n=204)	3.0	2.5	1.5	5.5	11	6.9	9.3	43	17
-MC									
EIP1/EIP1-TAP, cdc20/MET3::CDC20 (n=207)	37	16	9.7	5.8	32	0	0	0	0

[1]Percentage of cells showing the indicated patterns. Strain SS75 (*EIP1/EIP1-TAP-ARG4, cdc20::URA3/MET3::CDC20-HIS1*) was incubated in +MC or –MC medium for 5 h, fixed, and stained with DAPI.

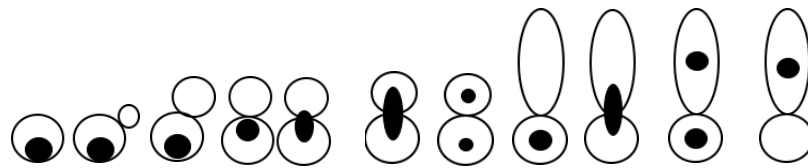**Table 3.5. Number and distribution of nuclei in Cdc20p-depleted cells after 8 h[1].**
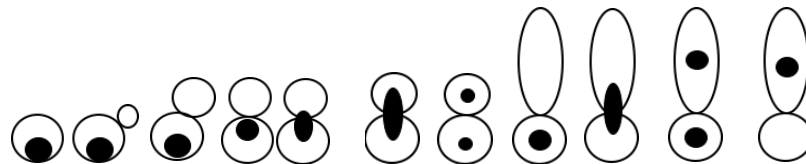
+MC									
EIP1/EIP1-TAP, cdc20/MET3::CDC20 (n=86)	8.3	5.9	4.8	1.2	3.6	7.1	4.8	55	12
-MC									
EIP1/EIP1-TAP, cdc20/MET3::CDC20 (n=227)	47	20	5.7	5.7	21	0	0	0	0

[1]Percentage of cells showing the indicated patterns. Strain SS75 (*EIP1/EIP1-TAP-ARG4, cdc20::URA3/MET3::CDC20-HIS1*) was incubated in +MC or –MC medium for 8 h, fixed, and stained with DAPI.

3.4.4 Absence of Cdc16p results in an enrichment in the mitotic cyclin Clb2p and Eip1p

In *S. cerevisiae*, the APC/C binds Cdc20p during early mitosis in order to target cyclin Clb2p and securin for degradation (Morgan, 2007). Later, the APC/C falls under control of Cdh1p for targeting and degrading the remainder of Clb2p, as well as other mitotic regulators including the remainder of Pds1p, Cdc20p and the polo-like kinase Cdc5p (Cohen-Fix et al., 1996; Irniger and Nasmyth, 1997; Hatano et al., 2016). In order to demonstrate the mechanisms of action of Cdc16p and determine whether it and the APC/C are important for mitotic protein degradation, we next investigated whether Cdc16p influenced turnover of the mitotic cyclin Clb2p. For this, we constructed a strain carrying a single copy of Clb2p tagged with the TAP epitope in a *CDC16*-conditional background. The strain was incubated in inducing (-MC) or repressing (+MC) medium for 5 or 8 h and processed for Western blot analysis. In the absence of Cdc16p, Clb2p was induced 1.9 or 1.4 times the level in cells containing Cdc16p, respectively (Figure 3.5). Thus, Cdc16p is important for turnover of the mitotic cyclin Clb2p, similar to its homologue in *S. cerevisiae*.

The securin Pds1p is significantly enhanced following down-regulation of the APC/C by depleting cells of Cdc20p (Visintin et al., 1997) or Cdc16p (Cohen-Fix et al., 1996). In order to confirm that the APC/C is important for Eip1p turnover, we next asked if Cdc16p influenced the levels of Eip1p. For this, a strain was constructed containing a single copy of Eip1p tagged with the TAP epitope in a *CDC16* conditional background (Figure S3.2). Cells were incubated in inducing or repressing medium and processed for Western blotting as described for Clb2p. In the absence of Cdc16p, Eip1p levels increased two fold relative to that in inducing conditions at 5 h, and this remained constant after 8 h (Figure 3.5). Thus, Eip1p is modulated in part by the APC/C, further demonstrating its similarity to other securins, and the APC/C subunit Cdc16p in *Candida albicans* shows conservation in contributing to APC/C-mediated targeting and degradation of important mitotic factors in *C. albicans*.

	CLB2/CLB2-TAP, cdc16/MET3::CDC16				EIP1/EIP1-TAP, cdc16/MET3::CDC16			
	5 h		8 h		5 h		8 h	
	-MC	+MC	-MC	+MC	-MC	+MC	-MC	+MC
A.R.D	1.0	1.9	1.0	1.4	1.0	1.8	1.0	2.0
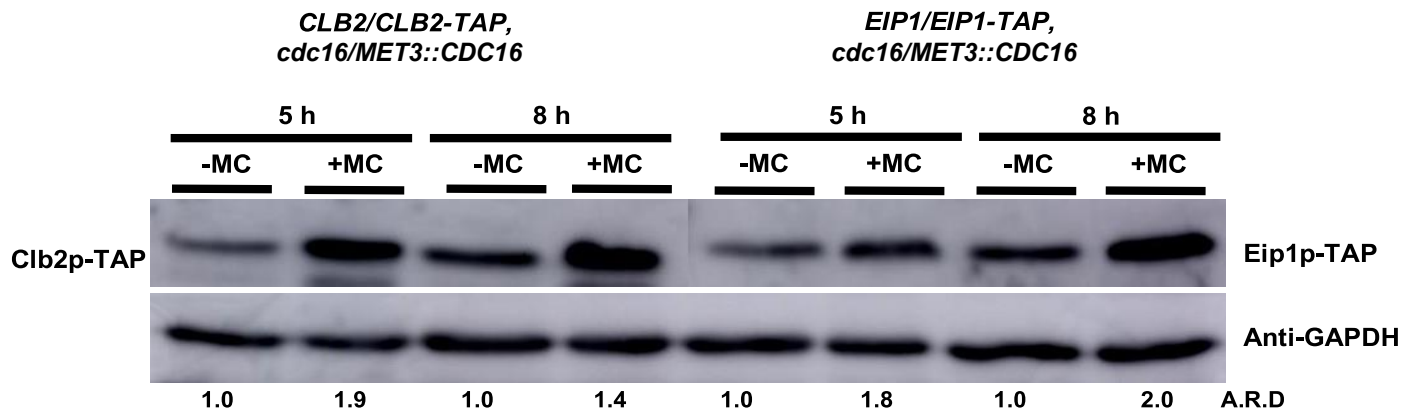
Figure 3.5. Depletion of Cdc16p results in increased levels of both Eip1p and Clb2p.
Strains SS87 (*CLB2/CLB2-TAP-ARG4, cdc16::URA3/MET3::CDC16-HIS1*) and SS75
(*EIP1/EIP1-TAP-ARG4, cdc16::URA3/MET3::CDC16-HIS1*) were incubated in inducing (-MC)
or repressing (+MC) medium. Samples were collected at 5 or 8 h and processed for Western blot
analysis using anti-TAP antibody. Anti-GAPDH antibody was used as a loading control.
Adjusted relative densities (A.R.D) of Clb2p-TAP or Eip1p-TAP bands were determined using -
MC medium as a reference, according to Chou et al., 2011.

3.4.5 Identification of Eip1p-interacting factors reveals Cdc14p phosphatase, APC subunit Apc2p and cohesin subunit Smc3p

We previously demonstrated that the separase-binding protein Eip1p is important for growth, chromosome organization, spindle orientation, and is regulated in part by degradation in mitosis. In order to gain further insight on its function and mechanisms of action, we investigated its interacting factors using affinity purification and mass spectrometry. For this, Eip1p was tagged with the TAP epitope and affinity purification was performed from exponential-growth phase cells. Mass spectrometry revealed Esp1p, the mitotic phosphatase Cdc14p as well as the cohesin subunit Smc3p (Table 3.6). Interestingly, additional co-purifying proteins included the core APC/C subunit Apc2p, Tom1p; a putative E3 ubiquitin ligase protein, the chromatin assembly protein Spo69p, and Rpn9p; a protein factor involved in proteasome assembly. Additional co-purifying factors included the RNA polymerase mediator protein Med1p, as well as Rna14p, which plays a role in RNA binding and DNA damage response. In order to optimize the assay and number of co-purifying peptides, we next tagged Eip1p with the TAP epitope in a *CDC20*-conditional background in order to synchronize cells in mitosis and potentially enhance protein yield. Affinity purification was conducted and samples were processed for mass spectrometry. Co-purifying peptides corresponded to proteins Eip1p, Esp1p, and Cdc14p, which was identified in three separate trials. Intriguingly, Cdc14p does not physically interact with Pds1p in *S. cerevisiae* (https://www.yeastgenome.org). In addition, several uncharacterized proteins including orf19.3213p and orf19.4011 co-purified (Table 3.7). Eip1p also co-purified with several factors associated with ubiquitination, such as Ubi3p, Tom1p, and the proteasome, including Apc2p, Rpn9p, Ecm29p, for example. In addition, several-filament-associated factors, including Kem1p, Fab1p and Opi1p, Ecm29p, and Uso6p also co-purified.

Since depletion of Cdc16p resulted in enrichment of Eip1p (Figure 3.5), we reasoned that affinity purification of Eip1p under these conditions may optimize identification of Eip1p-interacting proteins. We thus repeated the affinity purification of Eip1p-TAP from the *CDC16* conditional strain under repressing conditions, and performed mass spectrometry. While Eip1p was successfully affinity purified from cells (Figure 3.6), mass spectrometry did not reveal any co-purifying peptides, suggesting technical issues with the procedure. Overall, the results present

putative co-purifying factors of Eip1p, which reinforce its interaction with separase, a role in regulating chromatin segregation, and possibly other processes in mitosis as well.
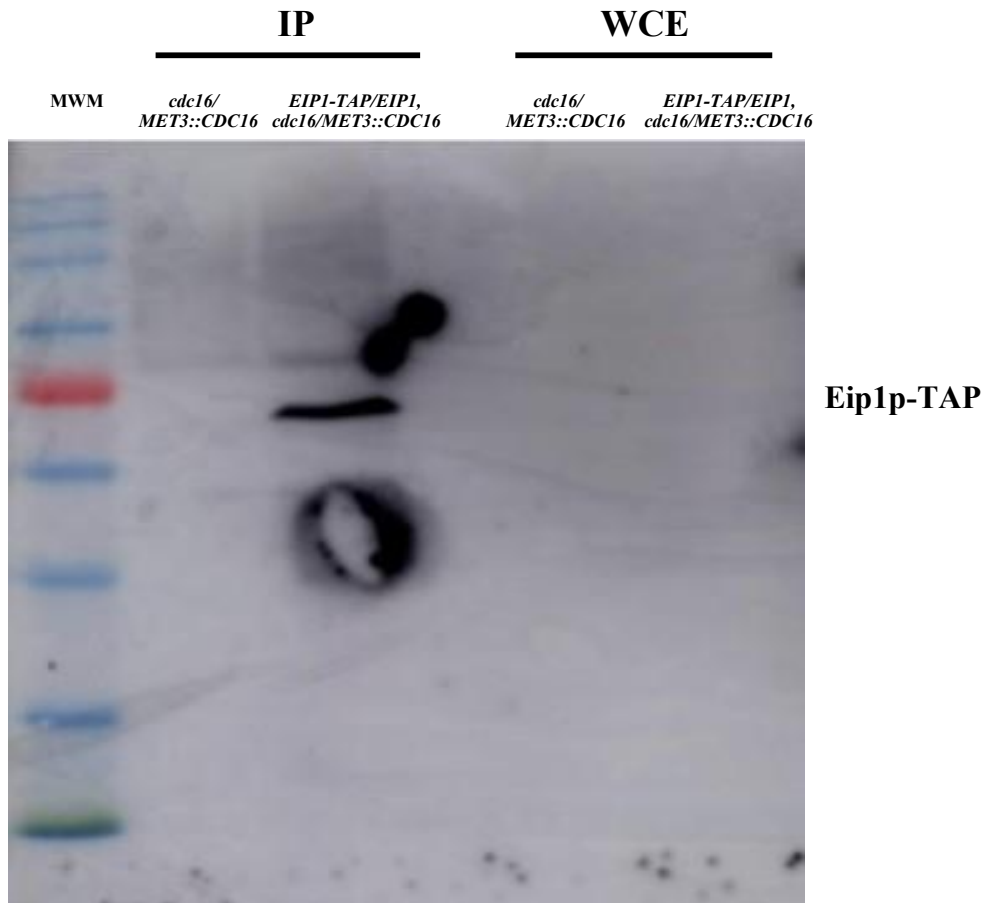
Figure 3.6. Tandem Affinity purification of Eip1p-TAP from *CDC16*-depleted cells. Protein extracted from 4 L cultures of strains SS82 (*cdc16::URA3/MET3::CDC16-HIS1*) and SS75 (*EIP1-TAP-ARG4/EIP1*, *cdc16::URA3/MET3::CDC16-HIS1*) were subjected to tandem affinity purification. Elutions were TCA precipitated and run on an SDS-PAGE gel for Western blot analysis.

Table 3.6. Orbitrap LC/MS analysis of putative Eip1p-interacting proteins from exponential-phase cells[1]

PROTEIN ID	No. of Peptides[2,3]	ORF	Identified Proteins	Frequency of Hits[4]
C4_07180W_A	6	UBI3	Fusion of ubiquitin with the S34 protein of the small ribosomal subunit; mRNA decreases upon heat shock, appears to be degraded; functional homolog of *S. cerevisiae RPS31*; Hap43-induced; Spider biofilm repressed	1
A0A0A6NJ08_CANAX	4	ESP1	Putative caspase-like cysteine protease; mutation confers increased sensitivity to nocodazole; periodic mRNA expression, peak at cell-cycle S/G2 phase; mRNA binds She3	2
C1_13420C_B	4	KEM1	5'->3' exoribonuclease of cytoplasmic stress granules; role in filamentous growth; complements slow growth/mating of *S. cerevisiae kem1* mutant; required for SD or Spider medium biofilm formation	1
C2_03180C_B	3	TOM1	Uncharacterized; putative E3 ubiquitin ligase	1
C3_02700W_B	3	SMC3	Protein similar to *S. cerevisiae* Smc3p, which is an ATPase involved in sister chromatid cohesion; likely to be essential for growth, based on insertional mutagenesis strategy	1
C3_06810W_B	2	APC2	Ortholog(s) have ubiquitin protein ligase activity and role in anaphase-promoting complex-dependent catabolic process, exit from mitosis, metaphase/anaphase transition of mitotic cell cycle, protein ubiquitination	1
tr|Q5AKI5 Q5AKI5_CANAL	2	EIP1	Putative securin-like protein	2
A0A0A6MFS1_CANAL	2	CDC14	Tyrosine-protein phosphatase CDC14 OS=*Candida albicans* (strain SC5314)	2
C7_01580W_B	2	SMC6	Putative structural maintenance of chromosomes (SMC) protein; Hap43-induced; cell-cycle regulated periodic mRNA expression; *S. cerevisiae* ortholog not cell-cycle regulated; Spider biofilm induced	1
sp|Q5AEE1|H2AZ_CANAL	2	H2A	Histone H2A.Z OS=*Candida albicans* (strain SC5314 / ATCC MYA-2876) GN=HTZ1 PE=3 SV=3	2

C4_07180W_B	2	RPL4B	Ribosomal protein 4B; repressed upon phagocytosis by murine macrophage; Spider biofilm repressed	1
C5_05050W_A	2	ADH1	Alcohol dehydrogenase; oxidizes ethanol to acetaldehyde; at yeast cell surface; immunogenic in humans/mice; complements *S. cerevisiae* adh1 adh2 adh3 mutant; fluconazole, farnesol-induced; flow model biofilm induced	2
C2_01320W_B	2	RPN9	Ortholog(s) have structural molecule activity, role in proteasome assembly, ubiquitin-dependent protein catabolic process and cytosol, nucleus, proteasome regulatory particle, lid subcomplex, proteasome storage granule localization	1
C2_01320W_B	2	SPO69	Orthologs have chromatin binding activity and role in meiotic sister chromatid cohesion, protein localization to chromosome, centromeric region, reciprocal meiotic recombination, synaptonemal complex assembly	1
C2_07530C_A	2	Orf19.6469	Predicted ORF in retrotransposon Tca11p with similarity to the Gag-Pol region of retrotransposons, which encodes nucleocapsid-like protein, reverse transcriptase, protease, and integrase	1
C2_08380C_A	2	DPB11	Ortholog(s) have DNA polymerase binding, molecular adaptor activity, protein kinase activator activity	1
C7_03490W_B	2	GYP7	Protein similar to *S. cerevisiae* Gyp7p (GTPase-activating protein for Ypt1p); caspofungin induced	1
C2_07530C_A	2	Orf19.1874	Ortholog(s) have protein serine/threonine kinase activity	1
CR_05080W_B	2	VMA13	Predicted proton-transporting ATPase; predicted role in ATP hydrolysis coupled proton transport; rat catheter biofilm repressed	1
C2_02250C_A	2	OPI1	Leucine zipper transcription factor; involved in regulation of filamentous growth; has putative Opi1-Sin3 interaction domain; interacts with ScSin3, but not CaSin3	1

C1_06760C_A	2	Orf19.6234	Putative U2 snRNP component; mutation confers hypersensitivity to 5-fluorocytosine (5-FC), 5-fluorouracil (5-FU), and tubercidin (7-deazaadenosine); Hap43-induced, Spider biofilm induced	1
C5_03250W_B	2	RMS1	Putative lysine methyltransferase; Hap43-induced; protein induced during mating; possibly essential, disruptants not obtained by UAU1 method; rat catheter and Spider biofilm induced	1
C1_03740W_B	2	WAR1	Zn(II)2Cys6 transcription factor; plays a role in resistance to weak organic acids; required for yeast cell adherence to	1
C2_10220C_A	2	PHO23	Ortholog(s) have methylated histone binding activity	1
C1_04960C_A	2	Orf19.500	Ortholog(s) have tRNA (adenine-N1-)-methyltransferase activity, role in tRNA methylation and nucleus, tRNA (m1A)	1
C2_02150C_A	2	RNA14	Ortholog(s) have RNA binding activity and role in mRNA polyadenylation, pre-mRNA cleavage required for polyadenylation, regulation of mRNA 3'-end processing, response to DNA damage checkpoint signaling	1
C1_01460W_A	2	Orf19.3332	Ortholog of Bre4 in *S. cerevisiae* has a role in brefeldin A resistance; a drug that affect intracellular transport; Spider biofilm induced	1
C2_01990C_B	2	FAB1	Phosphatidylinositol 3-phosphate 5-kinase; required for hyphal growth on solid media, and for wild-type vacuolar morphology and acidification; not required for wild-type virulence in mouse systemic infection or for adherence to HeLa cells	1
C1_10540C_A	2	Orf19.998	Putative adapter protein; links synaptojanins Inp52 and Inp53 to the cortical actin cytoskeleton in *S. cerevisiae*; mutants are viable	1
C1_13010W_B	2	Orf19.4942	Ortholog of *Candida albicans WO-1*: CAWG_00134	1

C2_03980C_B	2	MED1	Uncharacterized; RNA polymerase II mediator complex subunit; RNA polymerase II transcription cofactor	1
C3_07260C_B	2	ECM29	Putative scaffold protein; assists in association of the proteasome core particle with the regulatory particle; ortholog of *S. cerevisiae* Ecm29; transposon mutation affects filamentous growth; flow model biofilm repressed	1
C1_07590C_A	2	APL3	Uncharacterized; Ortholog(s) have AP-2 adaptor complex, cellular bud neck	1
C5_00770C_A	2	FOL1	Uncharacterized; Putative dihydroneopterin aldolase (dihydro-6-hydroxymethylpterin pyrophosphokinase); fungal-specific (no human or murine homolog)	1
C3_07660W_B	2	RAD4	Uncharacterized; Protein similar to *S. cerevisiae* Rad4p; down-regulation associated with azole resistance	1
C3_05310W_B	2	USO6	Uncharacterized; Putative vesicular transport protein; transcript induced by filamentous growth; rat catheter biofilm repressed	1
C6_03430C_A	2	CPS2	Uncharacterized; Predicted metallocarboxypeptidase; role in proteolysis; rat catheter biofilm repressed	1

[1]350 mg protein extracts from 4 L cultures of strain SS40 (*eip1/EIP1-TAP-URA3*) and BWP17(*EIP1/EIP1*) incubated in YPD medium until reaching an O.D.600nm of 0.8 were subjected to Tandem Affinity Purification. Elutions were TCA-precipitated and run just into the resolving portion of an SDS PAGE gel. The compressed bands were stained with Coomasie blue, cut from the gel, and analysed using an LTQ-Orbitrap Elite with nano-ESI.
[2]Peptides less than 2 were excluded from the results.
[3]Peptides identified in both the tagged strain and the untagged control strain were excluded from the table.
[4]Number of times indicated proteins were purified over total number of two affinity purification repeats.

Table 3.7. Orbitrap LC/MS analysis of putative Eip1p-interacting proteins in *CDC20-*depleted Cells[1]

PROTEIN ID	Number of Peptides[2,3]	ORF	Identified Proteins	Frequency of hits[4]
tr|C4YQT2|C4YQT2_CANAW	59	EIP1	Putative securin-like protein	1
sp|Q59NH8|CDC14_CANAL	15	CDC14	Tyrosine-protein phosphatase CDC14 OS=*Candida albicans* (strain SC5314)	1
sp|Q9UVZ8|ACT_CANDC	2	Orf19.3213	Uncharacterized ORF	1
tr|Q5AK09|Q5AK09_CANAL	2	Orf19.4011	Uncharacterized ORF	1
sp|Q5AEE1|H2AZ_CANAL	2	H2A	Histone H2A.Z OS=*Candida albicans* (strain SC5314 / ATCC MYA-2876) GN=HTZ1 PE=3 SV=3	1

[1]526 mg protein extracts from 4 L cultures of strain SS41 (*EIP1/EIP1-TAP-ARG4, cdc20::URA3/MET3::CDC20-HIS1*) and AG153(*MET3::CDC20-ARG4/cdc20::URA3, CLB2-HA-HIS1*) incubated in +MC medium until reaching an O.D.600nm of 0.4 were subjected totandem affinity purification. Elutions were TCA-precipitated and run just into the resolving portion of an SDS PAGE gel. The compressed bands were stained with Coomasie blue, cut from the gel, and analysed using an LTQ-Orbitrap Elite with nano-ESI.
[2]Peptides less than 2 were excluded from the results.
[3]Peptides identified in both the tagged strain and the untagged control strain were excluded from the table.
[4]Number of times indicated proteins were purified over total number of two affinity purification repeats.

3.5 Discussion

Timely progression of events involved in each phase of the cell cycle is critical in order to ensure proper DNA duplication and subsequent chromosome segregation. The metaphase-to-anaphase transition involves several key factors including separase, the separase regulator securin, the cohesin complex as well as the APC/C. Our previous work (Sparapani and Bachewich, 2019) identified Eip1p as a new separase-binding protein with many properties that suggested it is a securin. A diagnostic feature of all known securins is degradation at the metaphase-to-anaphase transition, mediated by APC/C$_{Cdc20p}$ activity (Morgan, 2007). However, previous work (Sparapani and Bachewich, 2019) demonstrated that depletion of Cdc20p in *C. albicans* did not strongly or consistently modulate the levels of Eip1p, in contrast to the situation in other systems (Irniger, 2002), questioning whether Eip1p is similar to other securins with respect to regulation. Further, many phenotypes of Eip1p-depleted cells suggest that Eip1p is important for chromosome segregation and possible other mitotic processes, but its mechanisms of action remain unclear.

Thus, we first addressed whether Eip1p levels are influenced by the APC/C. The function of the APC/C in *C. albicans* had not been previously explored, except for partial characterizations of the APC/C cofactors Cdc20p and Cdh1p (Chou et al., 2011). Here, we provide the first characterization of an APC/C subunit in *C. albicans,* Cdc16p. In *S. cerevisiae*, Cdc16p is a subunit of the APC/C containing several TPR repeat motifs that stabilize its binding to other APC/C subunits indlucing Cdc26p, as well as several substrates (Zhang et al., 2014). Cdc16p is highly conserved in *C. albicans*. A three-dimensional comparative analysis between Cdc16p in *C. albicans* and its homologue in *S. pombe*, Cut9p, revealed 100% confidence in alignment at a specific region. In *S. cerevisiae*, *CDC16* is essential, where its depletion results in large-budded cells containing a large mass of DNA lying either near or through the budneck (Lamb et al., 1994; Heichman and Robert, 1996). Consistent with this, its depletion in *C. albicans* resulted in a strong block in mitosis, suggestive of a metaphase arrest, based on the majority of cells containing a single undivided nucleus at the budneck. An analysis of corresponding spindle lengths using a *CDC16*-conditional strain carrying *TUB2-GFP* would help confirm this result. Further, we found that Cdc16p is required for degradation of the mitotic

114

cyclin Clb2p, consistent with the situation in *S. cerevisiae* (Irniger and Nasmyth, 1997). In addition, we provide evidence that Cdc16p-depleted cells are large-budded and form elongated filaments after a long period of depletion. A portion of filamentous cells demonstrated a distinct phenotype in that from a large bud emanated a filament. Interestingly, this growth pattern is also observed in cells depleted of the mitotic kinase Cdc15p. Cdc15p is recruited to spindle pole bodies during later stages of mitosis by the GTPase Tem1p, activating the kinase to recruit the Bub2p-Bfa1p GAP complex, which in turn drives the release of Cdc14p (Milne et al., 2014; Bates, 2018). Cells depleted of Cdc15p developed into large budded cells with filaments emanating from the bud, and contained two nuclei in addition to hyper-extended spindles, characteristic of a failure to exit mitosis (Bates, 2018). The data suggest that Cdc16p and by extension the APC/C is conserved in its role in regulating mitotic progression in *C. albicans*.

Based on this, we next explored whether Cdc16p is important for degradation of Eip1p. In *S. cerevisiae*, absence of Cdc16p resulted in enriched levels of the securin Pds1p (Cohen-Fix et al., 1996). Consistently, we showed that Eip1p was also enriched when Cdc16p was depleted. Additional experiments to confirm the relationship between Eip1p and the APC/C-mediated degradation at metaphase could include site-directed mutagenesis of the Destruction or KEN box motifs of Eip1p's amino acid sequence and measure modulation of Eip1p levels in the presence of the APC/C. In addition, levels of Eip1p could be measured in an unperturbed cell cycle to determine if its levels decrease during metaphase. One technique currently in progress includes tagging Eip1p in a *cpp1Δ* strain in order to synchronize cells in G1-phase using *α*-pheromone, releasing cells from the block and measuring the levels of Eip1p. The fact that Eip1p showed variable to little change in levels when Cdc20p was depleted (Sparapani and Bachewich, 2019) could be due to the weaker block in metaphase compared to Cdc16p-depleted cells, preventing a strong enrichment. In addition, the APC/C cofactor Cdh1p may also contribute to Eip1p degradation (Hatano et al., 2016). It would be informative to determine Eip1p levels in cells lacking Cdh1p, or in cells lacking both Cdc20p and Cdh1p. In addition, future studies should include characterization of all APC/C subunits in *C. albicans*. Overall, the results demonstrate that Eip1p is regulated in part by degradation mediated by the APC/C, and reinforce the notion that Eip1p is a new securin.

Through identifying Eip1p-interacting factors using affinity purification and mass spectrometry, we also provide new insights on potential functions and mechanisms of action of Eip1p. First, the data revealed that Esp1p co-purified with Eip1p, consistent with results from affinity purifying Esp1p and co-immunoprecipitation experiments (Sparapani and Bachewich, 2019). The data also revealed several chromatin-associated factors, including Smc3p, Spo69/Rec8p, Smc6p, Rad4p and Med1p, for example. While interaction between the cohesin subunit Smc3p and Eip1p could be indirect, based on Eip1p binding the separase Esp1p, it is noteworthy that the securin Pds1p has not been reported to physically bind Smc3p in *S. cerevisiae* (Costanzo et al., 2016). Whether this reflects a role for Eip1p in regulating cohesin directly remains to be determined. Co-immunoprecipitation and co-localization experiments could help address this question. Intriguingly, Spo69p/Rec8 is the meiotic equivalent of Scc1p (Kim et al., 2010), yet *C. albicans* does not undergo meiosis. Smc6p is part of the Smc5p/6p complex. In *S. cerevisiae*, this is required for resistance to DNA damage and damage-induced sister chromatid recombination (Ampatzidou et al., 2006). Intriguingly, the nucleotide excision repair protein Rad4p also co-purified, reinforcing a link between DNA damage and Eip1p (Sparapani and Bachewich, 2019). To date, securins have not been reported to bind either of these factors, or Med1p, which is involved in regulating genes transcribed by Polymerase II but also higher order chromatin organization (Chereji et al., 2017). The significance of these potential interactions on chromatin organization and function await further investigation.

Eip1p co-purified with several factors associated with ubiquitination, such as Ubi3p, Tom1p, and the proteasome, including Apc2p, Rpn9p, Ecm29p, for example. Pds1p has also been reported to bind subunits of the 26S proteasome and ubiquitin-specific protease (Schaefer and Morgan, 2011), and these putative interactions could reflect association with the APC/C and proteasome. The association between Eip1p and several factors that influence filamentous growth in *C. albicans*, including Kem1p, Fab1p and Opi1p, Ecm29p, and Uso6p, for example, are intriguing based on the report that cells depleted of Eip1p were impaired in their ability to form filaments in response to serum (O'Meara et al., 2015). Further investigations are required to distinguish whether these filamentation growth defects are solely due to general growth inhibition vs. including a role for Eip1p in influencing filamentation.

During three separate affinity purification trials, Eip1p co-purified with the mitotic phosphatase Cdc14p. In *S. cerevisiae*, Cdc14p functions in the FEAR network during early mitosis where it is released from its inhibitor, Net1p, which leads to the dephosphorylation of Cdc28p, initiating mitotic exit (Weiss, 2012). Accumulation of Cdc14p activates the MEN at the spindle pole bodies; allowing for one spindle pole body to enter the bud, initiating mitotic exit (Sanchez-Diaz et al., 2012). In *C. albicans*, Cdc14p is not essential, in contrast to *S. cerevisiae* (Clemente-Blanco et al., 2006). Cdc14p-depleted cells show defects in mitotic exit, but also cell separation (Clemente-Blanco et al., 2006), unlike in *S. cerevisiae*. We have demonstrated the interaction of Esp1p and Cdc14p in *C. albicans* (Sparapani and Bachewich, 2019) and a recent study has also confirmed this interaction in *C. albicans* (Kaneva et al., 2019). In *S. cerevisiae*, Esp1p functions with Slk19p, PP2A and Cdc55p as part of the FEAR network and has been shown to interact with Cdc14p in a genetic manner only (https://www.yeastgenome.org). Thus, the interaction between Eip1p and Cdc14p may be indirect due to Eip1p's interaction with Esp1p. However, due to the frequency with which Cdc14p co-purified with Eip1p, we cannot rule out a functional relationship and additional roles of Eip1p, possibly with respect to Cdc14p function. Previous work demonstrated that Eip1p-depleted cells formed a pleiotropic phenotype consisting of large budded, pseudohyphal and chains of cells (Sparapani and Bachewich, 2019). Taken together, this could imply that Eip1p influences cell separation in a proportion of cells in *C. albicans*. Future studies could include calcofluor staining in order to analyze cell walls, confirming all interactions between Eip1p and co-purifying proteins using co-immunoprecipitations and conducting functional analyses.

In summary, our work provides the first characterization of the APC/C subunit Cdc16p in *C. albicans*. The approaches used throughout the characterizations have expanded our understanding of how the metaphase-to-anaphase transition is regulated in addition to gaining a better understanding on the role of Eip1p during this process, as well as additional potential roles in mitotic exit, cell separation and morphogenesis.

3.6 Supplemental Figures and Tables

Table S3.1. Strains used in this study.

Strain	Genotype	Source
BWP17	*ura3:imm434/ura3:imm434, his1::hisG/his1::hisG arg4::hisG/arg4::hisG*	Wilson *et al.*,1999
AG153	*MET3::CDC20-ARG4/cdc20::URA3, CLB2-HA-HIS1*	Glory, 2014
SS41	*EIP1/EIP1-TAP-ARG4, cdc20::URA3/MET3::CDC20-HIS1*	This study
SS58	*EIP1/EIP1-TAP-ARG4*	This study
SS71	*EIP1/EIP1-TAP-ARG4, CDC16/MET3::CDC16-HIS1*	This study
SS75	*EIP1/EIP1-TAP-ARG4, cdc16::URA3/MET3::CDC16-HIS1*	This study
SS82	*cdc16::URA3/MET3::CDC16-HIS1*	This study
SS87	*CLB2/CLB2-TAP-ARG4, cdc16::URA3/MET3::CDC16-HIS1*	This study
SS88	*EIP1/EIP1-HA-ARG4*	This study
SS91	*EIP1/EIP1-HA-ARG4, CDC14/CDC14-MYC-HIS1*	This study

Table S3.2. Plasmids used in this study.

Plasmids	Description	Source
pFA-TAP-Ca*ARG4*	pFunctional Analysis Casette-TAP-ARG4	Lavoie. *et al.*, 2008
pFA-*MET3*-Ca*HIS1*	*MET3* promotor-Ca*HIS1*	Gola, S. *et al.*, 2003
pBS-Ca*URA3*	pBluescript-Ca*URA3*	A.J.P Brown
pMG2093	pFA6a-13myc-TRP1 ligated into pFA-GFP-HIS1	Bensen et al., 2005

Table S3.3. Oligonucleotides used in this study.

Oligonucleotide	Sequence in 5'-3' direction	Source
AG5F	ATC AGG AAG AGA TTT GTT TGA TGA ACG ATT ATC GAC CCA TAG GCT AAC ATT AGA AGA TGA TGA CGA AGA AGA AGA AAT AGT GGT AGC AGA AGC AGA AGA GGG TCG ACG GAT CCC CGG GTT	Chou et al., 2011
AG5R	ATT ATA GGG TAA TGC ACA TAA CTC ATG TTC ATC TTC TTT CAT TTC CTC ATT TAT GCA TTG TAA AGA TAA GAA CCT AGA TCC AAT AGT CAT CAA AAC TTT ATC GAT GAA TTC GAG CTC GTT	Chou et al., 2011
AG6R	AGT AGG ACA CCA ATG GGT TG	Chou et al., 2011
SS25R	GAG AAT CCG ATC AAT TTC CA	Sparapani, 2019
SS33F	GGA CTT TGA AGA TGA AAG TAA TGT TGG AGA AAT ACC AAT TAT TGA AGG TAT TGA TGA GGA AAT TGG TTT AAC TAG CGA TGA TTT GGA TAA TTT ATT AGG AGG TCG ACG GAT CCC CGG GTT	Sparapani, 2019
SS33R	ATC AGT TAC CCA AGT ACA ATC AGG ATA GAA AGT ATG AAC AAC AGG GGT ACG AGC AAT CAT GTG CCC AAC AAT AAT ACC ATG TAA ATA CTC AAT ATA TGA ATC GAT GAA TTC GAG CTC GTT	Sparapani, 2019

SS40F	GGA AGT GCT ACT ACC ACG ACT GCT AAT GTC	This study
SS40R	GGT AGC ATG CTT TAA GTA GCC ATC TCA TCA	This study
SS41F	TGT TGT TAG CGC TAC CAT AGT CGT CTA GTT	This study
SS41R	TTA TCT ATC TTC TAC TAT AAT CAC GTT ACC	This study
SS42F	TGA TGA GAT GGC TAC TTA AAG CAT GCT ACC/ TAT AGG GCG AAT TGG AGC TC	This study
SS42R	AAC TAG ACG ACT ATG GTA GCG CTA ACA ACA/ GAC GGT ATC GAT AAG CTT GA	This study
SS43F	TGG AGA CTT CAG TGG AAA ATT TCA AAC TAG	This study
SS43R	AAA TTT TAT TCA CAG TGT TGG ACG CGC TAA	This study
SS44F	ATG ACA ACA AAT CAA TCA ATC AAT ACA ACA	This study
SS44R	ATT GAA ATA TAC TTG ACC TAA CCA AAA TGC	This study
SS45F	TTA GCG CGT CCA ACA CTG TGA ATA AAA TTT GGA TCC TGG AGG ATG AGG AG	This study
SS45R	TGT TGT ATT GAT TGA TTG ATT	This study

	TGT TGT CAT CAT GTT TTC TGG GGA GGG TA	
SS46F	TTT CCC AAT CTT TAG TTC TC	This study
SS53F	GCT TCT GGA AAC TCA CAA ACA TCA AGA GCA CAC TCT GGT GGT GTG AGA AAG TTA AGT GGA AAG AAA CAT GGT GGT GGT CGG ATC CCC GGG TTA ATT AA	This study
SS53R	TTT CGA TAT ATT GGC TTT TGC ATA TGG TTC GGA AGA ACA AAT TGA AAT TGT TGA ACC AGC TTA TGA AGA AGA ATT CCG GAA TAT TTA TGA GAA AC	This study
SS54R	AGG TGA AGA ACG AAG ATG AA	This study
CaARG4F	ACT ATG GAT ATG TTG GCT AC	Glory, 2014
CaHIS1F	CCT GCA GCT GAT ATC CCA GT	Glory, 2014
CaHIS1R	ACT GGG ATA TCA GCT GCA GG	Glory, 2014
CaURA3R	GGT TGG AAT GCT TAT TTG AA	Glory, 2014

Figure S3.1. Confirmation of *EIP1/EIP1-TAP-ARG4*.

(A) Map and DNA gel showing the PCR screening strategy to confirm correct integration of *EIP1-TAP-ARG4* gene construct into strain BWP17. (B) Oligonucleotides SS25R and CaARG4F generate a 968bp band for the *EIP1-TAP-ARG4* construct. Negative strain BWP17 and positive strain SS58 are demonstrated. Vertical bars delineate the length of the transforming product. (C)Western blot showing confirmation of Eip1p-TAP expression.

Figure S3.2. Confirmation of *cdc16::URA3/MET3::CDC16-HIS1, EIP1/EIP1-TAP-ARG4*.
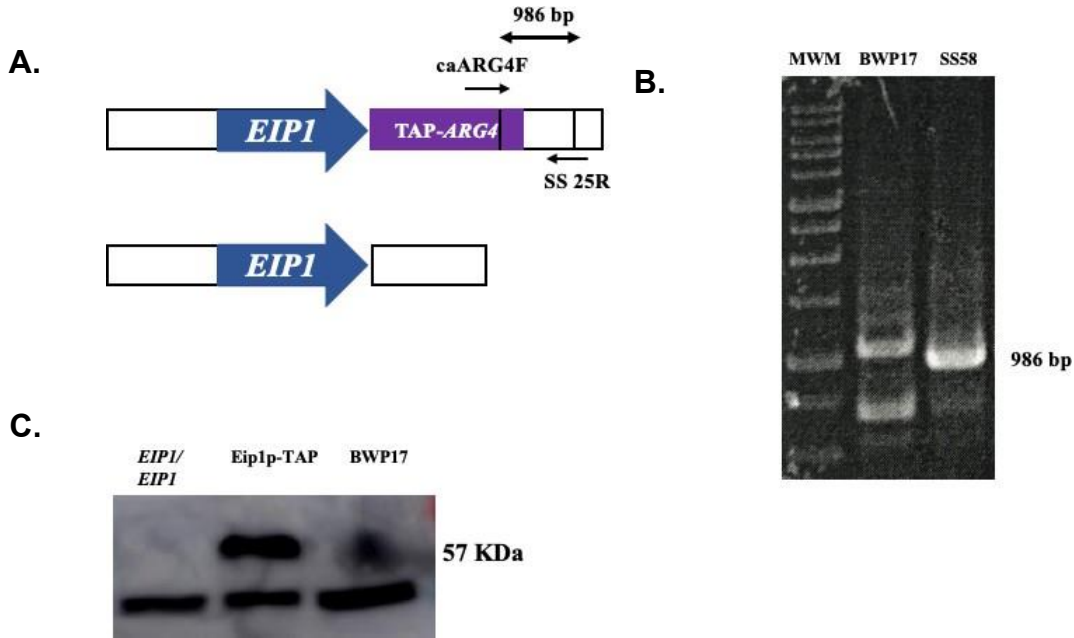(A)Map and DNA gel showing the PCR screening strategy to confirm correct integration of the
MET3-containing construct. Oligonucleotides SS25F and CaHIS1R generate a 1.1 kb band for
the *MET3* integration. Positive strain SS71 and the negative control strain BWP17 is
demonstrated. (B) Map and DNA gel showing the PCR screening strategy to confirm correct
integration of the *URA3* replacement. Oligonucleotides SS46F and CaURA3R generate a

2 kb band for the *URA3* integration. Negative strain BPW17, *CDC16/CDC16* transformants and positive strain SS75 are demonstrated. Vertical bars delineate the length of the transforming construct.
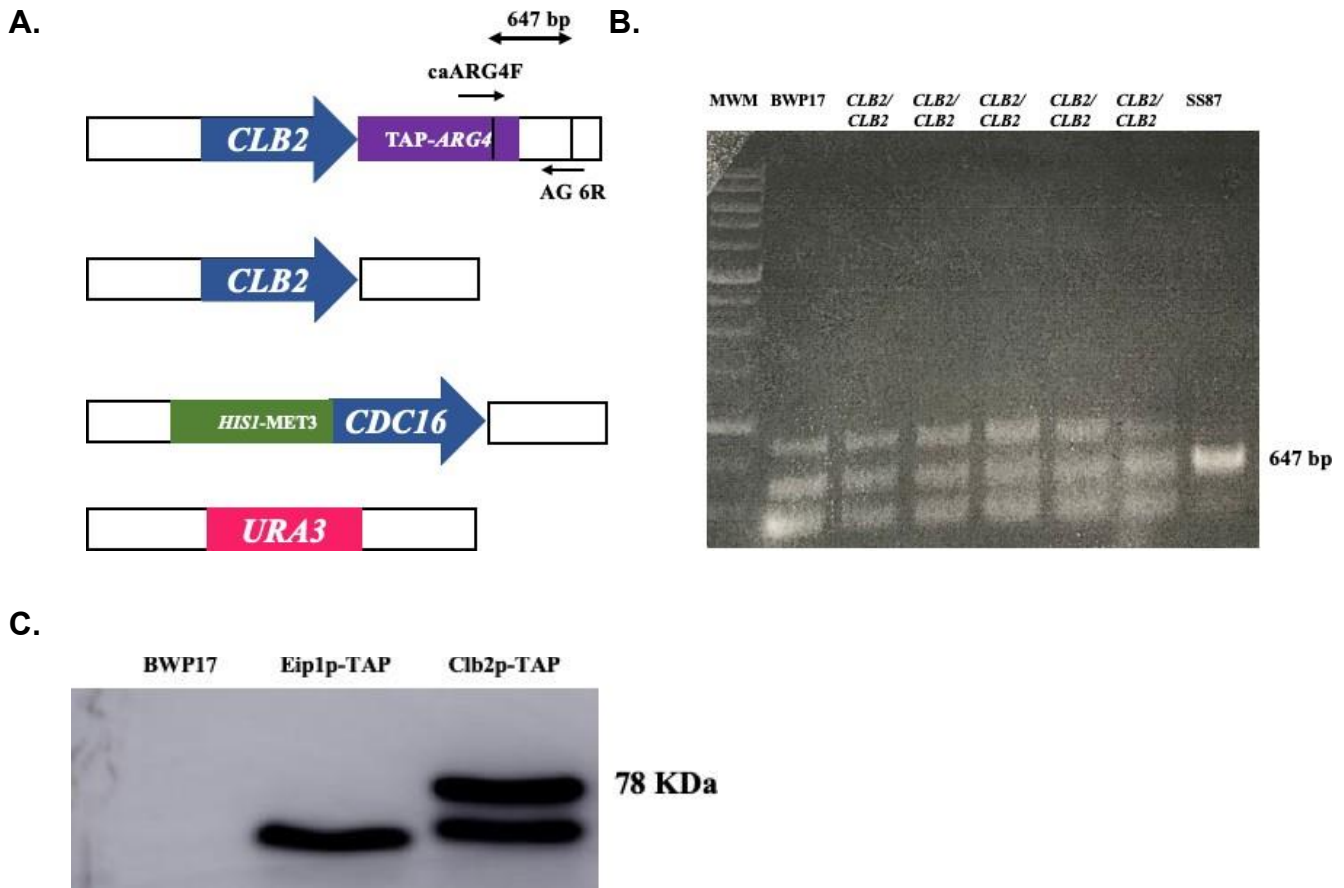
Figure S3.3. Confirmation of *CLB2/CLB2-TAP-ARG4*, *cdc16::URA3/MET3::CDC16-HIS1*. (A) Map and DNA gel showing the PCR screening strategy to confirm correct integration of *CLB2-TAP-ARG4* gene construct into strain SS82. (B) Oligonucleotides AG6R and CaARG4F generate a 647 bp band for the *CLB2-TAP-ARG4* construct. Negative strain BWP17, negative transformants *CLB2/CLB2*, and positive strain SS87 are demonstrated. Vertical bars delineate the length of the transforming product. (C)Western blot showing confirmation of Clb2p-TAP expression.
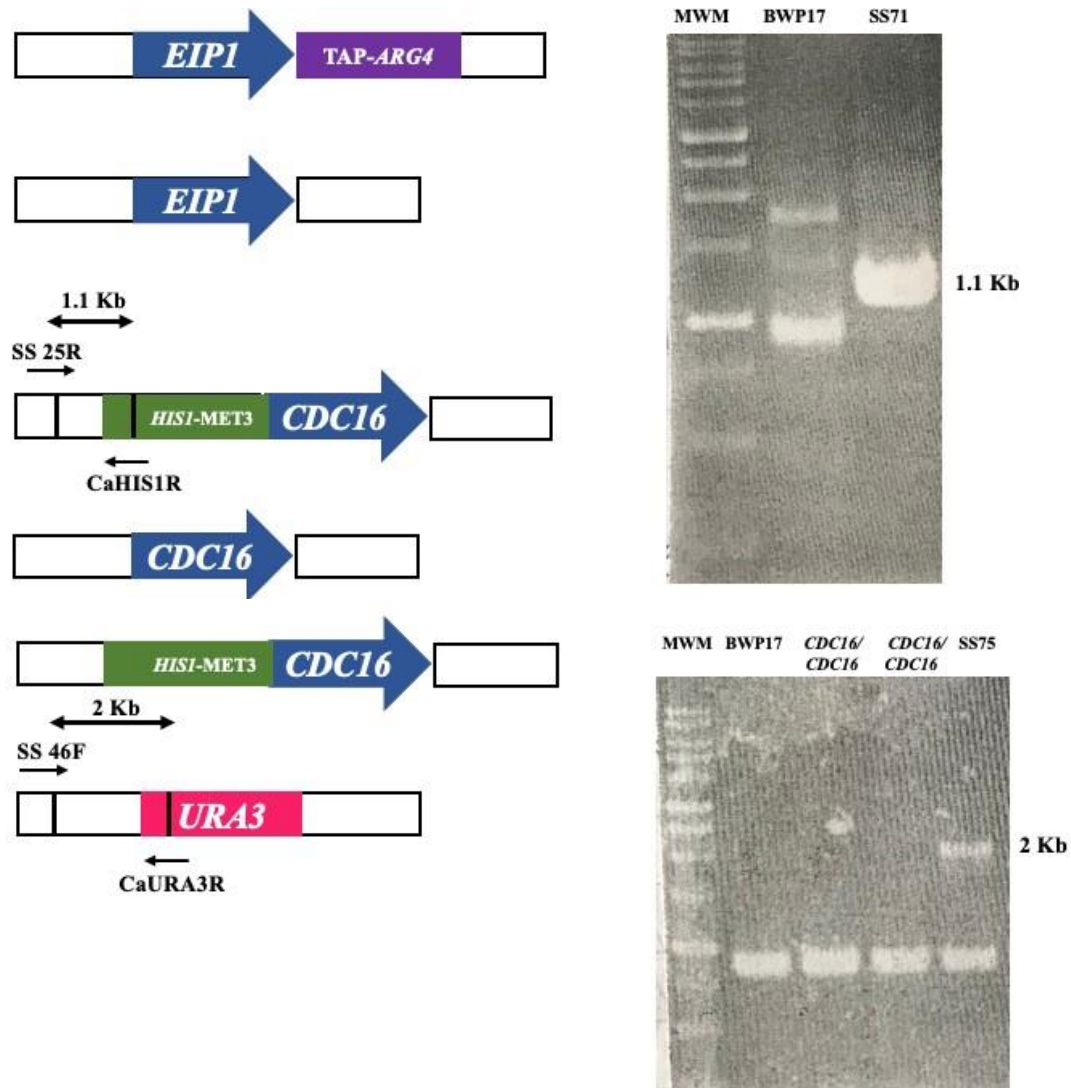
Figure S3.4. Confirmation of *EIP1/EIP1-HA-ARG4*.

(A)Map and DNA gel showing the PCR screening strategy to confirm correct integration of *EIP1-HA-ARG4* gene construct into strain BWP17. (B) Oligonucleotides SS25R and CaARG4F generate a 885bp band for the *EIP1-HA-ARG4* construct. Negative strain BWP17 and positive strain SS88 are demonstrated. Vertical bars delineate the length of the transforming product. (C)Western blot showing confirmation of Eip1p-HA expression.
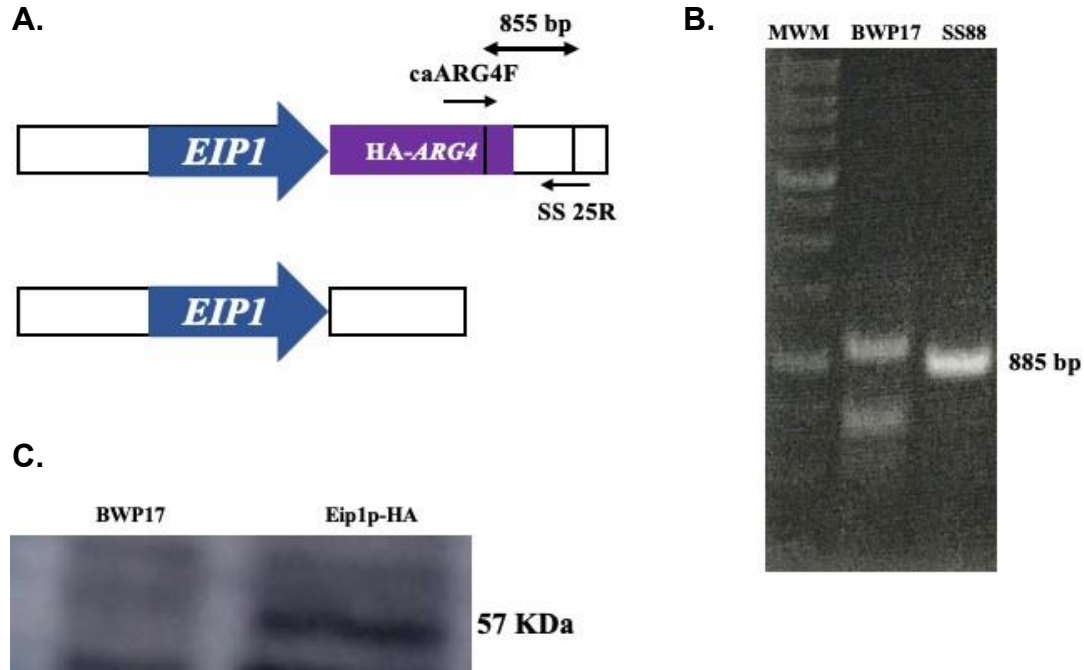
Chapter 4.0 Summary and Model

C. albicans is one of the most common opportunistic fungal pathogens of humans and its increase in resistance underscores the importance of identifying novel drug targets for therapeutic development. The cell cycle is an important virulence determining trait of *C. albicans*. Elucidating the networks that govern mitosis in the fungal pathogen will provide insights on the regulation of its cell proliferation, and identify potential new targets to treat infection. The metaphase-to-anaphase transition is critical for proper chromosome segregation and maintaining genomic stability. However, a comprehensive understanding of the various mechanisms that control the metaphase-to-anaphase transition in *C. albicans* is lacking. Previous characterization studies have shown functional conservation of several mitotic regulators including the APC/C cofactors Cdc20p and Cdh1p (Chou et al., 2011) as well as the polo-like kinase Cdc5p (Bachewich et al., 2003; 2005) and demonstrated their importance for the metaphase-to-anaphase transition and mitotic exit. Although these studies provide a partial framework for mitotic progression in *C. albicans*, characterization of additional mitotic factors important for the metaphase-to-anaphase transition, including separase and the APC/C remained elusive. Moreover, *C. albicans* lacked a sequence homologue of the separase regulator; securin. Thus, the objective of our studies involved gaining a better understanding of the regulation of the metaphase-to-anaphase transition in *C. albicans* by investigating the functions of several key mitotic factors involved in this process, and potentially identifying suitable drug targets for therapeutic development.

I have since characterized *C. albicans'* separase Esp1p and demonstrated its conserved function in the metaphase-to-anaphase transition. I have identified Eip1p, a novel separase-binding protein, demonstrating that its function and part of its regulation suggests it is a new securin. My work also raises the possibility for additional functions of Eip1p and thus suggests novel features of securins, and provides a first characterization of the APC/C subunit Cdc16p in *C. albicans*. This work uncovered a new fungal-specific protein and potential candidate target for therapeutic development as well as progresses our understanding of mitosis and the overall cell cycle in *C. albicans*.

In Chapter 2 we provided the first characterization of the *C. albicans* separase, Esp1p, and demonstrated it is important for chromosome segregation, since cells depleted of the protein contained large single masses of DNA and short spindles characteristic of G2/M or early anaphase (Figure 2.2). Esp1p depletion also resulted in filamentous formation after long periods of depletion, consistent with cell cycle arrest in *C. albicans* (Figure 2.1). Since the identification of securins is difficult using sequence-based homology searches given that little homology exists between securins in different organisms, we hypothesized that through identifying the interacting protein factors of Esp1p we could uncover a homologue of securin. We provided the first screen of interacting factors of Esp1p, and identified the phosphatase Cdc14p, as well as the functionally uncharacterized protein Eip1p. In *S. cerevisiae*, Esp1p interacts with the kinetochore protein Slk19p and the PP2A$_{Cdc55p}$ complex as part of the FEAR network that activates the partial release of Cdc14p into the cytoplasm from inhibition in the nucleolus. In contrast to our results, Esp1p and Cdc14p have been reported to interact in only a genetic rather than physical manner (https://www.yeastgenome.org). Interestingly, a recent screen for Cdc14p interacting factors in *C. albicans* uncovered Esp1p (Kaneva et al., 2019), consistent with our results. Homologues of Slk19p, and PP2A$_{Cdc55p}$ were not isolated in our Esp1p purification screens in *C. albicans,* and a FEAR pathway has not been identified in *C. albicans* to date. Our screen identified α- tubulin and proteins involved in RNA polymerase binding activity, consistent with other separases. Additional interactors included Cdc19p and Def1p, implying possible other new functions. These interactions require validation before additional characterization. Collectively, the data suggests Esp1p in *C. albicans* may have additional functions and play a role in other processes, in addition to regulating mitosis.

We proceeded to characterize Eip1p using comprehensive bioinformatic analyses and a variety of biochemical, molecular, and cell biological approaches. The data suggest Eip1p to be a divergent securin-like protein based on several features. First, the amino acid sequence of Eip1p contained motifs including KEN and Destruction box sequences unique to proteins targeted for degradation by the APC/C. BLAST searches of the amino acid sequence of Eip1p uncovered *Candida*-specific species only, and an analysis of its 3D structure showed 50% similarity with a portion of Pds1p from *S. cerevisiae*. Second, Eip1p levels are significantly reduced in the absence

128

of Cdc5p, consistent with Pds1p (Hilioti et al., 2001), suggesting that it is degraded during mitosis. Third, Eip1p levels are enriched in response to DNA damage or replication stress inducing agents such as MMS and HU, similar to Pds1p in *S. cerevisiae* (Palou et al., 2015). Further, depletion of Eip1p partially suppresses the MMS or HU-induced metaphase block and depletion of Eip1p results in enrichment of the cohesin subunit Mcd1p/Scc1p.

Intriguingly, depletion of Eip1p demonstrated some additional phenotypes that were novel compared to other securins, which suggest the possibility of additional roles in other processes. First, a proportion of cells had misoriented spindles and a stretched or misoriented DNA mass in the mother cell that subsequently re-oriented and segregated to the daughter cell, implying a possible role for Eip1p in spindle orientation. Second, a proportion of Eip1p-depleted cells maintained elongated spindles. Specifically, some cells displayed elongated spindles confined to the mother cell which could be a consequence of the activation of the spindle orientation checkpoint (SPOC) pathway and delayed mitotic progression and spindle disassembly. However, other cells contained elongated spindles spanning between the mother and daughter cells, suggesting a possible role of Eip1p in spindle disassembly or mitotic exit. Given that separase is required for mitotic exit (Hatano et al., 2016), and securins such as Pds1p block this activity and thus negatively regulate mitotic exit, we do not propose that Eip1p has some positive role in regulating mitotic exit, resulting in elongated spindles when depleted, but rather that Eip1p may be affecting spindle disassembly. Indeed, *pds1Δ* mutants did not demonstrate spindle maintenance in *S. cerevisiae*. Rather, some cells displayed multinuclei suggesting precocious mitotic exit (Hatano et al., 2016). Further, the novel phenotypes of Eip1-depleted cells, including abnormal nuclear movements, are also consistent with microtubule-related defects. We cannot rule out that the novel phenotypes are secondary effects of disregulated Esp1p. However, securins have additional separase-independent functions. For example, the human securin, PTTG1 has a separase-independent role in microtubule nucleation (Moreno-Mateos et al., 2011). In addition, Eip1p-depleted cells did not phenocopy Esp1p-depleted cells. Thus, Eip1p demonstrated both conserved and distinct phenotypes, which suggest possible roles in other mitotic pathways and processes, consistent with securins in some other systems.

We next addressed whether the APC/C demonstrated conserved function in maintaining Eip1p turnover during mitosis, as observed with other securins. Previously, we demonstrated that Eip1p was modulated when *C. albicans* cells were blocked in mitosis through depleting Cdc5p (Sparapani and Bachewich, 2019). However, when cells were blocked in mitosis due to Cdc20p-depletion, Eip1p was not significantly or consistently enriched, in contrast to Pds1p in *S. cerevisiae*. Although this could be due to variability in the mitotic arrest point of Cdc20p-depleted cells in *C. albicans*, it was also possible that the regulation of Eip1p during mitosis may involve other mechanisms. Given the differences in cell cycle circuitry in *C. albicans*, we explored this question in Chapter 3 by providing the first characterization of the APC/C subunit Cdc16p in *C. albicans*. A BLAST analysis of the amino acid sequence of Cdc16p identified *Candida*-specific species as well as the *S. pombe* Cdc16p homologue, Cut9p. *C. albicans'* Cdc16p and Cut9p shared 100% similarity in a portion of their 3D structures and Cdc16p contained TPR motifs characteristic of APC/C subunits in other organisms including *S. cerevisiae* and humans (Barford, 2011). DAPI analysis of Cdc16p-depleted cells resulted in a high proportion of cells containing a single mass of DNA at the bud-neck, consistent with Cdc16p in *S. cerevisiae* (Palmer et al., 1989). This suggested that Cdc16p was important for mitotic function. In order to address whether Cdc16p displayed functional conservation in regulating mitotic progression, we measured levels of the mitotic cyclin Clb2p. Upon depletion of Cdc16p, Clb2p levels were enriched, consistent with *S. cerevisiae* (Cohen-Fix et al., 1996). In order to determine the effect of the APC/C on Eip1p turnover, we next measured levels of Eip1p when Cdc16p was modulated. In the absence of Cdc16p, Eip1p levels were also enriched, consistent with Pds1p in *S. cerevisiae* (Cohen-Fix et al., 1996). Although, this was in contrast to Cdc20p-depletion, our studies suggest the APC/C is required for Eip1p turnover, consistent with other securins. Moreover, the lack of Eip1p enrichment in the absence of Cdc20p could have been due to variability in the mitotic block induced by Cdc20p depletion. Specifically, many Cdc20p-depleted cells contained two nuclei, suggesting they were not blocked at metaphase. In addition, the lack of enrichment in Eip1p levels upon Cdc20p-depletion could be due to Cdh1p preventing Eip1p protein enrichment or another form of regulation by Cdh1p. Additional assays addressing Eip1p regulation by the APC/C could include measuring Eip1p levels through Western blot analyses in cells released from a G1 synchronized state as they progress through the

cell cycle, coupled with DAPI and spindle morphology patterns to confirm cell cycle stage. To this end, I have tagged Eip1p in a *cpp1Δ* mutant background in order to synchronize cells in a G1 state when treated with α-pheromone. In *C. albicans*, *CPP1* is a phosphatase involved in the MAP kinase pathway, and its depletion activates the pheromone response pathway (Rastghalam et al., 2019), synchronizing cells in G1. In addition, site-directed mutagenesis of Eip1p's KEN and Destruction box motifs can further address regulation of Eip1p. In order to gain more information on the regulatory role of the APC/C in *C. albicans*, a preliminary assay could include the affinity purification of APC/C subunits to identify putative interacting protein factors.

While the various studies support a role for Eip1p as a securin, its mechanisms of action remained unclear. To this end, we conducted affinity purification analysis of Eip1p and mass spectrometry to identify its interacting factors. Among the purified proteins included Esp1p, the phosphatase Cdc14p, the APC/C subunit Apc2p and Tom1p, the cohesion subunit Smc3p, the chromatin binding protein Spo69p, RNA polymerase mediator protein Med1p, as well as several filament-associated protein factors including Kem1p. Optimization of Eip1p purification by arresting cells in mitosis through Cdc20p-depletion revealed several uncharacterized protein factors as well as Cdc14p and Esp1p. The co-purification of Cdc14p with Eip1p is unique since Pds1p and Cdc14p do not physically interact in *S. cerevisiae*, and is consistent with our finding of Esp1p binding Cdc14p. In addition, Cdc14p has recently been found to co-purify Esp1p in *C. albicans* (Kaneva et al., 2019). This data suggests that the co-purification with Eip1p could be indirect. However, in addition to this, and the frequency with which Cdc14p co-purified with Eip1p, this could suggest Eip1p, Esp1p and Cdc14p are functioning together in regulating mitosis. Accumulation of Cdc14p further activates APC/C$_{Cdh1p}$ promoting a positive feedback loop, suggesting a two-step degradation process of securin (Hatano et al., 2016). Thus, future investigations addressing the relationship between Cdc14p, Eip1p and separase in *C. albicans*, could include assessing modulation of Eip1p and Esp1p in the absence of Cdc14p. We cannot rule out additional roles of Eip1p, as suggested in Figure 4.1.
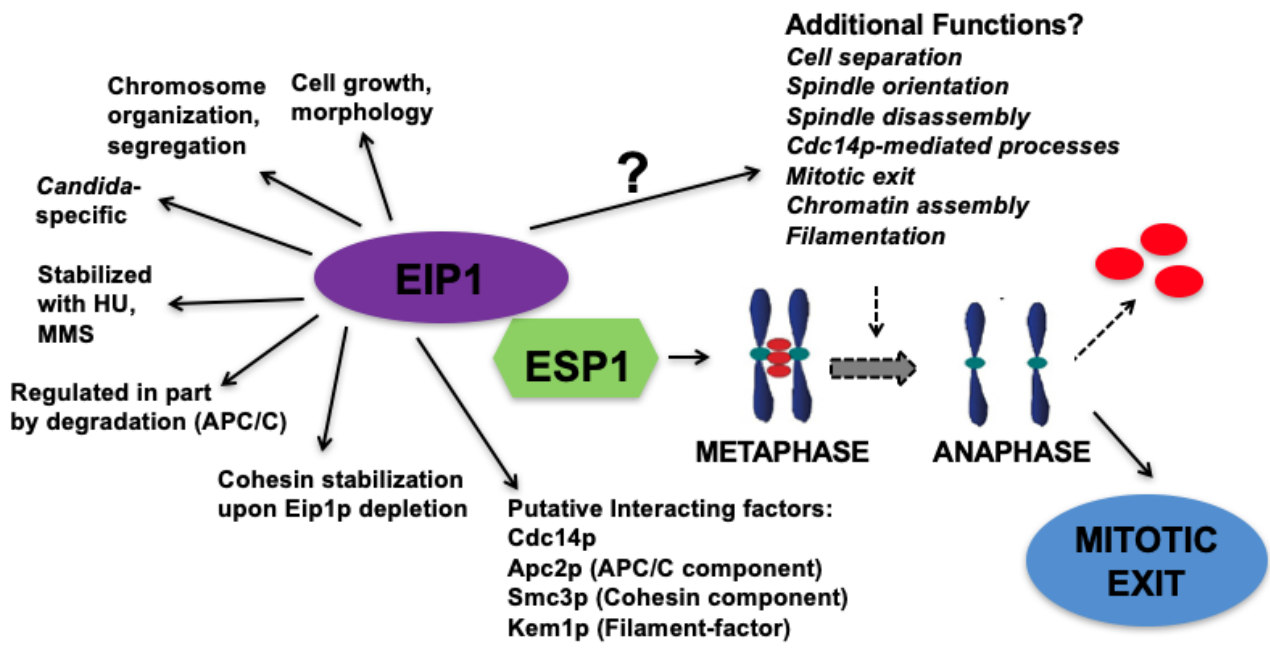
Figure 4.1. Conserved and putative novel functions of Eip1p in *C. albicans*

The regulation of the metaphase-to-anaphase transition has been studied extensively in other organisms including yeast and humans (Rahal and Amon, 2008b). Homologues of separase, the APC/C subunits, the APC/C cofactors Cdc20p and Cdh1p, as well as the polo-like kinase Cdc5p exist in yeast, flies, worms and humans. Securin homologues exist in yeast, flies, worms and humans, but are highly divergent in sequence. To date, securin homologues had not been identified in many fungi, and were only recently identified in plants (Cromer et al., 2019). Having identified a divergent securin-like protein in *C. albicans* that demonstrated both conserved and unique features underscores the difference in the cell cycle circuitry of this fungal pathogen. Overall, our studies have provided a better understanding of the role of separase and the APC/C during the metaphase-to-anaphase transition, and identified a functional securin in *C. albicans*. Although Eip1p appears to be functionally conserved in regulating separase, our work raises the possibility of additional, separase-independent roles. Given its importance in cell division as well as the fact that Eip1p is a *Candida*-specific protein, it is a candidate for therapeutic development.

Chapter 5.0 References

Acquaviva C, Pines J (2006). The anaphase promoting complex/cyclosome: APC. J Cell Biol 119, 2401-2404.

Agarwal R, Cohen-Fix O (2002). Phosphorylation of the mitotic regulator Pds1/securin by Cdc28 is required for efficient nuclear localization of Esp1/separase. Genes Dev 16, 1371-1382.

Alexandru G, Zachariae W, Schleiffer A, Nasmyth K (1999). Sister chromatid separation and chromosome re-duplication are regulated by different mechanisms in response to spindle damage. EMBO J 18, 2707-2721.

Alexandru G, Uhlmann F, Mechtler K, Poupart MA, Nasmyth K (2001). Phosphorylation of the cohesin subunit Scc1 by Polo/Cdc5 kinase regulates sister chromatid separation in yeast. Cell 105, 459-472.

Ampatzidou E, Irmisch A, O'Connell MJ, Murray JM (2006). SMC5/6 Is Required for Repair at Collapsed Replication Forks. Mol and Cell Biol 26, 9387-9401.

Atir-Lande A, Gildor T, Kornitzer D (2005). Role for the SCFCDC4 ubiquitin ligase in *Candida albicans* morphogenesis. Mol Biol Cell 16, 2772– 2785.

Bachewich C, Thomas D, Whiteway M (2003). Depletion of a polo-like kinase in *Candida albicans* activates cyclase-dependent hyphal-like growth. Mol Biol Cell 14, 2163-2180.

Bachewich C, Nantel A, Whiteway M (2005). Cell cycle arrest during S or M phase generates polarized growth via distinct signals in *Candida albicans*. Mol Microbiol 57, 942–959.

Bachmann G, Richards MW, Winter A, Beuron F, Morris E, Bayliss R (2016). A closed conformation of the *Caenorhabditis elegans* separase-securin complex. Open Biol 6, 160032.

Bai C, Ramanan N, Wang YM, Wang Y (2002). Spindle assembly checkpoint component CaMad2p is indispensable for *Candida albicans* survival and virulence in mice. Mol Microbiol 45, 31–44.

Barford D (2011). Structural insights into anaphase-promoting complex function and mechanism. Philos Trans R Soc Lond B Biol Sci 366, 3605–3624.

Bates S (2018). *Candida albicans* Cdc15 is essential for mitotic exit and cytokinesis. Sci Rep 8, 8899.

Baum P, Yip C, Goetsch L, Byers B (1988). A yeast gene essential for regulation of spindle pole duplication. Mol Cell Biol 8, 5386–5397.

Behl C, Ziegler C (2007). Cell Cycle: The Life Cycle of a Cell. Springer Briefs in Molecular Medicine 9-19.

Bensen ES, Filler SG, Berman J (2002). A forkhead transcription factor is important for true hyphal as well as yeast morphogenesis in *Candida albicans*. Eukaryot Cell 1, 787–798.

Bensen ES, Clemente-Blanco A, Finley KR, Correa-Bordez J, Berman J (2005). The Mitotic Cyclins Clb2p and Clb4p Affect Morphogenesis in *Candida albicans*. Mol Biol Cell 16, 3487-3400.

Berman J (2012). *Candida albicans*. Curr Biol 22, R620-622.

Bouchonville K, Forche A, Tang KE, Selmecki A, Berman J (2009). Aneuploid chromosomes are highly unstable during DNA transformation of *Candida albicans*. Eukaryot Cell 8, 1554–1566.

Care RS, Trevethick J, Binley KM, Sudbery PE (1999). The *MET3* promoter: a new tool for *Candida albicans* molecular genetics. Mol Microbiol 34, 792–798.

Cannon RD, Lamping E, Holmes AR, Niimi K, Tanabe K, Niimi M, Monk BC (2007). *Candida albicans* drug resistance another way to cope with stress. Microbiol 153, 3211-3217.

Carlisle PL, and Kadosh D (2013). A genome-wide transcriptional analysis of morphology determination in *Candida albicans*. Mol Biol Cell 24, 246-260.

Caydasi AK, Ibrahim B, Pereira G (2010). Monitoring spindle orientation: Spindle position checkpoint in charge. Cell div 5, 1-15.

Charles JF, Jaspersen SL, Tinker-Kulberg RL, Hwang L, Szidon A, Morgan DO (1998). The Polo-related kinase Cdc5 activates and is destroyed by the mitotic cyclin destruction machinery in *S. cerevisiae*. Curr Biol 8, 497–507.

Chereji RV, Bharatula V, Elfving N, Blomberg J, Larsson M, Morozov AV, Broach JR, Björklund S (2017). Mediator binds to boundaries of chromosomal interaction domains and to proteins involved in DNA looping, RNA metabolism, chromatin remodeling, and actin assembly. Nucleic Acids Res 45, 8806-8821.

Chestukhin A, Pfeffer C, Milligan S, DeCaprio JA, Pellman D (2003). Processing, localization, and requirement of human separase for normal anaphase progression. Proc Natl Acad Sci U S A 100, 4574-4579.

Chou H, Glory A, Bachewich C (2011). Orthologues of the anaphase-promoting complex/cyclosome coactivators Cdc20p and Cdh1p are important for mitotic progression and morphogenesis in *Candida albicans*. Eukaryot Cell 10, 696-709.

Ciosk R, Zachariae W, Michaelis C, Shevchenko A, Mann M, Nasmyth K (1998). An ESP1/PDS1 complex regulates loss of sister chromatid cohesion at the metaphase to anaphase transition in yeast. Cell 93, 1067-1076.

Clemente-Blanco A, González-Novo A, Machín F, Caballero-Lima D, Aragón L, Sánchez M, de Aldana CR, Jiménez J, Correa-Bordes J (2006). The Cdc14p phosphatase affects late cell-cycle events and morphogenesis in *Candida albicans*. J Cell Sci 119, 1130–1143.

Cohen-Fix O, Peters JM, Kirschner MW, Koshland D (1996). Anaphase initiation in *Saccharomyces cerevisiae* is controlled by the APC-dependent degradation of the anaphase inhibtitor Psd1p. Genes Dev 10, 3081–3093.

Cohen-Fix O, Koshland D (1997). The anaphase inhibitor of *Saccharomyces cerevisiae* Pds1p is a target of the DNA damage checkpoint pathway. Proc Natl Acad Sci U S A 94, 14361-14366.

Costanzo M, VanderSluis B, Koch EN, Baryshnikova A, Pons C, Tan G, Wang W, Usaj M, Hanchard J, Lee SD, Pelechano V, Styles EB, Billmann M, van Leeuwen J, van Dyk N, Lin ZY, Kuzmin E, Nelson J, Piotrowski JS, Srikumar T, Bahr S, Chen Y, Deshpande R, Kurat CF, Li SC, Li Z, Usaj MM, Okada H, Pascoe N, San Luis BJ, Sharifpoor S, Shuteriqi E, Simpkins SW, Snider J, Suresh HG, Tan Y, Zhu H, Malod-Dognin N, Janjic V, Przulj N, Troyanskaya OG, Stagljar I, Xia T, Ohya Y, Gingras AC, Raught B, Boutros M, Steinmetz LM, Moore CL, Rosebrock AP, Caudy AA, Myers CL, Andrews B, Boone C (2016). A global genetic interaction network maps a wiring diagram of cellular function. Science 353, aaf1420.

Côte P, Hogues H, Whiteway MS (2009). Transcriptional analysis of the *Candida albicans* cell cycle. Mol Biol Cell 20, 3363–3373.

Cromer L, Jolivet S, Singh DK, Berthier F, De Winne N, De Jaeger G, Sinichiro K, Prusicki MA, Schnittger A, Guérois R, Merciew R (2019). Patronus is the elusive plant securin, preventing chromosome separation by antagonizing separase. Proc Natl Acad Sci U S A 116, 16018-16027.

Cui J, Ren B, Tong Y, Dai H, Zhang L (2015). Synergistic combinations of antifungals and antivirulence agents to fight against *Candida albicans*. Virulence 6, 362-371.

Dabrieva Z, Pic-Taylor A, Boros J, Spanos A, Geymonat M, Reece RJ, Sedgwick SG, Sharrocks AD, Morgan BA (2003). Cell Cycle-Regulated Transcription through the FHA Domain of Fkh2p and the Coactivator Ndd1p. Curr Biol 13, 1740-1745.

da Silva Dantas A, Lee KK, Raziunaite I, Schaefer K, Wagener J, Yadav B, Gow NA (2016). Cell biology of *Candida albicans*-host interactions. Curr Opin Microbiol 34, 111-118.

Delaloye J, Calandra T (2014). Invasive candidiasis as a cause of sepsis in the critically ill patient. Virulence 5, 161–169.

De Souza CP, Osmani SA (2007). Mitosis, not just open or closed. Eukaryot Cell 6, 1521–1527.

Edenberg ER, Mark KG, Toczyski DP (2015). Ndd1 turnover by SCF(Grr1) is inhibited by the DNA damage checkpoint in Saccharomyces cerevisiae. PLoS genetics, *11* e1005162.

Finley KR, Berman J (2005). Microtubules in *Candida albicans* hyphae drive nuclear dynamics and connect cell cycle progression to morphogenesis. Eukaryot Cell 4, 1697-1711.

Finley KR, Bouchonville KJ, Quick A, Berman, J (2008). Dynein-dependent nuclear dynamics affect morphogenesis in *Candida albicans* by means of the Bub2p spindle checkpoint. J Cell Sci 121, 466-476.

Fournane S, Krupina K, Kleiss C, Sumara I (2013). Decoding Ubiquitin for Mitosis. Genes & Cancer 3, 697-711.

Funabiki H, Kumada K, Yanagida M (1996). Fission yeast Cut1 and Cut2 are essential for sister chromatid separation, concentrate along the metaphase spindle and form large complexes. EMBO J 15, 6617–6628.

Gladfelter A, Berman J (2009). Dancing genomes: Fungal nuclear positioning. Nat Rev Microbiol 7, 875–886.

Glory A, van Oostende C, Geitmann A, Bachewich C (2017). Depletion of the mitotic kinase Cdc5p in *Candida albicans* results in the formation of elongated buds that switch to the hyphal fate over time in a Ume6p and Hgc1p-dependent manner. Fungal Genet Biol 107, 51-66.

Gola S, Martin R, Walther A, Dunkler A, Wendland J (2003). New modules for PCR-based gene targeting in *Candida albicans*: rapid and efficient gene targeting using 100 bp of flanking homology region. Yeast 20, 1339–1347.

González-Novo A, Labrador L, Pablo-Hernando ME, Correa-Bordes J, Sánchez M, Jiménez J, De Aldana CR (2009). Dbf2 is essential for cytokinesis and correct mitotic spindle formation in *Candida albicans*. Mol Micro 72, 1364-1378.

Guacci V, Yamamoto A, Strunnikov A, Kingsbury J, Hogan E, Meluh P, Koshland D (1993). Structure and function of chromosomes in mitosis of budding yeast. Cold Spring Harb Symp Quant Biol 58, 677–685.

Gulati M, Nobile CJ (2016). *Candida albicans* biofilms: development, regulation, and molecular mechanisms. Microbes Infect 18, 310–321.

Harkness TAA (2018). Activating the Anaphase Promoting Complex to Enhance Genomic Stability and Prolong Lifespan. Int J Mol Sci 19, 1888.

Hatano Y, Naoki K, Suzuki A, Ushimaru T (2016). Positive feedback promotes mitotic exit via the APC/C-Cdh1-separase-Cdc14 axis in budding yeast. Cell Signal 28,1545-1554.

Hauf S, Roitinger E, Koch B, Dittrich CM, Mechtler K, Peters JM (2005). Dissociation of cohesin from chromosome arms and loss of arm cohesion during early mitosis depends on phosphorylation of SA2. PLoS Biol 3, 419-432.

Havens KA, Gardner MK, Kamieniecki RJ, Dresser ME, Dawson DS (2010). Slk19p of *Saccharomyces cerevisiae* regulates anaphase spindle dynamics through two independent mechanisms. Genetics 186, 1247-1260.

Hazan I, Sepulveda-Becerra M, Liu H (2002). Hyphal elongation is regulated independently of cell cycle in *Candida albicans*. Mol Biol Cell 13, 134–145.

Heichman KA, Roberts JM (1996). The yeast *CDC16* and *CDC27* genes restrict DNA replication to once per cell cycle. Cell 85, 39-48.

Hellmuth S, Pöhlmann C, Brown A, Böttger F, Sprinzl M, Stemmann O (2015). Positive and negative regulation of vertebrate separase by Cdk1-cyclin B1 may explain why securin is dispensable. J Biol Chem 290, 8002-8010.

Hilioti Z, Chung YS, Mochizuki Y, Hardy CF, Cohen-Fix O (2001). The anaphase inhibitor Pds1 binds to the APC/C-associated protein Cdc20 in a destruction box-dependent manner. Curr Biol 11, 1347-1352.

Holt LJ, Krutchinsky AN, Morgan DO (2008). Positive feedback sharpens the anaphase switch. Nature 454, 353–357.

Hornig NCD, Knowles PP, McDonald NQ, Uhlmann F (2002). The dual mechanism of separase regulation by securin. Curr Biol 12, 973–982.

Hotz M, Lengefeld J, Barral Y (2012). The MEN mediates the effects of the spindle assembly checkpoint on Kar9-dependent spindle pole body inheritance in budding yeast. Cell cycle 11, 3109-3116.

Huang MY, Woolford CA, May G, McManus CJ, Mitchell AP (2019). Circuit diversification in a biofilm regulatory network. PLOS Path 15, e1007787.

Irniger S, Nasmyth K (1997). The anaphase-promoting complex is required in G1 arrested yeast cells to inhibit B-type cyclin accumulation and to prevent uncontrolled entry into S-phase. J Cell Biol 110, 1523-1531.

Irniger S (2002). Cyclin destruction in mitosis: a crucial task of Cdc20p. FEBS Lett 532, 7-11.

Jäger H, Herzig A, Lehner CF, Heidmann S (2001). *Drosophila* Separase is required for sister chromatid separation and binds to PIM and THR. Genes Dev 15, 2572-2584.

Jaspersen SL, Charles JF, Morgan D (1999). Inhibitory phosphorylation of the APC regulator Hct1 is controlled by the kinase Cdc28 and the phosphatase Cdc14. Curr Biol 9, 227-36.

Jensen S, Segal M, Clarke DJ, Reed SI (2001). A novel role of the budding yeast separin Esp1 in anaphase spindle elongation: evidence that proper spindle association of Esp1p is regulated by Pds1. J Cell Biol 152, 27-40.

Jorgensen P, Tyers M (2004). How cells coordinate growth and division. Curr Biol 14, R1014–1027.

Kabir MA, Hussain MA, Ahmad Z (2012). *Candida albicans*: A Model Organism for Studying Fungal Pathogens. ISRN Microbio 1-15.

Kadosh D. (2017). Morphogenesis in *C. albicans*. In *Candida albicans: Cellular and Molecular Biology: Second Edition*. Springer International Publishing 41-62.

Kaneva, I, Sudbery, I, Dickman, M, Sudbery P. (2019). Proteins that physically interact with the phosphatase Cdc14 in *Candida albicans* have diverse roles in the cell cycle. Scientific Reports 9, 6258.

Kim KP, Weiner BM, Zhang L, Jordan A, Dekker J, Kleckner N (2010). Sister Cohesion and Structural Axis Components Mediate Homolog Bias of Meiotic Recombination. Cell 143, 924-937.

Kitamura E, Tanaka K, Kitamura Y, Tanaka TU (2007). Kinetochore microtubule interaction during S phase in *Saccharomyces cerevisiae*. Genes Dev 21, 3319-3330.

Kitagawa R, Law E, Tang LH, Rose AM (2002). The Cdc20 homolog, FZY-1, and its interacting protein, IFY-1, are required for proper chromosome segregation in *Caenorhabditis elegans*. Curr Biol 12, 2118-2123.

Kraft C, Herzog F, Gieffers C, Mechtler K, Hagting A, Pines J, Peters JM (2003). Mitotic regulation of the human anaphase-promoting complex by phosphorylation. EMBO J 22, 6598-6609.

Kramer ER, Scheuringer N, Podtelejniko AV, Mann M, Peters JM (2000). Mitotic Regulation of the APC Activator Proteins CDC20 and CDH1. Mol Cell Bio 11, 1555-1569.

Kumar R (2017). Separase: Function Beyond Cohesion Cleavage and an Emerging Oncogene. J Cell Biochem 118, 1283-1299.

Lamb JR, Michaud WA, Sikorski RS, Hieter PA (1994). Cdc16p, Cdc23p and Cdc27p form a complex essential for mitosis. EMBO J 13, 4321-4328.

Larkin MA, Blackshields G, Brown NP, Chenna R, McGettigan PA, McWilliam H, Valentin F, Wallace IM, Wilm A, Lopez R, Thompson JD, Gibson TJ, Higgins DJ (2007). Clustal W and Clustal X version 2.0, Bioinformatics 23, 2947–2948.

Lavoie H, Sellam A, Askew C, Nantel A, Whiteway M (2008). A toolbox for epitope-tagging and genome-wide location analysis in *Candida albicans*. BMC Genomics 9, 578.

Lazo BC, Bates S, Sudbery P (2005). The G1 cyclin Cln3 regulates morphogenesis in *Candida albicans*. Eukaryot Cell 4, 90 –94.

Li X, Hou Y, Yue L, Liu S, Du J, Sun S (2015). Potential Targets for Antifungal Drug Discovery Based on Growth and Virulence in *Candida albicans*. Antimicrob Agents Chemother. 59, 5885–5891.

Liang F, Richmond D, Wang Y (2013). Coordination of Chromatid Separation and Spindle Elongation by Antagonistic Activities of Mitotic and S-Phase CDKs. PLoS Genet 9, e1003319.

Lianga N, Doré C, Kennedy EK, Yeh E, Williams EC (2018). Cdk1 phosphorylation of Esp1/Separase functions with PP2A and Slk19 to regulate pericentric cohesin and anaphase onset. PLoS Genet 14, 1-34.

Lim HH, Goh PY, Surana U (1998). Cdc20p is essential for the cyclosome-mediated proteolysis of both Pds1p and Clb2p during M phase in budding yeast. Curr Biol 8, 231–234.

Lim CS, Rosli R, Seow HF, Chong PP (2012). Candida and invasive candidiasis: back to basics. Eur J Clin Microbiol Infect Dis 31, 21-31.

Listovsky T, Sal, JE (2013). Sequestration of CDH1 by MAD2L2 prevents premature APC/C activation prior to anaphase onset. J of Cell Biol 203, 87-100.

Liu HL, Osmani AH, Ukil L, Son S, Markossian S, Shen KF, Govindaraghavan M, Varadaraj A, Hashmi SB, De Souza CP, Osmani SA (2010). Single-step affinity purification for fungal proteomics. Eukaryot Cell 9, 831-833.

Lo HJ, Köhler JR, DiDomenico B, Loebenberg D, Cacciapuoti A, Fink GR (1997). Non filamentous *C. albicans* mutants are avirulent. Cell 90, 939-949.

Lu Y, Cross F (2009). Mitotic exit in the absence of separase activity. Mol Biol Cell 20, 1576-91.

Lundblad V, Szostak JW (1989). A mutant with a defect in telomere elongation leads to senescence in yeast. Cell 57, P633-643.

Luo S, Tong L (2018). Structural biology of the separase-securin complex with crucial roles in chromosome segregation. Curr Opin Struct Biol 49, 114-122.

Marston AL (2014). Chromosome segregation in budding yeast: Sister chromatid cohesion and related mechanisms. Genetics 196, 31-63.

May KM, Hardwick KG (2006). The spindle checkpoint. J Cell Sci 119, 4139-4142.

McLean JR, Chaix D, Ohi MD, Gould KL (2011). State of the APC/C: organization, function, and structure. Crit Rev Biochem Mol Biol 46, 118–136.

McGrew JT, Goetsch L, Byers B, Baum P (1992). Requirement for *ESP1* in the nuclear division of *Saccharomyces cerevisiae*. Mol Biol Cell 3, 1443-1445.

McKnite AM, Perez-Munoz ME, Lu L, Williams EG, Brewer S, Andreux PA, Bastiaansen JW, Wang X, Kachman SD, Auwerx J, Williams RW, Benson AK, Peterson DA, Ciobanu DC (2012). Murine gut microbiota is defined by host genetics and modulates variation of metabolic traits. PLoS One 7, e39191.

Mehta GD, Kumar R, Srivastava S, Ghosh SK (2013). Cohesin: functions beyond sister chromatid cohesion. FEBS Lett 587, 2299-2312.

Miller RK, Rose MD (1998). Kar9p is a novel cortical protein required for cytoplasmic microtubule orientation in yeast. J Cell Biol 140, 377-390.

Milne SW, Cheetham J, Lloyd D, Shaw S, Moore K, Paszkiewicz KH, Aves SJ, Bates S (2014). Role of *Candida albicans* Tem1 in mitotic exit and cytokinesis. Fungal Genet Biol 69, 84-95.

Moreno-Mateos MA, Espina ÁG, Torres B, Gámez del Estal MM, Romero-Franco A, Ríos RM, Pintor-Toro JA (2011). PTTG1/securin modulates microtubule nucleation and cell migration. Mol Biol Cell 22, 4302-4311.

Morgan DO (2007). The Cell Cycle Principles of Control. New Science Press Ltd, 96-98.

Moschou P, Bozhkov PV (2012). Separases: biochemistry and function. Physiol Plant 145, 67-76.

Ofir A, Kornitzer D (2010). *Candida albicans* cyclin Clb4 carries S-phase cyclin activity. Eukaryot Cell 9, 1311-1319.

Ofir A, Hofmann K, Weindling E, Gildor T, Barker KS, Rogers PD, Kornitzer D (2012). Role of a *Candida albicans* Nrm1/Whi5 homologue in cell cycle gene expression and DNA replication stress response. Mol Microbiol 84, 778-794.

O'Meara TR, Veri AO, Ketela T, Jiang B, Roemer T, Cowen LE (2015). Global analysis of fungal morphology exposes mechanisms of host cell escape. Nat Commun 6, 1-10.

Onoda F, Takeda M, Seki M, Maeda D, Takima J, Ui A, Yagi H, Enomoto T (2004). SMC6 is required for MMS-induced interchromosomal and sister chromatid recombinations in *Saccharomyces cerevisiae*. DNA Repair Amst 4, 429-439.

Orellana-Muñoz S, Dueñas-Santero E, Arnáiz-Pita Y, Del Rey F, Correa-Bordes J, Vázquez de Aldana CR (2018). The anillin-related Int1 protein and the Sep7 septin collaborate to maintain cellular ploidy in *Candida albicans*. Sci Rep 8, 2257.

Palmer RE, Koval M, Koshland D (1989). The dynamics of chromosome movement in the budding yeast *Saccharomyces cerevisiae*. J Cell Biol 109, 3355–3366.

Palou G, Palou R, Zeng F, Vashisht AA, Wohlschlegel JA, Quintana DG (2015). Three Different Pathways Prevent Chromosome Segregation in the Presence of DNA Damage or Replication Stress in Budding Yeast. PLoS Genet 11, 1-22.

Palou R, Palou G, Quintana DG (2017). A role for the spindle assembly checkpoint in the DNA damage response. Curr Genet 63, 275-280.

Parente-Rocha JA, Bailão AM, Amaral AC, Taborda CP, Paccez JD, Borges CL, Pereira M (2017). Antifungal Resistance, Metabolic Routes as Drug Targets, and New Antifungal Agents: An Overview about Endemic Dimorphic Fungi. Mediators Inflamm 9870679.

Peters JM (2006). The anaphase promoting complex/cyclosome: a machine designed to destroy. Mol Cell Biol 7, 644-656.

Peters JM, Tedeschi A, Schmitz J (2008). The cohesin complex and its roles in chromosome biology. Genes Dev 22, 3089-3114.

Piskadlo E, Oliveira RA (2017). A Topology-Centric View on Mitotic Chromosome Architecture. Int J Mol Sci 18, 2751.

Qiao R, Weissmann F, Yamaguchi M, Brown NG, VanderLinden R, Imre R, Jarvis MA, Brunner MR, Davidson IF, Litos G, Haselbach D, Mechtler K, Stark H, Schulman BA, Peters JM (2016). Mechanism of APC/CCDC20 activation by mitotic phosphorylation. Proc Natl Acad Sci U S A. 113, 2570-2580.

Queralt E, Uhlmann F (2008). Cdk-counteracting phosphatases unlock mitotic exit. Curr Opin Cell Biol 20, 661-668.

Rahal R, Amon A (2008a). The Polo-like kinase Cdc5 interacts with FEAR network components and Cdc14. Cell Cycle 7, 3262-3272.

Rahal R, Amon A (2008b). Mitotic CDKs control the metaphase–anaphase transition and trigger spindle elongation. Genes Dev 22, 1534-1548.

Ramos-Morales F, Dominguez A, Romero F, Luna R, Multon MC, Pintor Toro JA, Tortolero M (2000). Cell cycle regulated expression and phosphorylation of hPTTG proto-oncogene product. Oncogene19, 403–409.

Raspelli, E, Cassani, C, Chiroli, E and Fraschini R. (2015). Budding Yeast Swe1 Is Involved in the Control of Mitotic Spindle Elongation and Is Regulated by Cdc14 Phosphatase during Mitosis. J Biol Chem 290, 1-12.

Rastghalam G, Parvizi Omran R, Alizadeh M, Fulton D, Mallick J, Whiteway M (2019). MAP Kinase Regulation of the *Candida albicans* Pheromone Pathway. mSphere 4, 1-14.

Rigaut G, Shevchenko A, Rutz B, Wilm M, Mann M, Séraphin B (1999). A generic protein purification method for protein complex characterization and proteome exploration. Nat Biotechnol 17, 1030-1032.

Robert X, Gouet P (2014). Deciphering key features in protein structures with the new ENDscript server. Nucleic Acids Res W320-324.

Rose MD, Winston F, Hieter P (1990). Methods in Yeast Genetics: A Laboratory Course Manual. Cold Spring Harb Laboratory Press.

Rosenberg A, Enez IV, Bibi M, Zakin S, Shtifman E, Ziva N, Dahan AM, Lopes-Colombo A, Bennet RJ, Berman J (2018). Antifungal tolerance is a subpopulation effect distinct from resistance and is associated with persistent candidemia. Nat Commun 9, 1-14.

Sajman J, Zenvirth D, Nitzan M, Margalit H, Simpson-Lavy KJ, Reiss Y, Cohen I, Ravid T, Brandeis M (2015). Degradation of Ndd1 by APC/C$_{Cdh1}$generates a feed forward loop that times mitotic protein accumulation. Nat Commun 6, 1-10.

Sanchez Y, Bachant J, Wang H, Hu F, Liu D, Tetzlaff M, Elledge SJ (1999). Control of the DNA damage checkpoint by chk1 and rad53 protein kinases through distinct mechanisms. Science 286, 1166-1171.

Sanchez-Diaz A, Nkosi PD, Murray S, Labib K (2012). The Mitotic Exit Network and Cdc14 phosphatase initiate cytokinesis by counteracting CDK phosphorylations and blocking polarized growth. EMBO J 31, 3620-3634.

Sellam A, Whiteway M (2016). Recent advances on *Candida albicans* biology and virulence. F1000Res 5, 2582.

Selmecki A, Forche A, and Berman, J (2010). Genomic plasticity of the human fungal pathogen *Candida albicans*. Eukaryot Cell 9, 991-1008.

Schaefer JB, Morgan DO (2011). Protein-linked ubiquitin chain structure restricts activity of deubiquitinating enzymes. J Biol Chem 286, 45186–45196.

Sherwood RK, Bennett RJ (2008). Microtubule motor protein Kar3 is required for normal mitotic division and morphogenesis in *Candida albicans*. Eukaryot Cell 7, 1460-1474.

Shi QM, Wang YM, Zheng XD, Lee RT, Wang Y (2007). Critical role of DNA checkpoints in mediating genotoxic-stress-induced filamentous growth in *Candida albicans*. Mol Biol Cell 18, 815-826.

Si H, Hernday AD, Hirakawa MP, Johnson AD, Bennett RJ (2013). *Candida albicans* white and opaque cells undergo distinct programs of filamentous growth. PLoS Pathog 9, e1003210.

Siomos MF, Badrinath A, Pasierbek P, Livingstone D, White J, Glotzer M, Nasmyth K (2001). Separase is required for chromosome segregation during meiosis I in *Caenorhabditis elegans*. Curr Biol 11, 1825-1835.

Sivakumar S, Gorbsky GJ (2015). Spatiotemporal regulation of the anaphase-promoting complex in mitosis. Nat Rev Mol Cell Biol 16, 82–94.

Sparapani S (2015). Characterization of a putative separase Esp1p and a novel interacting protein in regulating mitosis in the fungal pathogen *Candida albicans*. Masters thesis, Concordia University.

Sparapani S, Bachewich C (2019). Characterization of a novel separase-interacting protein and candidate new securin, Eip1p, in the fungal pathogen *Candida albicans*. Mol Biol Cell 30, 2469-2489.

Stegmeier F, Visintin R, Amon A (2002). Separase, polo kinase, the kinetochore protein Slk19, and Spo12 function in a network that controls Cdc14 localization during early anaphase. Cell 108, 207-220.

Stratmann R, Lehner CF (1996). Separation of sister chromatids in mitosis requires the *Drosophila* pimples product, a protein degraded after the metaphase/anaphase transition. Cell 84, 25-35.

Sudakin V, Chan GK, Yen TJ (2001). Checkpoint inhibition of the APC/C in HeLa cells is mediated by a complex of BUBR1, BUB3, CDC20, and MAD2. J Cell Biol 154, 925-936.

Sudbery P (2011). Growth of *Candida albicans* hyphae. Nat Rev Microbiol 16, 737-748.

Sullivan M, Uhlmann F (2003). A non-proteolytic function of separase links the onset of anaphase to mitotic exit. Nat Cell Biol 5, 249–254.

Tinker-Kulberg RL, Morgan DO (1999). Pds1 and Esp1 control both anaphase and mitotic exit in normal cells and after DNA damage. Genes Dev 13, 1936-1949.

Uhlmann F, Lottspeich F, Nasmyth K (1999). Sister-chromatid separation at anaphase onset is promoted by cleavage of the cohesin subunit Scc1. Nature 400, 37-42.

Uhlmann F, Wernic D, Poupart MA, Koonin EV, Nasmyth K (2000). Cleavage of Cohesin by the CD Clan Protease Separin Triggers Anaphase in Yeast. Cell 103, 375-386.

Visintin, R, Prinz, S, Amon A. (1997). CDC20 and CDH1: a family of substrate-specific activators of APC-dependent proteolysis. Science 278, 460-463.

Waizenegger IC, Gimenez-Abian JF, Wernic D, Peters JM (2002). Regulation of Human Separase by Securin Binding and Autocleavage. Curr Biol 12, 1368-1378.

Wang H, Liu D, Wang Y, Qin J, Elledge SJ (2001). Pds1 phosphorylation in response to DNA damage is essential for its DNA damage checkpoint function. Genes Dev 15, 1361-1372.

Wang H, Gao J, Li W, Wong AHH, Hu K, Chen K, Wang Y, Sang J (2012). Pph3 Dephosphorylation of Rad53 Is Required for Cell Recovery from MMS-Induced DNA Damage in *Candida albicans*. PLoS One 7, 1-13.

Wang W, Deng Z, Wu H, Zhao Q, Li T, Zhu W, Wang X, Tang L, Wang C, Cui SZ, Xiao H, Chen J (2019). A small secreted protein triggers a TLR2/4-dependent inflammatory response during invasive *Candida albicans* infection. Nat Commun 10, 1-14.

Weiss E (2012). Mitotic Exit and Separation of Mother and Daughter Cells. Genetics 192, 1165-1202.

Williams AE (2012). Basic concepts in Immunology, in Immunology: Mucosal and Body Surface Defences. John Wiley & Sons, Ltd, Chichester UK 4-6.

Woodruff JB, Drubin DG, Barnes G (2010). Mitotic spindle disassembly occurs via distinct subprocesses driven by the anaphase-promoting complex, Aurora B kinase, and kinesin-8. J Cell Biol 191, 795-808.

Yamamoto A, Guacci V, Koshland D (1996a). Pds1p is required for faithful execution of anaphase in the yeast *Saccharomyces cerevisiae*. J Cell Biol 133, 85-97.

Yamamoto A, Guacci V, Koshland D (1996b). Pds1p, an inhibitor of anaphase in budding yeast, plays a critical role in the APC and checkpoint pathway(s). J Cell Biol 133, 99-110.

Yanagida M (2000). Cell cycle mechanisms of sister chromatid separation; roles of Cut1/separin and Cut2/securin. Genes to cells 5, 1-8.

Yellman CM, Roeder GS (2015). Cdc14 Early Anaphase Release, FEAR, Is Limited to the Nucleus and Dispensable for Efficient Mitotic Exit. PLoS One 10, 1-24.

Zhang J, Wan L, Dai X, Sun Y, Wei W (2014). Functional characterization of Anaphase Promoting Complex/Cyclosome (APC/C) E3 ubiquitin ligases in tumorigenesis. Biochim Biophys Acta 1845, 277–293.

Zhu J, Thompson CB (2019). Metabolic regulation of cell growth and proliferation. Nat Rev Molec Cell Biol 20, 436–450.

Zou H, McGarry TJ, Bernal T, Kirschner MW (1999). Identification of a vertebrate sister-chromatid separation inhibitor involved in transformation and tumorigenesis. Science 285, 418–422.

Chapter 6.0: Appendices

6.1 Appendix 1

Hof1 plays a checkpoint related role in MMS induced DNA damage response in *Candida albicans*

Jinrong Feng, Amjad Islam, Aashima Goyal, Bjorn Bean, **Samantha Sparapani**, Manjari Shrivastava, Jia Feng, Raha Parvizi Omran, Jaideep Mallick, Malcolm Whiteway

6.1.1 Introduction and Purpose

DNA damage and stress induces genomic instability and morphological changes in the fungal pathogen *Candida albicans*. The DNA damage checkpoint pathway plays a critical role in ensuring external stressors are dealt with prior to the cell progressing through mitosis and undergoing cytokinesis. The DNA damage response pathway is composed of several key proteins, some of which include Rad53p and Hof1p, with Hof1p recently shown to play a role in cytokinesis (Smolka et al., 2006). In *C. albicans*, when exposed to DNA damaging agents such as methyl methane sulfate (MMS), the conditional *HOF1* mutant showed sensitivity. This manuscript sought to further investigate the potential function of Hof1p in the DNA damage response pathway in *C. albicans*. Using my experience in conducting MMS-induced cell cycle arrest assays and fluorescent microscopy, my contribution to this manuscript involved evaluating the nuclear segregation in *hof1* and *rad53* mutant cells in order to determine whether genomic instability in the presence of MMS was due to chromosomal segregation defects.

6.1.2 Materials & Methods

The MMS assay was conducted using strains SN148 (*HOF1/HOF1*), JC23 (*rad53::HIS1/rad53::HIS1*), JC28 (*hof1::HIS1/hof1::HIS1*), and JC24 (*rad53::HIS1/rad53::HIS1, hof1::ARG4/hof1::ARG4*). Overnight cells were diluted down to an OD_{600} of 0.2 in YPD with and without 0.02% Methyl Methane Sulfate (MMS) and incubated for 6 h. In order to visualize DNA, cells were fixed in fresh 70% ethanol for 20 min, washed with sterile water, incubated in 1.0 µg/ml of 4′, 6′-diamidino-2-phenylindole dihydrochloride (DAPI; Sigma-Aldrich) for 20 min, washed twice with sterile water, and mounted on slides. Cells were imaged on a LeicaDM6000B microscope (Leica Microsystems Canada Inc., Richmond Hill, ON, Canada) equipped with a Hamamatsu-ORCA ER camera (Hamamatsu Photonics, Hamamatsu City, Japan) and the HCX PL APO 63x NA 1.40-0 oil or HCX PLFLUO TAR 100x NA 1.30-0.6 oil objectives. Differential Interference Contrast (DIC) optics, or epifluorescence with DAPI (460nm) filters were utilized. Images were captured with Volocity software (Improvision Inc., Perkin-Elmer, Waltham, MA).

6.1.3 Results

Cells were incubated in the presence or absence of MMS, fixed, stained with DAPI and imaged. In wildtype cells incubated in the absence of MMS, 40% arrested in metaphase and 50% in telophase (n=58). In contrast, approximately 20% of cells in the *hof1* mutant arrested in metaphase and 30% in telophase, with 50% of cells in both phases showing either binucleate or non-compact nuclei (n=56). In the presence of MMS 90% of wildtype cells arrested in metaphase whereas 40% of cells predominantly shifted to a metaphase arrest in the *hof1* mutant with 43% of cells demonstrating binucleate and non-compact DNA masses (Table 6.1). These results suggest that *hof1* mutants show aberrant cell cycle progression and increase binucleate DNA, consistent with a defect in cytokinesis.

Table 6.1. Nuclear segregation of Hof1 and Rad53 mutant cells.
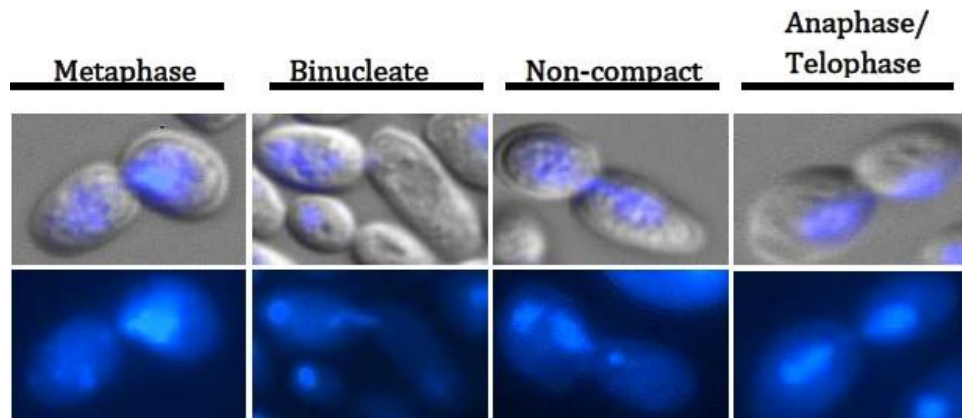
	Metaphase	Binucleate	Non-compact	Anaphase/Telophase
No MMS				
WT (n=62)	43.4	0	3.3	53.3
rad53Δ/rad53Δ (n=52)	42.8	3.5	0	53.8
hof1Δ/hof1Δ (n=56)	19.2	36.0	16.0	27.8
rad53Δ/rad53Δ, hof1Δ/hof1Δ (n=66)	41.9	24.8	8.4	24.8
+ 0.02% MMS				
WT (n=58)	90.4	0	0	9.6
rad53Δ/rad53Δ (n=57)	23.5	26.5	26.5	23.5
hof1Δ/hof1Δ (n=59)	40.0	30.0	13.4	16.7
rad53Δ/rad53Δ, hof1Δ/hof1Δ (n=80)	17.4	19.6	23.5	39.2

6.1.4 References

Smolka MB, Chen SH, Maddox PS, Enserink JM, Albuquerque CP, Wei XX, Desai A, Kolodner RD, Zhou H (2006). An FHA domain-mediated protein interaction network of Rad53 reveals its role in polarized cell growth. J Cell Biol 175, 743-753.